

# Simulating Bark Beetle Outbreak Dynamics and their Influence on Carbon Balance Estimates with ORCHIDEE r7791

Guillaume Marie<sup>1\*</sup>, Jina Jeong<sup>2\*</sup>, Hervé Jactel<sup>3</sup>, Gunnar Petter<sup>4</sup>, Maxime Cailleret<sup>5</sup>, Matthew J. McGrath<sup>1</sup>, Vladislav Bastrikov<sup>6</sup>, Josefine Ghattas<sup>7</sup>, Bertrand Guenet<sup>8</sup>, Anne Sofie Lansø<sup>9</sup>, Kim Naudts<sup>11</sup>, Aude Valade<sup>10</sup>, Chao Yue<sup>12</sup>, Sebastiaan Luyssaert<sup>2</sup>

<sup>1</sup> Laboratoire des Sciences du Climat et de l'Environnement, CEA CNRS UVSQ UP Saclay, 91191 Orme des Merisiers, Gif-sur-Yvette, France

<sup>2</sup> Faculty of Science, A-LIFE, Vrije Universiteit Amsterdam, 1081 ~~HV~~BT Amsterdam, the Netherlands

<sup>3</sup> INRAE, University of Bordeaux, umr Biogeco, 33612 Cestas, France

<sup>4</sup> ETH Zürich, Department of Environmental Systems Science, Forest Ecology, 8092 Zürich, Switzerland

<sup>5</sup> INRAE, Aix-Marseille Univ, UMR RECOVER, 13182 Aix-en-Provence, France

<sup>6</sup> Science Partner, France

<sup>7</sup> Institut Pierre-Simon Laplace – Sciences du climat (IPSL), 75105 Jussieu, France

<sup>8</sup> Laboratoire de Géologie, Ecole Normale Supérieure, CNRS, PSL Research University, IPSL, 75005 Paris, France

<sup>9</sup> Department of Environmental Science, Aarhus Universitet, Frederiksborgvej 399, 4000 Roskilde, Denmark

<sup>10</sup> Eco & Sols, Univ Montpellier, CIRAD, INRAE, 34060 Institut Agro, IRD, Montpellier, France

<sup>11</sup> Department of Earth Sciences, Vrije Universiteit Amsterdam, 1081 HV Amsterdam, the Netherlands

<sup>12</sup> State Key Laboratory of Soil Erosion and Dryland Farming on the Loess Plateau, Northwest A & F University, Yangling, Shaanxi, China

\* These authors contributed equally to this study

**Corresponding author:** Guillaume Marie, [guillaume.marie@lsce.ipsl.fr](mailto:guillaume.marie@lsce.ipsl.fr), Jina Jeong, [j.jeong@vu.nl](mailto:j.jeong@vu.nl), Sebastiaan Luyssaert, [s.luyssaert@vu.nl](mailto:s.luyssaert@vu.nl)

**Abstract :** New (a)biotic conditions, resulting from climate change, are expected to change disturbance dynamics, e.g., wind throw, forest fires, droughts, and insect outbreaks, and their interactions. Unprecedented natural disturbance dynamics might alter the capability of forest ecosystems to buffer atmospheric CO<sub>2</sub> increases in the atmosphere, even leading to the risk that forests transform from sinks into sources of CO<sub>2</sub>. This study aims to enhance the capability of the ORCHIDEE land surface model to study the impacts of climate change on bark beetle dynamics and subsequent effects on forest functioning. The bark beetle outbreak model is ~~based on~~ inspired by previous work ~~by~~ from Temperli et al. 2013 for the LandClim landscape model. The new implementation of this model in ORCHIDEE r7791 accounts for the following differences between ORCHIDEE and LandClim: (1) the

coarser spatial resolution of ORCHIDEE, (2) the higher temporal resolution of ORCHIDEE, and (3) the pre-existing process representation of ~~wind-throw~~windthrow, drought, and forest structure in ORCHIDEE. ~~Qualitative evaluation~~Simulation experiments demonstrated the model's ability to simulate a wide range of observed post-disturbance forest dynamics: (1) resistance to bark beetle infestation— even in the presence of windthrow events; (2) slow transition (~~3–71~~9 years) from an endemic into an epidemic bark beetle population following ~~medium-intensity windthrow events at cold locations~~; and (3) ~~fast transition (1–3 years) from endemic to epidemic triggered by strong~~windthrow events. Although all simulated sites eventually recovered from disturbances, the time needed to recover varied from ~~5 to 107~~ to 14 years depending on the disturbance dynamics. In addition to enhancing the functionality of the ORCHIDEE model, the new bark beetle model represents a fundamental change in the way mortality is simulated as it replaces a framework in which mortality is conceived as a continuous process by one in which mortality is represented by abrupt events. Changing the mortality framework provided new insights into carbon balance estimates, showing the risk of overestimating the short term sequestration potential under the commonly used continuous mortality framework.

## 1. Introduction

~~Considerable uncertainties remain about the magnitude of Earth system impacts from all future climate change scenarios, even the most modest (Pörtner et al., 2022). One major source of uncertainty is that future~~Future climate will likely bring new abiotic constraints through the co-occurrence of multiple connected hazards, e.g., “hotter droughts”, which are droughts combined with heat waves (Allen et al., 2015; Zscheischler et al., 2018), but also new biotic conditions from interacting natural and anthropogenic disturbances, e.g., insect outbreaks following ~~wind-throw~~windthrow or forest fires (Seidl et al., 2017). Unprecedented natural disturbance dynamics might alter biogeochemical cycles specifically the capability of forest ecosystems to buffer the CO<sub>2</sub> increase in the atmosphere (Hicke et al., 2012; Seidl et al., 2014) and the risk that forests are transformed from sinks into sources of CO<sub>2</sub> (Kurz et al., ~~2008~~2008a). The magnitude of such alteration, however, remains uncertain principally due to the lack of impact studies that include disturbance regime shifts at global scale (Seidl et al., 2011).

Land surface models are used to study the relationships between climate change and the biogeochemical cycles of carbon, water, and nitrogen (Cox et al., 2000; Ciais et al., 2005; Friedlingstein et al., 2006; Zaehle and Dalmonech, 2011; Luysaert et al., 2018). Many of these models use background mortality to obtain an equilibrium in their biomass pools. ~~Moreover, the~~This classic approach of ~~studying towards~~studying forest dynamics, which assumes steady-state conditions over long periods of time, may not be suitable for assessing the impacts of disturbances on shorter time scales under a ~~climate of accelerating changes. This is important because such~~fast changing climate. This could be considered a shortcoming in the land surface models because disturbances can have significant impacts on ecosystem services, such as water regulation, carbon sequestration, and biodiversity (Quillet et al., 2010). ¶

Mechanistic approaches that account for a variety of mortality ~~drivers~~causes, such as age, size, competition, climate, and disturbances, are now being ~~used~~considered and tested to simulate forest dynamics more accurately (Migliavacca et al., 2021). For example, the ~~ORCHIDEE model considers mortality induced by~~land surface model

ORCHIDEE accounts for mortality from interspecific competition for light in addition to background mortality. Incorporating (Naudts et al., 2015). Implementing a more mechanistic view on mortality is important thought to be essential for improving our understanding of the impacts of climate change on forest dynamics and the provision of ecosystem services.

Land surface models also face the challenge of better describing mortality particularly when it comes to ecosystem responses to “cascading disturbances”, where legacy effects from one disturbance affect the next (Zscheischler et al., 2018; Buma, 2015). Biotic disturbances, such as bark beetle outbreaks, strongly depend on previous disturbances as their infestation capabilities are higher when tree vitality is low, for example following drought or storm events (Seidl et al., 2018). This illustrates how interactions between biotic and abiotic disturbances can have significant substantial effects on ecosystem dynamics and must be incorporated into accounted for in land surface models to improve our understanding of the impacts of climate change on forest dynamics (Temperli et al., 2013; Seidl et al., 2011). While progress has been made towards including abrupt mortality from individual disturbance types such as wildfire (Yue et al., 2014; Lasslop et al., 2014; Migliavacca et al., 2013), windthrow (Chen et al., 2018) and drought (Yao et al., 2022), the interaction of biotic and abiotic disturbances remains both a knowledge and modeling gap (Kautz et al., 2018).

Bark beetle outbreaks infestations are becoming increasingly important biotic disturbances across the world (Seidl recognized as disturbance events of regional to global importance (Kurz et al., 2018 2008b; Bentz et al., 2010). A massive bark beetle outbreak in the Canadian and American Rocky Mountains damaged more than 90% of the Engelmann spruce trees across 325,000 ha from 2005 to; Seidl et al., 2018). Notably, a bark beetle outbreak ravaged over 90% of Engelmann spruce trees across approximately 325,000 hectares in the Canadian and American Rocky Mountains between 2005 and 2017 (Andrus et al., 2020). Damage caused by In Europe, the spruce bark beetle, *Ips typographus* is also on the rise in Europe, and is responsible for as much as, has been involved in up to 8% of all total tree mortality due to natural disturbances in Europe between 1850 and 2000 (Hlásny et al., 2021). In particular, a strong link between previous windthrow and bark beetle outbreaks has been reported (Pasztor from 1850 to 2000 (Hlásny et al., 2021a). A recent increase in beetle activity, particularly following mild winters (Kurz et al., 2008b; Andrus et al., 2020), windthrow (Mezei et al., 2017), and droughts (Nardi et al., 2023) have been well-documented (Hlásny et al., 2021a; Pasztor et al., 2014), underscoring the need to integrate bark beetle dynamics into land surface modeling.

Past studies used a variety of approaches to model the impacts of bark beetles on forests. While some model treated bark beetle outbreaks as background mortality (Naudts et al., 2014; Mezei 2016; Luysaert et al., 2017). These observations justify the inclusion of bark beetle dynamics into land surface models. Hence, the 2018), others dynamically modeled these outbreaks within ecosystems (Temperli et al., 2013; Seidl and Rammer, 2016; Jönsson et al., 2012). Studies with prescribed beetle outbreaks tend to focus on the direct effects of the outbreak on forest conditions and carbon fluxes, but are likely to overlook more complex feedback processes, such as interactions with

other disturbances and longer-term impacts. Conversely, dynamic modeling of beetle outbreaks, provides a more comprehensive view by incorporating the lifecycle of bark beetles, tree defense mechanisms, and ensuing alterations in forest composition and functionality.

Simulation experiments for *Ips typographus* outbreaks using the LPJ-GUESS vegetation model highlighted regional variations in outbreak frequencies, pinpointing climate change as a key exacerbating factor (Jönsson et al., 2012). Simulation experiments with the iLand landscape model suggested that almost 65% of the bark beetle outbreaks are aggravated by other environmental drivers (Seidl and Rammer, 2016). A 4°C temperature increase could result in a 265% increase in disturbed areas and a 1800% growth in average patch size (Seidl and Rammer 2016). Disturbance interactions were ten times more sensitive to temperature changes, boosting the disturbance regime's climate sensitivity. The results of these studies justify the inclusion of interacting disturbances in land surface models, such as ORCHIDEE, which are used in future climate predictions and impact studies (Boucher et al., 2020).

The objectives of this study are: (1) to develop and implement a spatially implicit bark beetle (*Ips Typographus*) outbreak model in the land surface model ORCHIDEE based on the work by Temperli et al. (2013), and (2) use a simulation experiment to evaluate the performance of simulation experiments to characterize the behavior of this newly added model functionality.

## **2. Methods and material** **Model description**

### **2.1. The land surface model ORCHIDEE**

ORCHIDEE is the land surface model of the IPSL (Institut Pierre Simon Laplace) Earth system model (Krinner et al., 2005; Boucher et al., 2020). ORCHIDEE can, however, also be run off-line as a stand-alone land surface model forced by temperature, humidity, pressure, precipitation, and wind conditions. Unlike the coupled setup, which needs to run on the global scale, the stand-alone configuration can cover any area ranging from a single grid point to the global domain.

ORCHIDEE does not enforce any particular spatial resolution. The spatial resolution is an implicit user setting that is determined by the resolution of the climate forcing (or the resolution of the atmospheric model in a coupled configuration). ORCHIDEE can run on any temporal resolution. This apparent flexibility is somewhat restricted as processes are formalized at given time steps: half-hourly (e.g., photosynthesis and energy budget), daily (i.e., net primary production), and annual (i.e. vegetation demographic processes). Hence, With the current model architecture meaningful simulations should have a temporal resolution of one minute to one hour for the calculation of energy balance, water balance, and photosynthesis.

ORCHIDEE is a vegetation distribution model that utilizes meta-classes to describe different types of vegetation. The model includes 13 meta-classes by default, including one class for bare soil, eight classes for various combinations of leaf-type and climate zones of forests, two classes for grasslands, and two classes for croplands.

Each meta-class can be further subdivided into an unlimited number of plant functional types (PFTs). The current default setting of ORCHIDEE distinguishes 15 PFTs. ~~Within a single meta-class, various PFTs can be defined based on specific parameters, such as species-specific parameters and age classes. As a simple example, different types of broadleaf temperate forest PFTs, such as beech and oak species, could be simulated using different photosynthetic rates or phenology threshold values~~ where the C3 grasslands have now a separate PFT in the boreal, temperate and tropical zone.

At the beginning of a simulation, each forest PFT in ORCHIDEE contains a monospecific forest stand that is defined by a user-defined but fixed number of diameter classes (three by default). Throughout the simulation, the boundaries of the diameter classes are adjusted to accommodate changes in the stand structure, while the number of classes remains constant. Flexible class boundaries provide a computationally efficient approach to simulate different forest structures. For instance, an even-aged forest is simulated by using a small diameter range between the smallest and largest trees, resulting in all trees belonging to the same stratum. Conversely, an uneven-aged forest is simulated by applying a wide range between diameter classes, such that different classes represent different strata.

The model uses allometric relationships to link tree height and crown diameter to ~~tree stem~~ diameter. Individual tree canopies are not explicitly ~~represented~~ represented, instead a canopy structure model based on simple geometric forms ~~developed by~~ (Haverd et al. (2012) has been included in ORCHIDEE (Naudts et al., 2015). Diameter classes represent trees with different mean diameter and height, which informs the user about the social position of trees within the canopy. Intra-stand competition is based on the basal area of individual trees, which accounts for the fact that trees with a higher basal area occupy dominant positions in the canopy and are therefore more likely to intercept light and thus contribute more to stand-level photosynthesis and biomass growth compared to suppressed trees (Deleuze et al., 2004). If recruitment occurs, diameter classes evolve into cohorts. However, in the absence of recruitment, all diameter classes contain trees of the same age.

~~The allocation scheme is based on the pipe model theory (Shinozaki et al., 1964) and its implementation by Sitch et al. (2003); Zachle and Friend (2010); Zachle and Dalmonech (2011). According to this scheme, carbon is allocated to different biomass pools (leaves, fine roots, and sapwood) while respecting differences in basal area and tree height between diameter classes as well as longevity and hydraulic conductivity between biomass pools of the same diameter class (Naudts et al., 2015).~~

Individual tree mortality from self-thinning, wind storms, and forest management is explicitly simulated. Other sources of mortality are implicitly accounted for through a so-called constant background mortality rate. Furthermore, age classes (four by default) can be used after land cover change, forest management, and disturbance events to explicitly simulate the regrowth of the forest. Following a land cover change, biomass and soil carbon pools (but not soil water columns) are either merged or split to represent the various outcomes of a land cover change. The ability of ORCHIDEE to ~~simulate~~ simulate dynamic canopy structures (Naudts et al., 2015; Ryder et al., 2016; Chen et al., 2016), a feature essential to simulate both the biogeochemical and biophysical effects of natural and anthropogenic disturbances, is exploited in other parts of the model, i.e., precipitation interception,

transpiration, energy budget calculations, the radiation scheme, and the calculation of the absorbed light for photosynthesis.

Since revision 7791, mortality from bark beetle outbreaks is now explicitly accounted for and thus conceptually excluded from the so-called environmental background mortality. Subsequently, changes in canopy structure resulting from growth, forest management, land cover changes, wind storms, and bark beetle outbreaks are accounted for in the calculations of the carbon, water, and energy exchanges between the land surface.

ORCHIDEE's functionality that is not of direct relevance for this study, e.g., energy budget calculations, soil hydrology, snow phenology, albedo, roughness, photosynthesis, respiration, phenology, carbon and nitrogen allocation, land cover changes, product use, and the nitrogen cycle are detailed in (Krinner et al., 2005; Zaehle and Friend, 2010; Naudts et al., 2015; Vuichard et al., 2019).

## 2.2. ~~Bark beetle outbreaks in ORCHIDEE~~

### 2.3. ~~Origin of the bark beetle module: the LANDCLIM legacy~~

Although mortality from windthrow (Chen Yi-Ying et al., 2018) and forest management (Naudts et al., 2015; Luyssaert et al., 2018) were already accounted for in ORCHIDEE prior to r7791, insect outbreaks and their interaction with other disturbances were not. The LandClim model (Schumacher et al., 2004) approach and more specifically the bark beetle module developed by Temperli et al. (2013) ~~were adjusted~~ has been used as basis to develop the bark beetle module in ORCHIDEE r7791.

LandClim is a spatially explicit stochastic landscape model in which forest dynamics are simulated at a yearly time step for 10–100 km<sup>2</sup> landscapes consisting of 25 m × 25 m patches. Within a patch recruitment, growth, mortality and competition among age cohorts of different tree species are simulated with a gap model (Bugmann, 2001; 1996) in response to monthly mean temperature, climatic drought, and light availability. LandClim, for which a detailed description can be found in Schumacher (Schumacher, 2004; Temperli et al., 2004; 2013), includes the functionality to simulate the decadal dynamics and consequences of bark beetle outbreaks at the landscape-scale (Temperli et al., 2013). In the LandClim approach, the extent, occurrence and severity of beetle-induced tree mortality are driven by the landscape susceptibility, beetle pressure, and infested tree biomass. While the LandClim beetle module was designed and structured to be generally applicable for northern hemisphere climate-sensitive bark beetle-host systems, it was originally parameterized to represent disturbances by the European spruce bark beetle (*Ips typographus* Linnaeus) in Norway spruce (*Picea abies* Karst.; Temperli et al. 2013).

As ~~ORCHIDEE and LandClim~~ LandClim and ORCHIDEE are developed for different purposes, their temporal and spatial scales differ. These differences in model resolution ~~justified adjusting the original~~ justify developing a new model while still following the principles embedded in the LandClim approach. LandClim assesses bark beetle damage at 25 m x 25 m patches and to do so it uses information from other nearby patches as well as landscape characteristics such as slope, aspect and altitude. The susceptibility of a landscape to bark beetle infestations is

calculated using multiple factors such as drought-induced tree resistance, age of the oldest spruce cohort, proportion of spruce in the patch's basal area, and ~~windthrow-damaged spruce biomass~~ spruce biomass damaged by windthrow. These factors, presented as ~~a sigmoidal relationship, range~~ sigmoidal relationships, ranging from 0 to 1, ~~indicating no~~ (denoting none to maximum susceptibility respectively. ~~The~~) are combined in a susceptibility index for each Norway spruce cohort in a patch. ~~is then calculated and used to estimate the biomass of trees killed by bark beetles.~~ Bark beetle pressure is quantified as the potential number of beetles that can infest a patch, ~~calculated considering factors like~~ and its calculation considers, among others, previous beetle activity, maximum possible spruce biomass that beetles could kill, and ~~a temperature-dependent bark beetle phenology model. This allows the determination of the total infested tree biomass, accounting for stochastic processes with a beta distribution.~~ Finally, ~~the~~ the susceptibility index and beetle pressure are used to estimate the total infested tree biomass and total biomass killed by bark beetles ~~is estimated~~ for each cohort within a patch. ~~The main equations used in this approach, as well as required modifications to account for differences between the LandClim and ORCHIDEE models, are summarized in Table S1.~~

In ORCHIDEE, however, the simulation unit is about six orders of magnitude larger, i.e., 25 km x 25 km. Hence, a single pixel in ORCHIDEE exceeds the size of an entire landscape in LandClim. Where landscape characteristics in LandClim can be represented by a statistical distribution, the same characteristics in ORCHIDEE are summarized in a single value. These differences between LandClim and ORCHIDEE imply that the original bark beetle module cannot be implemented in ORCHIDEE without adjustments. ~~We develop a pixel-level model that does not require spatial information and statistical distributions of landscape characteristics. The main equations used in this approach, as well as required modifications to account for differences between the LandClim and ORCHIDEE models, are summarized in Table S1.~~

#### 2.4. Bark beetle outbreak development stages

Bark beetle outbreak development stages are useful to understand the dynamics of an outbreak (Fig. 1) and have been described in numerous studies (Wermelinger, 2004; Edburg et al., 2012; Hlásny et al., 2021a). Nonetheless, in ORCHIDEE r7791, we design a model framework which simulates the dynamic of bark beetle outbreak as a continuous process. Hence, endemic, epidemic, build-up and post-epidemic stages are not explicitly simulated and these stages were only introduced to structure the model description. If needed, these stages could be distinguished while post-processing the simulation results if (arbitrary) thresholds are set for specific variables such as  $i_{\text{beetles pressure}}$ ,  $i_{\text{beetles mass attack}}$ , or  $B_{\text{beetles kill}}$  (these variables are defined further below).

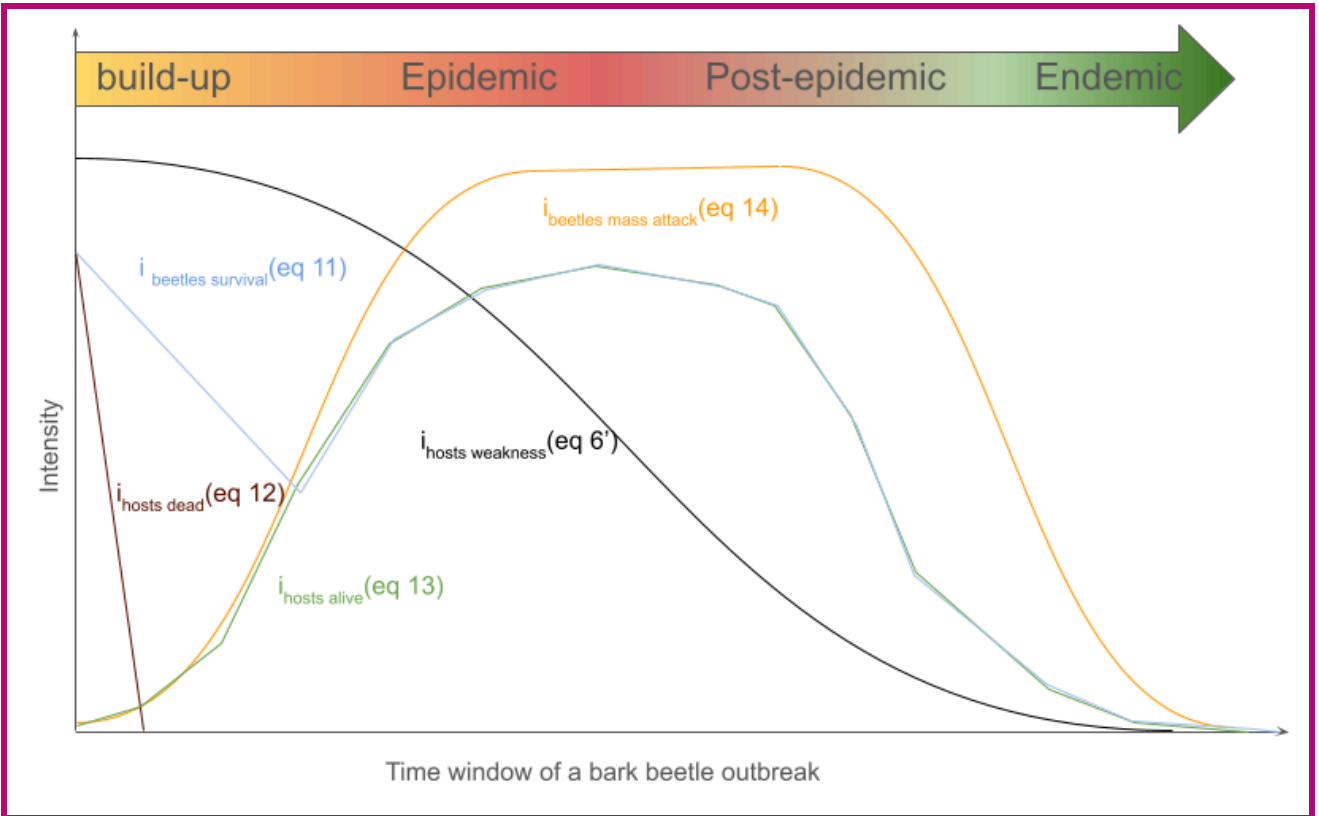


Figure 1 : This figure illustrates the dynamic interplay of factors during a bark beetle outbreak. It depicts the intensity and timeline of key variables such as beetle survival, host tree mortality, and host weakness. The time window spans four phases: build-up, epidemic, post-epidemic, and endemic. The curves represent key variables, showing the escalation of beetle attacks and subsequent decline in host population, which eventually leads to a stabilization of the system in the endemic phase.

## 2.5. Bark beetle damage in ORCHIDEE

Table 1: List of symbols

| Symbol | Description | Units |
|--------|-------------|-------|
|--------|-------------|-------|



|                                      |   |                      |
|--------------------------------------|---|----------------------|
| $\alpha$                             | Alpha parameter from the self thinning relationship               | unitless             |
| $\beta$                              | Beta parameter from the self thinning relationship                | unitless             |
| $act_{limit}$                        | $B_{kill}/B_{total}$ at which $i_{beetles\ activity} = 0.5$       | $gC.m^{-2}$          |
| $B_{beetles\ kill}$                  | Biomass of spruce killed by bark beetle annually                  | $gC.m^{-2}$          |
| $B_{windthrow\ kill}$                | Biomass of spruce killed by windthrow event                       | $gC.m^{-2}$          |
| $B_{beetles\ attacked}$              | Biomass of spruce attacked by bark beetle annually                | $gC.m^{-2}$          |
| $B_{total}$                          | Total living spruce stand biomass                                 | $gC.m^{-2}$          |
| $B_{wood}$                           | Spruce woody biomass  | $gC.m^{-2}$          |
| $BP_{limit}$                         | $i_{beetle\ pressure}$ at which $i_{beetles\ mass\ attack} = 0.5$ | unitless             |
| $D_{max}$                            | Maximum Tree stand density  | $tree.ha^{-1}$       |
| $D_{age\ class}$                     | Spruce age classes stand density                                  | $tree.ha^{-1}$       |
| $DD_{eff}$                           | Cumulative effective Degrees Day                                  | $^{\circ}C.Day^{-1}$ |
| $DD_{ref}$                           | Reference Degrees Day to fulfill one beetle generation            | $^{\circ}C.Day^{-1}$ |
| $Dia_{quadratic}$                    | Mean quadratic diameter   | meters               |
| $DR_{beetles}$                       | $B_{beetles\ kill}/B_{total} * 100$                               | %                    |
| $DR_{windthrow}$                     | $B_{windthrow\ kill}/B_{total} * 100$                             | %                    |
| $F_{spruce}$                         | Spruce stand area fraction  | unitless             |
| $F_{age\ class}$                     | Spruce age classes area fraction                                  | unitless             |
| $F_{non-spruce}$                     | Non-spruce area fraction  | unitless             |
| $G_{limit}$                          | Beetles generation number at which $i_{beetle\ generation} = 0.5$ | Generation           |
| $i_{hosts\_competition}$             | Spruce trees under competition pressure                           | unitless             |
| $i_{hosts\_weakness}$                | Weak to bark beetle attack spruce trees                           | unitless             |
| $i_{hosts\_attractivity}$            | Spruce attractiveness for bark beetles                            | unitless             |
| $i_{hosts\_dead}$                    | defenseless spruce trees uprooted or cutted                       | unitless             |
| $i_{hosts\_alive}$                   | Potential living spruce hosts for bark beetle                     | unitless             |
| $i_{hosts\_defence}$                 | Spruce trees capacity to resist to a bark beetle attack           | unitless             |
| $i_{hosts\_share}$                   | Spruces hidden by other species to bark beetle detection          | unitless             |
| $i_{hosts\_competition, age\_class}$ | Weak to bark beetle attack spruce trees                           | unitless             |
| $i_{hosts\_defence, age\_class}$     | Spruce trees capacity to resist to a bark beetle attack           | unitless             |
| $i_{hosts\_health, age\_class}$      | Spruce trees health condition                                     | unitless             |
| $i_{beetles\_pressure}$              | Proxy of bark beetle population level                             | unitless             |
| $i_{beetles\_survival}$              | Bark beetle winter survival index                                 | unitless             |
| $i_{beetles\_generation}$            | Bark beetle generation index                                      | unitless             |
| $i_{beetles\_activity}$              | Previous bark beetles activity index                              | unitless             |
| $i_{beetles\_mass\_attack}$          | Bark beetles mass attack capability                               | unitless             |
| $max_{N_{wood}}$                     | Value of $N_{wood}$ at which $i_{hosts\ dead} = 1.0$              | unitless             |
| $N_{wood}$                           | Spruce wood necromass   | $gC.m^{-2}$          |

|                                 |   |          |
|---------------------------------|---|----------|
| $P_{\text{success, age class}}$ | Probability of successful attack  | unitless |
| $P_{\text{attack}}$             | Probability of beetles attack   | unitless |
| $PWS_{\text{max}}$              | Maximum long term Spruce water stress                                   | unitless |
| $PWS_{\text{spruce}}$           | Spruce water stress   | unitless |
| $PWS_{\text{age class}}$        | Spruce age classes water stress   | unitless |
| $PWS_{\text{limit}}$            | Spruce water stress at which $i_{\text{hosts defense}} = 0.5$           | unitless |
| $RDi_{\text{limit}}$            | Relative density index at which $i_{\text{hosts competition}} = 0.5$    | unitless |
| $RDi_{\text{weakness}}$         | Relative density index at which $i_{\text{host weakness}} = 0.5$        | unitless |
| $RDi_{\text{spruce}}$           | Spruce stand relative density index [0,1]                               | unitless |
| $RDi_{\text{age class}}$        | Spruce age classes relative density index [0,1]                         | unitless |
| $S_{\text{competition}}$        | Shape parameter in the calculation of $i_{\text{hosts competition}}$    | unitless |
| $S_{\text{weakness}}$           | Shape parameter in the calculation of $i_{\text{hosts weakness}}$       | unitless |
| $S_{\text{drought}}$            | Shape parameter in the calculation of $i_{\text{hosts defense}}$        | unitless |
| $S_{\text{share}}$              | Shape parameter in the calculation of $i_{\text{hosts share}}$          | unitless |
| $S_{\text{activity}}$           | Shape parameter in the calculation of $i_{\text{beetle activity, y-1}}$ | unitless |
| $S_{\text{generation}}$         | Shape parameter in the calculation of $i_{\text{beetle generation}}$    | unitless |
| $Sh_{\text{spruce}}$            | Share fraction of Spruce  | unitless |
| $Sh_{\text{limit}}$             | Share fraction at which $i_{\text{hosts share}} = 0.5$                  | unitless |
| $T_{\text{air}}$                | Air Temperature   | °C       |

~~Hence, the original bark beetle module was modified to obtain a pixel-level model that does not account for the spatial information and statistical distribution of landscape characteristics.¶~~

~~In the following we will detail the development of the bark beetle outbreak module into ORCHIDEE by following the forest stand stages and bark beetle outbreak stages introduced in Fig. 1. For clarity, we explain the mechanisms of infestation (section 2.2.2) and mortality (section 2.2.3) separately.¶~~

~~¶~~

### ~~2.5.1. Mechanisms of infestation¶~~

~~As in LandCLIM (see table S1), the ORCHIDEE model represents the density of the bark beetle population indirectly through the beetle pressure index (BPI):~~

~~The biomass of trees killed by bark beetles in one year and one pixel ( $B_{\text{beetles kill}}$ ) is calculated as the product of the biomass of trees attacked by bark beetle ( $B_{\text{beetles attacked}}$ ) and the probability of a successful attacks ( $P_{\text{success, age class}}$ ) averaged over the number of age classes and weighted by their actual fraction ( $F_{\text{age class}}$ ) for a given tree species ( $F_{\text{spruce}}$ ). The approach assumes that a successful beetle colonization always results in the death of the attacked tree which is a simplification from reality (A. Leufvén et al. 1986).~~

$$BPI = C_{bp} \cdot S_i \cdot \frac{(G + Act_{y-1})}{2} B_{\text{beetles kill}} = \sum_{\text{nb age classes}}^{age\ class=1} P_{\text{success, age class}} \times B_{\text{beetles attacked}} \times \frac{F_{\text{age class}}}{F_{\text{spruce}}} \quad (1)$$

During the endemic stage,  $B_{\text{beetles attacked}}$  and  $B_{\text{beetles kill}}$  are at their lowest values and the damage from bark beetles has little impact on the structure and function of the forest. Losses from  $B_{\text{beetles kill}}$  can be considered background mortality.

The biomass of trees attacked by bark beetles ( $B_{\text{beetles attacked}}$ ) is defined as an attempt from the bark beetles to overcome the tree defenses and thus succeeding in boring holes in the bark in order to reach the sapwood.  $B_{\text{beetles attacked}}$  is calculated at the pixel level by multiplying the actual stand biomass of spruce ( $B_{\text{total}}$ ) and the probability that bark beetles attack spruce trees in the pixel ( $P_{\text{attacked}}$ ).

$$B_{\text{beetles attacked}} = B_{\text{total}} \times P_{\text{attacked}} \quad (2)$$

$P_{\text{attacked}}$  represent the ability of the bark beetles to spread and to locate new suitable spruce trees as hosts for breeding.  $P_{\text{attacked}}$  is calculated by the product of two indexes (all indexes in this study are denoted  $i$  and are analogue the susceptibility indexes from Temperli et al. 2013): (1) the beetle pressure index ( $i_{\text{beetles pressure}}$ ) which a proxy of the bark beetle population and (2) the stand attractiveness index ( $i_{\text{hosts attractiveness}}$ ) which is a proxy of the overall stand health. Health was here defined as the ability of the forest to resist an external stressor such as bark beetle attacks.

$$P_{\text{attacked}} = i_{\text{hosts attractiveness}} \times i_{\text{beetles pressure}} \quad (3)$$

## 2.6. Stand attractiveness

The stand attractiveness index ( $i_{\text{hosts attractiveness}}$ ) varies between 0.5 and 1. When  $i_{\text{hosts attractiveness}}$  tends to 0.5, the stand is constituted mainly by healthy trees which are less attractive for beetles whereas an  $i_{\text{hosts attractiveness}}$  approaching 1 represents a highly stressed forest suitable for colonization by bark beetles. Factors that contribute to the stress of a forest in ORCHIDEE are: nitrogen limitation, limited carbohydrate reserves, and monospecific spruce forest. Trees experiencing extended periods of environmental stress are expected to have less carbon and nitrogen reserves available for defense compounds, making them vulnerable for bark beetle attacks even at relatively low beetle population densities (Raffa et al., 2008). Nonetheless, reserves pools in ORCHIDEE r7791 have not yet been evaluated so, instead proxies were used such as long term drought ( $PWS_{\text{max}}$ ) and relative density index (RD<sub>i</sub>) which were already simulated in ORCHIDEE r7791.

$$i_{\text{hosts attractiveness}} = \max(i_{\text{hosts competition}}, i_{\text{hosts defense}}) \times i_{\text{hosts share}} \quad (4)$$

Where  $i_{\text{hosts competition}}$  and  $i_{\text{hosts defense}}$  both represent proxies for the reduction of the nitrogen and carbohydrate reserve due to strong competition for light and soil resources, and repetitive years that are drier than average. For this study, the average drought intensity during the last three years is considered, as a proxy of spruce stand healthiness:

$$i_{hosts\ defense} = 1 / (1 + e^{S_{drought} \cdot (1 - PWS_{max} - PWS_{limit})}) \quad (45a)$$

The BPI is driven by the number of beetle generations (G) that could occur in the current year, the bark beetle damage from the previous year ( $Act_{y-1}$ ), and the stand's susceptibility to infestation by bark beetles ( $S_i$ ), which are calculated as an index ranging from 0 to 1:

Where,

$$G = 1 / (1 + e^{-r \cdot (rDD - m)}) \cdot PWS_{max} = \sum_{nb\ age\ class}^{age\ class=1} \max(PWS_{spruce}, \dots, PWS_{spruce, n-3}) \quad (2)$$

Where r and m are parameters of the logistic function formalizing the relationship with the number of generations (rDD). rDD is calculated as:

$$rDD = \frac{sumTeff}{k} \times \frac{F_{age\ class}}{F_{spruce}} \quad (5b)$$

Where  $PWS_{max}$  is the maximum plant water stress index during the last 3 years,  $PWS_{limit}$  is the plant water stress below which the healthiness of the stand will strongly be affected. In addition to drought, overstocked forest may also decrease the overall healthiness of a spruce stand ( $i_{hosts\ competition}$ ).

$$i_{hosts\ competition} = 1 / (1 + e^{S_{competition} \cdot (RDi_{spruce} - RDi_{limit})}) \quad (6a)$$

In ORCHIDEE, the relative density index (RDi) is used to quantify the competition between trees at the stand level. At an RDi of 1, the forest is expected to be at its maximum density given the carrying capacity of the site, implying the highest level of competition between trees.  $RDi_{limit}$  represents the limit at which the bark beetle outbreak starts to decline because of lack of suitable host trees. At the spatial scale of the ORCHIDEE model,  $RDi_{limit}$  could be considered as a parameter for spatial upscaling since it describes how many trees survive after an outbreak which is very dependent on the size of the pixel. When a pixel represents a single stand (~1 ha) all trees may be killed during an outbreak so  $RDi_{limit}$  will be setup close to 0. When an ORCHIDEE pixel is used to represent an area of 2500 km<sup>2</sup>, not all trees will be killed which is reflected in setting  $RDi_{limit} = 0.4$ .

$RDi_{spruce}$  is computed as follows:

$$RDi_{\text{spruce}} = \sum_{\text{nb age class}}^{\text{age class}=1} \frac{D_{\text{age class}}}{D_{\text{max}}} \times \frac{F_{\text{age class}}}{F_{\text{spruce}}} \quad (6b)$$

Where  $D_{\text{age class}}$  is the current tree density of an age class and  $F_{\text{age class}}$  is the fraction of spruce in the pixel that resides in this age class.  $D_{\text{max}}$  represents the maximum stand density of a stand given its diameter. In ORCHIDEE  $D_{\text{max}}$  is calculated based on the mean quadratic diameter (cm) of the age class and two species specific parameters,  $\alpha$  and  $\beta$ :

$$D_{\text{max}} = (Dia_{\text{quadratic, age class}} / \alpha)^{(1/\beta)} \quad (6c)$$

The index  $i_{\text{hosts share}}$  (used in eq. 4) takes into account that in a mixed tree species landscape, even a few non-host trees may chemically hinder bark beetles in finding their host trees (Zhang and Schlyter, 2004) explaining why insect pests, including *Ips typographus* outbreaks, often cause more damage in pure compared to mixed stands (Nardi et al., 2023). ORCHIDEE r7791 does not simulate multi-species stands but does account for landscape-level heterogeneity of forests with different plant functional types. The bark beetle module in ORCHIDEE assumes that within a pixel, the fraction of spruce over other tree species is a proxy for the degree of mixture:

$$i_{\text{hosts share}} = 1 / (1 + e^{S_{\text{share}} \cdot (sh_{\text{spruce}} - sh_{\text{limit}})}) \quad (7a)$$

Where,

$$Sh_{\text{spruce}} = F_{\text{none-spruce}} / F_{\text{spruce}} \quad (7b)$$

## 2.7. Implicit representation of bark beetle populations

The bark beetle pressure Index ( $i_{\text{beetles pressure}}$ ) is formulated based on two components: (1) the bark beetle breeding index of the current year ( $i_{\text{beetles generation}}$ ), and (2) an index of the loss of tree biomass in the previous year due to bark beetle infestation ( $i_{\text{beetles activity}}$ ).  $i_{\text{beetles activity}}$  is thus a proxy of the previous year's bark beetle activity. The expression accounts for the legacy effect of bark beetle activities by averaging activities over the current and previous years. In this approach, the susceptibility index ( $i_{\text{beetles survival}}$ ) serves as an indicator for increased bark beetle survival which could result from favorable conditions for beetle demography (see next section).

$$i_{\text{beetles pressure}} = i_{\text{beetles survival}} \times \frac{(i_{\text{beetles generation}} + i_{\text{beetles activity}})}{2} \quad (8)$$

The model calculates  $i_{\text{beetles generation}}$  from a logistic function, which depends on the number of generations a bark beetle population can sustain within a single year:

$$i_{\text{beetles generation}} = 1 / (1 + e^{-S_{\text{generation}} \cdot (\frac{DD_{\text{eff}}}{DD_{\text{ref}}} - G_{\text{limit}})}) \quad (39)$$

Where  $\text{sumTeff}$

Where  $S_{\text{generation}}$  and  $G_{\text{limit}}$  are tuning parameters for the logistic function,  $DD_{\text{eff}}$  represents the sum of effective temperatures for bark beetle reproduction in  $^{\circ}\text{C} \cdot \text{day}^{-1}$ , while  $DD_{\text{ref}}$  denotes the thermal sum of degree days for one bark beetle generation in  $^{\circ}\text{C} \cdot \text{day}^{-1}$ .  $DD$  can reach up to three or in exceptional cases even four generations, but the index  $G$  reaches its maximum value of one when 2.5 or more generations occur in a single growing season. The  $\text{sumTeff}$  is incremented. Saturation of  $i_{\text{beetles generation}}$  represents the lack of available breeding substrate when many generations develop over a short period.

$DD_{\text{eff}}$  is calculated from January 1<sup>st</sup> until the diapause of the first generation. In ORCHIDEE, diapause is triggered when daylength exceeds 14.5 hours (e.g., April 27<sup>th</sup> for France). Each day before the diapause with a daily average temperature above 8°C is accounted for in  $\text{sumTeff}$ . This approach simulates the phenology of bark beetles, which tend to breed earlier when winter and spring are warmer, thus allowing for multiple generations in the same year (Hlásny et al., 2021).

The BPI is also driven by the bark beetle damage index from the previous year ( $\text{Act}_{y-1}$ ) (2021a). More details on the phenology model are available in Temperli et al. 2013.

The bark beetle activity of the previous year ( $i_{\text{beetles activity}}$ ) is calculated as:

$$\text{Act}_{y-1} = \frac{Bdb_{y-1}}{Bt \cdot Cst} i_{\text{beetles activity}} = 1 / (1 + e^{-S_{\text{activity}} (\frac{B_{\text{kill}, y-1}}{B_{\text{total}}} - \text{act}_{\text{limit}})}) \quad (4) \quad (10)$$

Where  $Bdb_{y-1}$  denotes the bark beetle damage from biomass of the stand damaged by bark beetles in the previous year,  $Bt_{\text{total}}$  is the total biomass of the stand, and  $Cst$  is a temporal scaling factor that has to be adjusted depending on the temporal resolution of the bark beetle outbreak module.

The stand's susceptibility to infestation by bark beetles ( $S_i$ ) is the third driver of BPI.  $S_{\text{activity}}$  and  $\text{act}_{\text{limit}}$  are parameters that drive the intensity of this negative feedback.

During the build-up stage (Fig. 1) the population of bark beetles can either return to its endemic stage (Fig. 1) if tree defense mechanisms are preventing bark beetles from successfully attacking healthy trees, or evolve into an epidemic stage (Fig. 1) if the tree defense mechanisms fail. During this stage, tree canopies remain green, therefore,

this stage is also known as the green stage (Fig. 1). During the post-epidemic stage, the forest is still subject to higher mortality than usual but signs of recovery appear (Hlásny et al., 2021a). Recovery may help the forest ecosystem to return to its original state or switch to a new state (different species, change in the forest structure) depending on the intensity and the frequency of the disturbance (Van Meerbeek et al., 2021).

## 2.8. Bark beetle survival

The capacity of the bark beetles to survive the winter in between two breeding seasons is a crucial mechanism explaining massive tree mortality due to an outbreak. During regular winters, winter mortality for bark beetles is around 40% for the adults and 100% for the juveniles (Jönsson et al. 2012). In our scheme, this mortality rate is implicitly accounted for in the calculation of the bark beetle survival index ( $i_{\text{beetles survival}}$ ). A lack of data linking bark beetle survival to anomalous winter temperatures prevented us from including this information as a modulator of  $i_{\text{beetles survival}}$ . Instead the model simulates the excess of survival due to the abundance of suitable tree hosts which decreases the competition for shelter and food:

$$Si = Siw \cdot Ww + Sir \cdot Wr + Sid \cdot Wd + Sis \cdot Ws \quad i_{\text{beetles survival}} = \max(i_{\text{hosts dead}}, i_{\text{hosts alive}})$$

(5)

¶

Where,  $Siw$ ,  $Sir$ ,  $Sid$ , and  $Sis$  denote the susceptibilities of bark beetles to various environmental factors: breeding substrate ( $Siw$ ), availability of trees weakened due to water stress ( $Sir$ ), availability of trees weakened due to inter-tree competition ( $Sid$ ), and prevalence of monospecific stands ( $Sis$ ). Similarly,  $Ww$ ,  $Wr$ ,  $Wd$ , and  $Ws$  represent the weights associated with these susceptibilities. In ORCHIDEE  $Ws$  and  $Wd$  are fixed at 0.1. The absolute values for the remaining weights,  $Wr$  and  $Ww$ , change depending on the stage of the bark beetle outbreak.¶

The transition in the outbreak stage from endemic to epidemic is determined by a risk index, which is computed as  $RI = SI * BPI$ . If the risk index surpasses the threshold of 0.1 (a value deemed high enough to confidently classify it as a critical threshold), the epidemic flag is switched to 1 and the weights  $Wr$  and  $Ww$  are computed as

$$(11)$$

The availability of wood necromass from trees that died recently, particularly following windstorms, plays a critical role in bark beetle survival and proliferation. In the year following a windstorm, uprooted and broken trees may offer an ideal breeding substrate for bark beetles, facilitating their population growth.

In Temperli et al. (2013) an empirical correlation between windthrow events and bark beetle susceptibility was established. ORCHIDEE enhances realism by considering the actual suitable hosts (living or recently dead trees) as the primary driver of bark beetle survival. To avoid overestimating bark beetle population growth,  $\max_{N_{\text{wood}}}$  has been introduced. This ensures that an excess of breeding substrate does not artificially inflate beetle numbers, acknowledging that recent dead trees lose their freshness and thus suitability for breeding after a year. Any addition of dead trees beyond  $\max_{N_{\text{wood}}}$  is considered ineffective in affecting the bark beetle population.

This relationship is quantitatively represented in ORCHIDEE through the dead host index,  $i_{\text{hosts dead}}$ , which is driven by the availability of recent dead trees. The formulation of  $i_{\text{hosts dead}}$  is as follows:

$$W_r = \frac{1}{(1 + e^{(r1 \cdot (Si \cdot BPI - r2))})^{-1}} \cdot (1 - W_s - W_d) i_{\text{hosts dead}} = \min\left(\frac{N_{\text{wood}}}{B_{\text{wood}} / \max_{N_{\text{wood}}}, 1}\right) \quad (6)$$

$$(12)$$

Here,  $N_{\text{wood}}$  represents the quantity of woody necromass from the current year,  $B_{\text{wood}}$  is the

$$W_w = 1 - (W_r + W_s + W_d) \quad (7)$$

On the other hand, if the bark beetle outbreak stage is endemic,  $W_r$  and  $W_w$  are computed as:

$$W_r = 1 - (W_d + W_s), W_w = 0 \quad (8)$$

By changing the susceptibility weights between the two stages, ORCHIDEE simulates hysteresis of the drivers that lead to an epidemic and the drivers that allow the forest exit the epidemic stage. Hysteresis in ecology relates to the concept that the path of “recovery” is not the same as the path of “degradation”, often due to complex interactions and feedback loops within the ecosystem (e.g. Staal et al., 2020).

The trigger that increases a forest stand's susceptibility to bark beetle infestation is the volume of trees that have recently died. The primary natural source of this woody biomass pool is windstorms. Up until about one year following a windstorm, uprooted and broken stems can be colonized by bark beetles, providing a suitable substrate for breeding and population increase (Nageleisen and Grégoire, 2022). ORCHIDEE formalizes this dependency by using a breeding substrate susceptibility index ( $Siw$ ):

$$\text{If } Siw < 1, Siw = \frac{Litw}{B_w} / Litt; \text{ Else, } Siw = 1 \quad (9)$$

where  $Litw$ ,  $B_w$ , and  $Litt$  indicate the quantity of breeding substrate for bark beetles, total woody biomass of in the stand, and  $\max_{N_{\text{wood}}}$  is the threshold at which of the ratio  $Litw/B_w$  is considered maximum, respectively. A windthrow event causes a sudden increase, or pulse, in the breeding substrate in ORCHIDEE, which is employed in computation of the breeding substrate susceptibility index. This  $N_{\text{wood}}/B_{\text{wood}}$  signifying the maximum level. This index captures the immediate increase in dead trees post-windthrow, which may drive bark beetle breeding. However, after a year, this substrate becomes unsuitable for beetle breeding after one year, according to Nageleisen and Grégoire (2022), and is henceforth excluded from the calculation of the breeding substrate susceptibility. This susceptibility index ranges from 0 (indicating no fresh woody biomass available in the litter) to 1 (equivalent to 30% or more of the litter being fresh woody biomass).



In the original formulation of Temperli et al. (2013) the relationship between windthrow and susceptibility was empirical (correlative relationship). In our version, we try to add more realism by introducing the breeding substrate which is a consequence of windthrow and is the real driver of windthrow susceptibility. The threshold (Litt) value of 0.3 was introduced to prevent excess breeding substrate from artificially boosting the bark beetle population, as fresh woody litter does not remain fresh for more than one year. The implication is that more than 30% of new woody litter in one year cannot be exploited by a bark beetle population. In other words, adding more fresh woody litter is thought to have no further impact on the bark beetle population (Hervé Jactel personal communication). As a result, regions or younger forests with a smaller wood volume tend to have a lower threshold than mature forests. However, the susceptibility index (SI) of younger and less dense forests is also limited by susceptibility to interspecific competition. ¶

ORCHIDEE determines the susceptibility of forests to infestation using three additional susceptibility indices: ¶

¶

- Susceptibility of weakened trees (Sid). Trees defend themselves against beetle attacks by producing secondary metabolites (Huang et al., 2020). The high carbon and nitrogen costs of these compounds limit their production to periods with environmental conditions favorable for growth (Lieutier, 2002). Trees experiencing extended periods of environmental stress are expected to have less carbon and nitrogen reserves available for defensive substance production, making them more vulnerable to successful bark beetle attacks even at relatively low beetle population densities (Raffa et al., 2008). For this study, the average drought intensity during the last three years is considered, as a proxy of tree health. ¶

¶

$i_{hosts\ dead}$  calculation.

Finally,  $max_{N_{wood}}$  can also be considered as a parameter that depends on the spatial scale of the simulation. The mortality rate of trees ( $DR_{windthrow}$ ) that will trigger an outbreak is very different across spatial scales. Where a relatively high share of dead wood is needed to trigger an outbreak at the patch-scale, a much lower share of dead wood suffices at the landscape-scale to trigger a widespread bark beetle outbreak. So these parameters must be set up according to the spatial resolution of the simulation experiment.

$i_{hosts\ alive}$  denotes the survival of bark beetles which is facilitated by the abundance of suitable trees which reduces the competition among bark beetles for breeding substrates and therefore increases their survival.

$$Sid = \sum_{nac}^{ac=1} (1 + e^{d1 \cdot ((1 - M_{ac}^{max}) - d2)})^{-1} \cdot \frac{Frac_{ac}}{nac}$$

$$i_{hosts\ alive} = i_{beetles\ mass\ attack} \times i_{hosts\ weakness} \quad (10) \quad ¶$$

With, (13)

The amount of suitable tree hosts.  $i_{\text{hosts weakness}}$  is driven by two factors: (1) the abundance of weak trees which can be more easily infected by bark beetles. ORCHIDEE does not explicitly represent weak trees, but tree health is thought to decrease with an increasing density given the stand diameter. The index for host suitability is thus calculated by making use of the relative density index ( $RDI_{\text{spruce}}$ ).

$$i_{\text{hosts weakness}} = \frac{MO_{ac}}{\max(MO_1, \dots, MO_{n-3})} = 1 / (1 + e^{S_{\text{weakness}} \cdot (RDI_{\text{spruce}} - RDI_{\text{weakness}})}) \quad (11)$$

¶

~~Susceptibility due to between-tree competition (Sir). Interspecific competition among trees for limited resources leads to decreased photosynthesis and thus less carbohydrate reserves, resulting in lower investments in defense compounds. In ORCHIDEE, the relative density index (RDI) is used to estimate the average competition between trees at the stand level. At an RDI of 1, the forest is expected to be at its maximum density given the carrying capacity of the site, implying the highest level of competition between trees:6a')~~

Equation 6a' is close to equation 6a but the parameter  $S_{\text{weakness}}$  has been reduced by a factor of two in order to reflect that  $i_{\text{hosts weakness}}$  are more sensitive to RDI than  $i_{\text{hosts competition}}$ . (2)  $i_{\text{hosts mass attack}}$  which represent the ability of bark beetles to attack healthy trees when the number of bark beetles is large enough. This index only depends on the size of the bark beetle population ( $i_{\text{beetles pressure}}$  see eq. 8)

$$i_{\text{hosts mass attack}} = \frac{a1 + (1 - a1) / (1 + e^{a2 \cdot (RDI_{\text{sp}} - a3)})}{1 + e^{S_{\text{mass attack}} \cdot (i_{\text{beetles pressure}} - BP_{\text{limit}})}} \quad (12)$$

¶

~~Susceptibility to forest species purity (Sis). Many forest pests cause more damage in pure forests than in mixed stands (Jactel et al., 2021). Ips typographus outbreaks are also more frequent in pure spruce stands (Nardi et al., 2022). Even just a few non-host trees, like deciduous trees, may disrupt the host searching behavior of dispersing beetles due to the emission of non-host volatile compounds (Zhang and Schlyter, 2004). ORCHIDEE r7791 cannot simulate multi-species stands but does account for landscape-level heterogeneity of forests with different plant functional types. The bark beetle module in ORCHIDEE assumes that within a pixel, the fraction of spruce over other tree species of trees is a proxy for the degree of mixture14)~~

Where  $S_{\text{hosts mass attack}}$  and  $BP_{\text{limit}}$  are parameters.  $S_{\text{mass attack}}$  controls the steepness of the relationship while  $BP_{\text{limit}}$  is the bark beetle pressure index at which the population is moving from endemic to epidemic stage where mass attacks are possible.

The epidemic stage corresponds to the capability of bark beetles to mass attack healthy trees and overrule tree defenses (Biedermann et al., 2019). At this point in the outbreak, all trees are potential targets irrespective of their

health. Owing to the widespread mortality of individual trees, the forest dies resulting in a stage also known as the red stage (Fig. S2, stage 3). Three causes may explain the end of an epidemic: (1) the most likely cause is a high interspecific competition among beetles for tree host when the density is decreasing (decreasing  $i_{\text{hosts alive}}$ ) (Pineau et al., 2017; Komonen et al., 2011), (2) a series of very cold years will decrease their ability to reproduce (decreasing  $i_{\text{beetles generation}}$ ), and (3) a rarely demonstrated increasing population of beetle predators (Berryman, 2002). In ORCHIDEE r7791, the first two causes are represented but the last, i.e., the predators are not represented.

## 2.9. Tree mortality from bark beetle infestation

When bark beetles attack a tree, the success of their attack will likely depend on the capacity of the tree to defend itself from the attack. Trees defend themselves against beetle attacks by producing secondary metabolites (Huang et al., 2020). The high carbon and nitrogen costs of these compounds limit their production to periods with environmental conditions favorable for growth (Lieutier, 2002). The probability of a successful bark beetle attack is driven by the size of the bark beetle population ( $i_{\text{beetle pressure}}$ ) and the weakness of each tree. ORCHIDEE, however, is not simulating individual trees but rather diameter classes within an age class. An index of tree weakness for each age class ( $i_{\text{hosts health, age class}}$ ) was calculated as:

$$P_{\text{success, age class}} = i_{\text{hosts health, age class}} \times i_{\text{beetles pressure}} \times \left(1 + e^{-s1 \cdot (sh_{sp} - s2)}\right)^{-1}, \text{ With } Sh_{sp} = \frac{Fae_{others}}{Frac_{sp}} \quad (13)$$

Finally the infested biomass ( $B_{inf}$ ) is calculated as :

$$B_{inf} = Bt \cdot Cst \cdot SI \cdot BPI \quad (14)$$

Note that the susceptibility of forest to infestation ( $SI$ ), and the beetle pressure index ( $BPI$ ) are calculated for the pixel as a whole, despite the existence of multiple age classes.

### Mechanisms of mortality

A tree rarely dies solely from bark beetle damage (except during mass attacks). However, as female beetles often carry blue-stain fungi, which colonizes the phloem and sapwood, blocking the water-conducting vessels of the tree. This results in tree death from carbon starvation or desiccation (Nageleisen and Grégoire, 2022). As ORCHIDEE r7791 does not simulate the effects of changes in sapwood conductivity on photosynthesis and the resultant probability of tree mortality, susceptibility due to weakened trees ( $S_{id}$ ) and susceptibility due to between-tree competition ( $S_{ic}$ ) are used as proxies in calculating the fraction of infected trees that eventually die, i.e., the mortality rate ( $S_{iac}$ ). The index of weakened trees index ( $i_{\text{hosts health, age class}}$ ) makes use of two proxies similarly to equation 5 and 6 but simplified to be calculated only for one age class at the time:

$$S_{iac} = S_{ir} \cdot W_r + S_{id} \cdot (1 - W_r) i_{hosts\ health, age\ class} = \frac{(i_{hosts\ competition, age\ class} + i_{hosts\ defense, age\ class})}{2} \quad (15)$$

Finally, the killed woody biomass ( $B_{db}$ ) is calculated as the product of the actual wood biomass (as a function of the basal area, BA) and the mortality rate.

$$B_{db} = \sum_{nac}^{ac=1} \frac{S_{iac} + BPI}{2} \cdot D_{inf} \cdot \frac{BA_{ac}}{BA_{sp}} i_{hosts\ defense, age\ class} = 1 / (1 + e^{S_{drought} \cdot (1 - PWS_{age\ class} - PWS_{limit})}) \quad (16)$$

Mortality happens on the tree level in ORCHIDEE, and thus the killed biomass must be converted into the number of trees per diameter class. Mortality first affects trees from the largest diameter class (those preferred by bark beetles) before affecting smaller diameter classes until the killed woody biomass ( $B_{db}$ ) has been met. The aboveground and belowground biomass pools (e.g., leaves, sapwood, heartwood) in the trees killed by bark beetles are then transferred directly into the respective litter pools.

### 2.9.1. Difference from the original formulation from LANDCLIM

The main changes between the model implemented in ORCHIDEE and the original model from Temperli et al., 2013 include various modifications to account for the difference in spatial scale, as ORCHIDEE operates at the landscape rather than a patch. This primarily affected the calculation of the susceptibility. The ORCHIDEE version is also based on dynamic biomass values, as the maximum biomass is not fixed and instead depends on factors like soil fertility, climate, and human management.

Further changes were made to account for the different temporal scales in ORCHIDEE and the fact that ORCHIDEE does not distinguish individual species but groups them into plant functional types (PFTs). The model was also adjusted to account for practices like salvage logging and to incorporate different methods of quantifying plant water stress. Finally, the susceptibility of each age class within a pixel was introduced instead of each cohort within a forest patch.

### 2.9.2. Bark beetle development stages

In ORCHIDEE r7791, only two bark beetle development stages are explicitly simulated: endemic and epidemic. Simulated mechanisms of positive and negative feedback on the bark beetle pressure index mimic implicitly two transition stages. Transition stages, referred to as the build-up and post-epidemic stage, were added to the model output as an additional post-processing step in order to facilitate the evaluation and presentation of the simulation results. The thresholds proposed for these transitions affect the figures and subsequent discussion but not the course of the actual simulation as they are only added after the simulations have finished.

¶

### ~~2.9.2.1. The endemic stage (a)~~¶

~~During the endemic stage both the bark beetle population and the number of trees killed are at their lowest values (Fig. 1). At low population densities, beetles can only attack weakened trees or trees that were uprooted or broken within the previous year. In the endemic stage, the susceptibility of a forest mainly depends on the amount of breeding substrate (Litw, see table 2). In ORCHIDEE, during the endemic stage bark beetle damage to the forest stand has little impact on the structure and function of the ecosystem. Losses can be considered as background mortality.~~¶

¶

### ~~2.9.2.2. The build-up stage (b)~~¶

~~During the build-up stage, the beetle population is fuelled by an increased availability of breeding substrate that enables the beetle population to grow beyond its endemic size. The build-up stage is a transitory stage during which the population of bark beetles can either return to its endemic stage or evolve into an epidemic stage. In the build-up stage, tree defense mechanisms are activated preventing bark beetles from successfully attacking healthy trees. Consequently, tree canopies remain green and therefore this stage is also known as the green stage (Fig. 1).~~¶

~~As the build-up stage is not explicitly represented in ORCHIDEE, we cannot precisely tag the start and the end of the stage. Nonetheless it was estimated during post-processing by considering two thresholds:~~¶

- ~~• The threshold at which the BPI is too high to represent an endemic population. Based on the simulation results, a  $BPI > 0.13$  was selected as the post-processing threshold to mark the end of the endemic stage.~~¶
- ~~• The second threshold represents the value of BPI which inevitably results in an epidemic stage. Again, based on the simulation results a  $BPI > 0.3$  will always lead to an epidemic stage.~~¶

¶

~~During the build up stage, the number of beetle generations and the susceptibility of forest to get infested determine the future of the outbreak. Increasing values for these two drivers will increase bark beetle activity ( $Act_{year-1}$ ) which can subsequently result in a positive feedback on the BPI in the following years leading to an epidemic. When the beetle generations index and the susceptibility of the forest to infestation are not favorable, e.g., cold and wet years, the bark beetles will consume all accessible breeding substrate ( $Siw$ ) leading to a decrease in both  $Siw$  and beetle pressure index.~~¶

¶

### ~~2.9.2.3. The epidemic stage (c)~~¶

~~The epidemic stage corresponds to the capability of bark beetles to mass attack healthy trees and overrule tree defenses (Biedermann et al., 2019). At this point in the outbreak, all trees are potential targets irrespective of their health. Owing to the widespread mortality of individual trees, the forest dies resulting in a stage also known as the red stage (Fig. 1, stage 3). In order to simulate mass attacks in ORCHIDEE, the weights of two specific susceptibilities ( $Siw$  and  $Sid$ ) in the calculation of the susceptibility index ( $Si$ ) are different compared to the endemic stage (eq. 6a). In the epidemic stage  $Ww = 0$  because beetles can access all trees whether healthy or not.~~

Consequently, the weight for  $W_r$  is equal to one as it represents the breeding substrate susceptibility accounting for every tree.

Three causes may explain the end of an epidemic: (1) the most likely cause is a high interspecific competition among beetles for breeding substrate when the density of tree hosts is decreasing (decreasing  $S_r$ ) (Pineau et al., 2017; Komonen et al., 2011), (2) extreme climate events such as heat waves, flood, and frost can abruptly decrease the beetle population (decreasing  $S_{id}$ ), and (3) a rarely demonstrated increasing population of beetle predators (Reeve and Turchin, 2002). In ORCHIDEE r7791, the first two causes are represented but the last, i.e., the predators are not represented.

¶

#### 2.9.2.4. The post-epidemic stage (d)

Similar to build-up, the post-epidemic stage is a transitory stage delineated during the post-processing of ORCHIDEE r7791 simulation results. During this stage, the forest is still subject to higher mortality than usual but signs of recovery appear (Hlásny et al., 2021). Recovery may help the forest ecosystem to return to its original state or switch to a new state (different species, change in the forest structure) depending on the intensity and the frequency of the disturbance (Van Meerbeek et al., 2021; Fig. 1).

¶

#### 2.10. Simulation experiments

Eight locations were selected which represent the range of climatic conditions within the distribution area of spruce in Europe (*Picea Abies* Karst L.) as shown in Table 4. Half-hourly weather data from the FLUXNET database (Pastorello et al., 2020) for these locations were used to drive ORCHIDEE. Some of these locations (FON, SOR, HES, COL, WET) are not populated with spruce but all are located within the species distribution. For each location, a pure spruce stand was simulated and the available FLUXNET data was looped to simulate a 100-year period. The study did not investigate the effect of species mixture in the simulation experiments. Other inputs, including soil texture, pH and soil color were obtained from the USDA map derived from Eswaran et al. (2003), for the corresponding pixel.

The amount of fresh breeding woody substrate inputs used by the bark beetles to breed was controlled by modifying the maximum wind speed of a windthrow event in ORCHIDEE. Seven wind speeds ranging between 19 m/s and 40 m/s were selected (Table 3). This range is justified by the observation that mean wind speeds below 19 m/s could not trigger a windthrow event in ORCHIDEE (Chen et al., 2018) while for wind speeds exceeding 40 m/s, more than 60% of the trees are uprooted, leaving too few living trees to trigger a bark beetle outbreak within the same pixel.

To investigate the impact of windthrow intensity and background climate on bark beetle outbreaks, the study conducted a total of 56 [8 sites x 7 wind speed intensity] simulations as given in table 3. The same 56 simulations were also used to analyze the sensitivity of the carbon balance of spruce forests to windthrow intensity and background climate.

Contrary to equation 5a,  $PWS_{age\ class}$  is the plant water stress from the current year.

$$i_{\text{hosts competition, age class}} = 1 / (1 + e^{S_{\text{competition}} \cdot (RD_{i \text{ age class}} - RD_{i \text{ limit}})}) \quad (6a'')$$

$$RD_{i \text{ age class}} = \frac{D_{\text{age class}}}{D_{\text{max}}} \quad (6b'')$$

To access the Bark beetle damage rate ( $DR_{\text{beetles}}$ ), we simply divide  $B_{\text{beetles kill}}$  by  $B_{\text{total}}$ .

## 2.11. Flow of the calculations

As the equations presented above contain feedback loops the flow of the calculation is shown in Fig. 2.

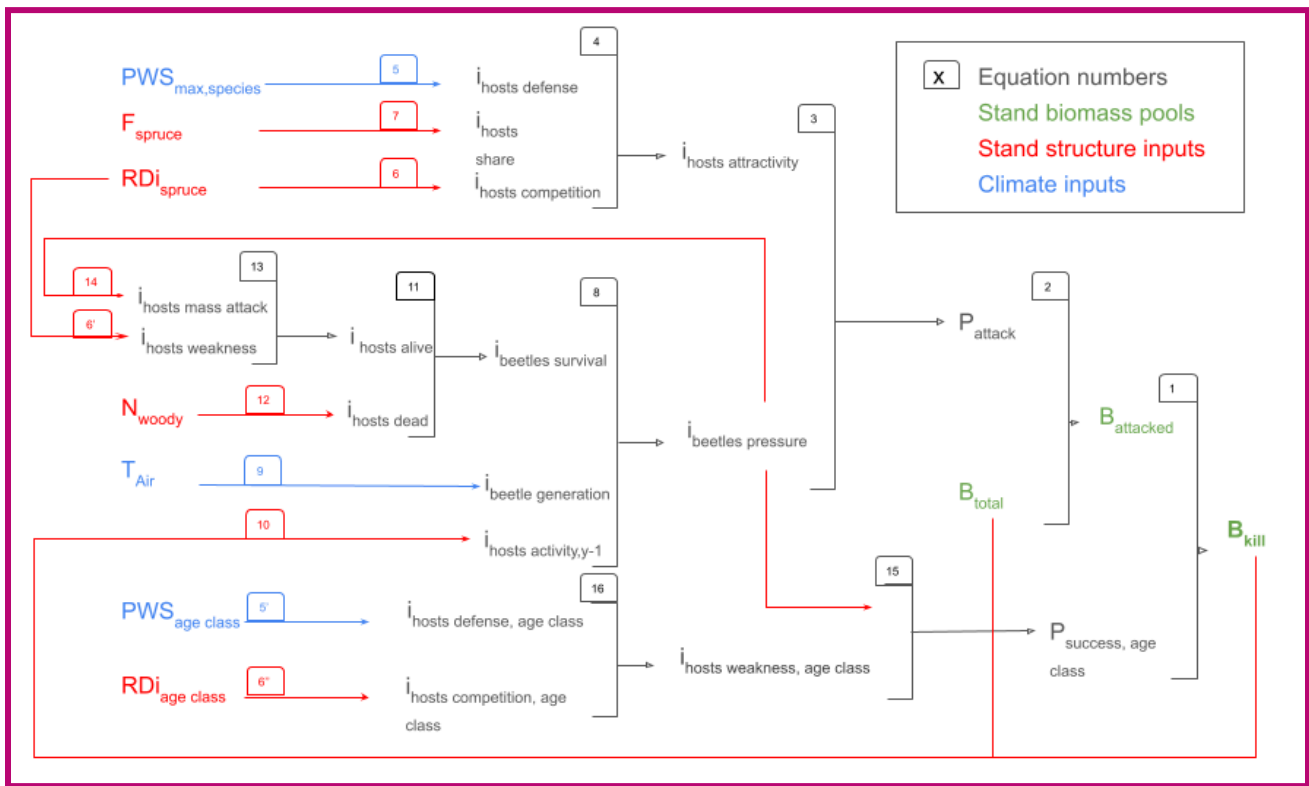


Figure 2: Flow of the calculations in the bark beetle outbreak module developed in this study. The numbers correspond to the equation numbers provided in this study.

## 3. Methods and material

### 3.1. Model configuration

Given the large-scale nature of the ORCHIDEE we carried out a sensitivity experiment of the bark beetle outbreak functionality rather than focusing the evaluation on matching observed damage volumes at specific case studies. Such an approach is thought to reduce the risk of overfitting the model to specific site conditions (Abramowitz et al., 2008).

ORCHIDEE r7791 including the bark beetle module was run for 8 FLUXNET sites, selected to simulate a credible temperature and precipitation gradient for spruce (see further below). For each location, the half-hourly meteorological data from the flux tower were gap filled and reformatted so that they could be used as climate forcing by the ORCHIDEE. Boundary conditions for ORCHIDEE, such as soil texture, pH and soil color were retrieved from the USDA map, for the corresponding pixel. The observed land cover and land use for the pixel were ignored and set to pure spruce because this study did not investigate the effect of species mixture in the simulation experiments. The resolution of the pixel chosen for this analysis is 2500 km<sup>2</sup>. It corresponds to a fine resolution for ORCHIDEE large-scale simulations but a coarse resolution for studying bark beetle outbreaks.

The climate forcings were looped over as much as needed to bring the carbon, nitrogen, and water pools to equilibrium during a 340 years long spinup followed by a windthrow event and a 100-years simulation. The results presented in this study come from the 100-years long site simulations. Given the focus on even-aged monospecific spruce forests in regions where spruce growth is not constrained by precipitation, variables such as  $i_{\text{hosts share}}$  and  $i_{\text{hosts defense}}$  were omitted from this study. Note that ORCHIDEE do not account for possible acclimation of the bark beetle population to each location.

### 3.2. Site selection

Bark beetle populations are known to be sensitive to temperature as they are more likely to survive a mild winter (Lombardero et al., 2000) and tend to breed earlier when winter and spring are warmer than usual, allowing for multiple generations in the same year (Hlásny et al., 2021a). In order to assess the temperature effect of the bark beetle outbreak module in ORCHIDEE, eight locations in Europe were selected (Table 2) which represent the range of climatic conditions within the distribution area of Norway spruce (*Picea Abies* Karst L.) which is the main host plant for *Ips typographus*, the bark beetle species under investigation.



**Table 2: Climate characteristics of the eight sites used in the simulation experiments gradient underlying our experimental setup. The site acronyms refer to the site names used in the FLUXNET database (Pastorello et al. 2020).**

| Site<br>(FLUXNET)                              | HYY      | SOR     | THA      | WET      | HES    | FON           | REN   | COL        |
|--|----------|---------|----------|----------|--------|---------------|-------|------------|
| Full name                                      | Hyytiala | Soroe   | Tharandt | Wetstein | Hesse  | Fontainebleau | Renon | Collelongo |
| Country  | Finland  | Danmark | Germany  | Germany  | France | France        | Italy | Italy      |
| Latitude (°N)                                  | 61.8     | 55.5    | 50.9     | 49.0     | 48.4   | 48.7          | 46.5  | 41.8       |
| Longitude (°E)                                 | 24.3     | 11.6    | 13.6     | 14.8     | 7.1    | 2.8           | 11.4  | 13.6       |
| MAT (°C)                                       | 3.8      | 8.2     | 8.2      | 7.7      | 9.5    | 10.2          | 4.7   | 6.3        |
| MinAT (°C)                                     | -10.8    | 2.7     | -3.9     | -5.2     | 0.1    | -1.1          | -6.3  | -3.8       |
| MAP (mm.y <sup>-1</sup> )                      | 522      | 811     | 734      | 587      | 653    | 989           | 752   | 1050       |
| Mean annual net radiation (w.m <sup>-2</sup> ) | 42.1     | 49.4    | 52.5     | 68.0     | 53.7   | 50.3          | 67.7  | 68.3       |

For these eight locations, half-hourly weather data from the FLUXNET database (Pastorello et al., 2020) were used to drive ORCHIDEE. Some of these locations (FON, SOR, HES, COL, WET) are in reality not covered by spruce but all sites are, however, located within the distribution of Norway spruce. In this study, site locations were selected to use observed weather data to simulate a credible temperature and rainfall gradient for spruce.

### 3.3. Sensitivity to model parameters

The sensitivity assessment evaluates the responsiveness of four key variables ( $i_{\text{hosts weakness}}$ ,  $i_{\text{beetles mass attack}}$ ,  $i_{\text{beetles generation}}$ ,  $i_{\text{beetles activity}}$ ) of the bark beetle model of ORCHIDEE. The assessment aims to demonstrate the ability of ORCHIDEE to simulate diverse dynamics of bark beetle infestations. The selection of  $i_{\text{hosts weakness}}$ ,  $i_{\text{beetles activity}}$ ,  $i_{\text{beetles mass attack}}$ , and  $i_{\text{beetles generation}}$  was based on two criteria: (1) their substantial influence on the dynamics of the bark beetle epidemic, and (2) their independence from direct measurable data, rendering them less suitable for evaluation through literature review.

For each variable, three distinct values were assigned to two parameters labeled “S” and “limit”. The S parameter determines the shape of the logistic relationship, with three values tested for each variable: (a)  $S=-1$ , yielding a linear relationship, (b)  $-1 < S < -100$ , resulting in a logistic curve, and (c)  $S > -100$ , turning the logistic relationship into a step function.

The second parameter called “Limit” determines the threshold, derived from expert insights, at which the logistic relationship will reach its midpoint value of 0.5 ( $RDI_{\text{weakness}}$ ,  $BP_{\text{limit}}$ ,  $Act_{\text{limit}}$  or  $G_{\text{limit}}$ ). For instance,  $RDI_{\text{weakness}}$  is set at 0.55, indicating  $i_{\text{hosts weaknes}}$  midpoint sensitivity (Eq. 6’). Setting  $BP_{\text{limit}}$  at 0.12 results in an  $i_{\text{beetles mass attack}}$  midpoint when  $i_{\text{beetles pressure}}$  is 0.12, selected for its proximity to scenarios where  $i_{\text{hosts dead}}$  equals 1.0 (Eq. 14).  $Act_{\text{limit}}$  was positioned at 0.06, signifies  $i_{\text{beetles activity}}$  midpoint at a  $DR_{\text{beetles}} = 6\%$  from the preceding year, exceeding endemic levels yet not reaching epidemic outbreaks (Eq. 10). Lastly,  $G_{\text{limit}}$  is fixed at 1.0, denoting  $i_{\text{beetles generation}}$ 's midpoint upon completing one generation annually, underpinning the rarity of bark beetle outbreaks with fewer than one generation per year (Eq. 9). Starting from these reference values, a “restrictive” simulation was run in which the “Limit” parameter values were reduced by 50%. Likewise a “permissive” simulation was run to test 50% higher “Limit” parameter values.

This assessment explores 36 parameters value combinations (3 x 3 parameter values x 4 parameters). The simulations were run for the THA site, where they were repeated for a  $DR_{\text{windthrow}}$  of 0.1 and 10%. The effect of the parameters with a negligible windthrow event, i.e., killing only 0.1% of the trees, was tested to confirm that the selected parameters did not simulate false positives, i.e. ORCHIDEE simulating a bark beetle outbreak in the absence of windthrow. Note that this sensitivity analysis aims to document model behavior, rather than seeking precise parameter values (see section 3.4).

### 3.4. Parameter tuning

The simulation experiment presented in this section was repeated for all eight sites and those results were used to tune key model parameters. In order to select parameters values for  $i_{\text{hosts weaknes}}$ ,  $i_{\text{beetles mass attack}}$ ,  $i_{\text{beetles generation}}$ ,  $i_{\text{beetles activity}}$  that resulted in simulations reproducing observed dynamics of bark beetle outbreaks, the literature was searched for peer-reviewed papers that reported quantitative characteristics of bark beetle outbreaks (Table 3). Four characteristics could be documented:

- The delay between the windthrow event and the start of the bark beetle outbreak.
- The length of the bark beetle outbreak is defined by the number of years required for a bark beetle population to go back to its endemic level.
- The cumulative number of trees per unit area, killed by the bark beetles at the end of an outbreak.
- The tree mortality rate ( $DR_{\text{beetles}}$ ) during an endemic stage.

As already mentioned in the section 2.4, at landscapes scale we do not expect that the all spruces in the landscape will be killed by an outbreak, so we choose to set  $RDI_{\text{limit}}$  to 0.4 which mean that an outbreak will not kill more than 60 % of the trees in one pixel irrespective of the outbreak intensity.

**Table 3 : Literature-based summary of characteristics of large-scale bark beetle outbreaks.**

| <b>Outbreak characteristics</b>       | <b>Observations/model outputs from literatures</b>   | <b>How to check in ORCHIDEE ?</b>  |
|---------------------------------------|--|--|
| Delay before the start of an outbreak | A notable surge in the population of <i>I. typographus</i> , a species of bark beetle, was observed in windthrow areas during the second to third summer following the storm (Wichmann and Ravn, 2001; Wermelinger, 2004; Kärvelo and Schroeder, 2010; Havašová et al., 2017). | Using the tree mortality rate by bark beetles ( $DR_{beetles}$ ), one can measure the number of years since the storm before reaching the maximum mortality rate (epidemic stage). |
| Length of an outbreak                 | Studies suggest that bark beetle outbreaks in Europe can last anywhere from 11 to 17 years (Hlásny et al., 2021b; Mezei et al., 2014; Bakke, 1989).  | Using the tree mortality rate by bark beetles ( $DR_{beetles}$ ), one can measure the number of years since the storm before reaching the minimum mortality rate (endemic stage).  |
| Severity rate of an outbreak          | A severe bark beetle outbreak resulted in a 52%-60% reduction in tree numbers at large landscape scale (>2000km <sup>2</sup> ) (Pfeifer et al., 2011; Morehouse et al., 2008)  | Count the number of trees killed by bark beetles until the end of the outbreak, then divide by the number of trees just after the storm event.                                     |
| Endemic mortality rate                | Total background mortality is around 1.2%/year. Bark beetles are estimated to account for 40% of the total mortality ( $\approx 0.5\%/year$ ) (Das et al., 2016; Berner et al., 2017; Hlásny et al., 2021b).   | After the end of the outbreak, count the number of trees that die every year. Then average it.   |

### 3.5. Impact of climate and windthrow : simulation experiment

In this simulation experiment, the amount of fresh dead tree hosts ( $N_{wood}$ ) used by the bark beetles to breed was controlled by modifying the maximum damage rate of a windthrow event ( $DR_{windthrow}$ ) in ORCHIDEE. Seven  $DR_{windthrow}$  were simulated (i.e. 0.1%, 5%, 7.5%, 10%, 15%, 20%, 35%). Given the monotonic nature of the relationships between  $DR_{windthrow}$  and  $i_{hosts\ dead}$  (Eq. 12), each event triggers a proportional increase in the dead host availability ( $i_{hosts\ dead}$ ) scaling between 0 and 1 (Fig. 3). Through its equations, ORCHIDEE assumes that for damage rates above 20%  $i_{hosts\ dead}$  will always be equal to 1.0.  $RDi_{spruce}$ , however, may further decrease with increasing windthrow damage, which makes the 35% damage rate still interesting to investigate. Although the simulations were run for all  $DR_{windthrow}$ , only four windthrow damage rates were presented to enhance the readability of the result section including a windstorm resulting in a 35% damage rate (Fig. 3).

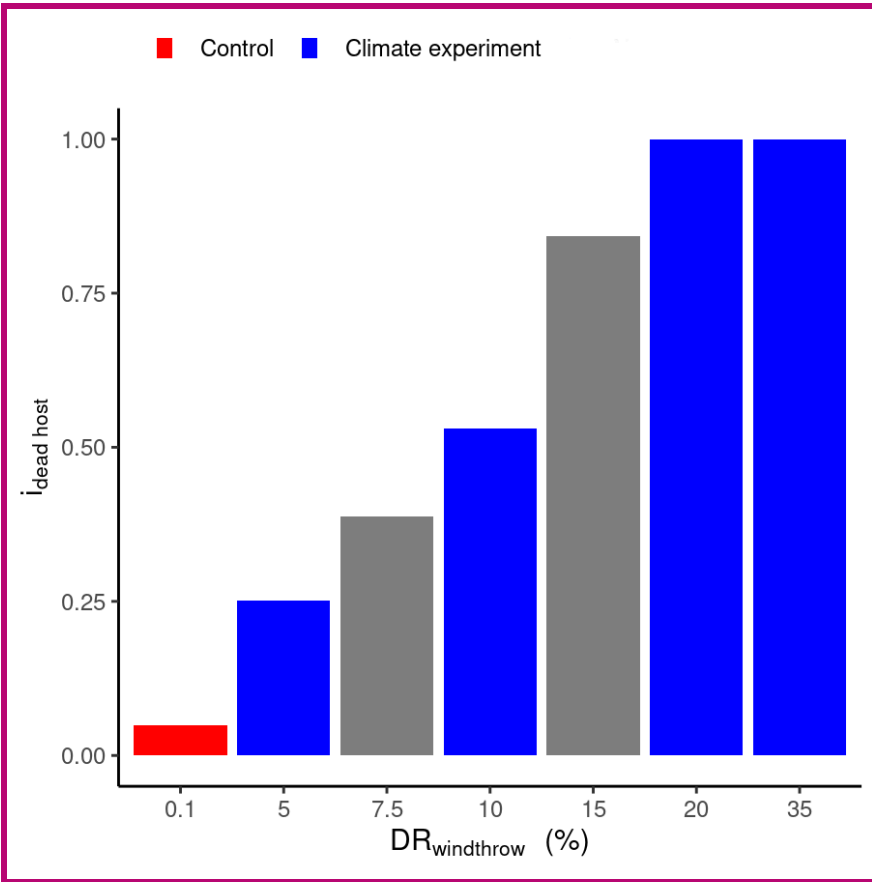


**Figure 3: Relationship between windthrow damage rate ( $DR_{windthrow}$ ) and dead host index ( $i_{hosts\ dead}$ ). For each site a  $DR_{windthrow}=0.1\%$  was used as the control simulation because an endemic bark beetle population is expected following such a low intensity event. Four  $DR_{windthrow}$  were selected for subsequent presentation of the results because they cover the entire range for the  $i_{hosts\ dead}$ .**

Site selection was based on the average numbers of generation a bark beetle population can achieve in one year. As described in Temperli 2013, the main driver of numbers of generation a bark beetle population can achieve in one year is the number of days higher than  $7.5^{\circ}\text{C}$  during winter time which is the reason why temperature is so important for bark beetle reproduction. By taking REN, THA, WET and HES, we can investigate a range in bark beetle generations between 0.8 and 3.5 (Fig. 3) which is a relevant range already observed in Europe. Restraining our analysis to only four sites will simplify the presentation in the results section.

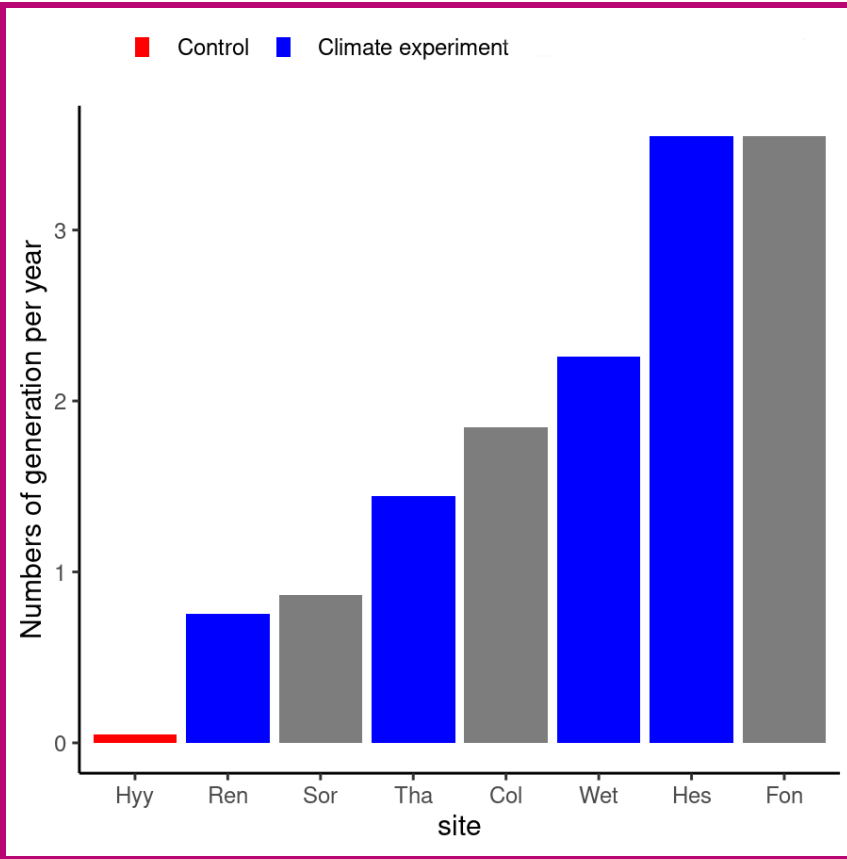


**Figure 4: Average number of bark beetle generations during the 5 years following the wind storm for the 8 sites. The HYY site in Finland was selected as the control site for the REN, THA, WET and HES sites. Only results from the control and selected sites are shown in the results to enhance readability of the figures. Although all simulations were also run for SOR, COL and FON their results were found to be too similar to the results of selected sites to present them as well.**

For the climate gradient, the HYY site was chosen to serve as a control since the numbers of generation is lower than 1 for which no outbreak should happen under any circumstances. Under present climate conditions, an outbreak in HYY should be considered as a false positive. Likewise, a  $DR_{windthrow}=0.1\%$  is considered too low to trigger an outbreak and was therefore used as the control for the wind damage rate tests.

The experiment consisted of 25 simulations, i.e., 5 selected sites (including a control) x 5 wind damage rates (including a control). Three output variables were assessed: bark beetle damage rate ( $DR_{beetles}$ ), total biomass ( $B_{total}$ ), and net primary production (NPP). Total was investigated over 100 years whereas  $DR_{beetles}$  and NPP were assessed for the first 20 years following a windthrow.

### 3.6. Continuous vs abrupt mortality

Where most land surface models use a turnover time to simulate continuous mortality (Turner et al., 2014, 2017; Pugh et al., 2019, 2017), ecological reality is better described by abrupt mortality events. An idealized simulation experiment was used to qualify the impact of abrupt mortality on net biome productivity by changing from a framework in which mortality is approximated by a constant background mortality to a framework in which mortality occurs in abrupt, discrete events. To test the impact of a change in mortality framework two versions of ORCHIDEE were compared to create an idealized simulation experiment: (1) a version simulating mortality as a continuous process, labeled "the continuous smooth version", and (2) the version capable of simulating abrupt mortality from windthrow and subsequent bark beetle outbreaks, labeled "the abrupt version". The effect of simulating abrupt mortality was evaluated over 20, 50, and 100 year time horizons.

The effect of changing the framework of simulating mortality from continuous to abrupt was qualified on the basis of 112 simulations (8 sites x 7 wind speeds x 2 model versions) of 100 years each. The simulations with abrupt mortality were run first. Subsequently, the number of trees killed was quantified and used as a reference value for the continuous mortality set-up. This approach resulted in the same quantities of dead trees at the end of the simulation for both frameworks, which then differed only in the timing of the simulated mortality. This precaution is necessary to avoid comparing two different mortality regimes where the result would mainly be explained by the intensity of the mortality rather than by its underlying mechanisms.

### 3.7. Quantitative evaluation ¶¶

~~This study presents a qualitative evaluation, whereas a quantitative evaluation is the topic of an ongoing study. The qualitative evaluation assesses whether the newly developed bark beetle model in ORCHIDEE is capable of reproducing bark beetle outbreak behavior along climate and windthrow gradients. As shown in Fig. 1, a bark beetle outbreak is driven by the beetle population dynamics resulting in structural and functional changes in the forest ecosystem. The length of the development stage of a bark beetle outbreak are not prescribed in ORCHIDEE, but emerge from the implemented processes. The evaluation of the beetle's population dynamics covers the 12 years following a disturbance event. The literature was searched for peer-reviewed papers that present the length of one or several of the outbreak stages. Eleven papers were identified and used in the evaluation (Table 6). ¶¶~~

~~Changes in forest functioning were evaluated through the temporal evolution of the net primary production (NPP) over a 15-year time frame and net biome productivity (NBP) over a 100-year time frame. NBP is defined as the regional net carbon accumulation after considering losses of carbon from fire, harvest, and other episodic disturbances. NBP is a key variable in the carbon cycle of forest ecosystems (Chapin et al., 2006; Galloway and Melillo, 1998) as it integrates photosynthesis, autotrophic, and heterotrophic respiration. In ORCHIDEE, NBP is calculated as proposed in (Chapin et al., 2006)). Changes in net biome productivity are thus the result of changes in photosynthesis, which in turn is driven by changes in leaf area, autotrophic respiration, and heterotrophic respiration. The latter is influenced by the availability of litter inputs, including litter from trees that died from the bark beetle outbreak. ¶¶~~

¶¶

## 4. Results

### 4.1. Sensitivity of bark beetles outbreaks to temperature and windthrow intensity

#### 4.1.1. Back beetle outbreak dynamic along a temperature gradient.

The variation in mean annual temperature across the eight examined locations spanned from a low of 4.3°C in HYY, Finland, to a high of 11.2°C in FON, France, over the simulation period. The hottest sites, FON and HES, witnessed a substantial bark beetle outbreak in ORCHIDEE following a windthrow event, resulting in a minimum of 12% timber loss. In contrast, the coldest sites, HYY and REN, remained unaffected by bark beetles, regardless of the severity of the windthrow event. Interestingly, the four sites with a similar average annual temperature (ranging between 7.2°C and 8.7°C) did not conform to the large-scale temperature gradient that governs bark beetle outbreaks in ORCHIDEE, as was the case in HYY, REN, FON, and COL. For instance, despite having an average annual temperature of 7.2°C, COL experienced an outbreak, while THA (8.7°C) only endured the buildup phase before reverting to the endemic phase with 12% timber loss. Additionally, SOR, which had an average annual temperature of 8.2°C, did not experience any outbreak in the simulations.

Examining the dynamics of net primary production during the outbreak, it's noticeable that warmer sites like FON, HES, and COL recovered more quickly (within 2-3 years) than colder sites (which took 3-5 years) following a disturbance event. This held whether or not the bark beetle population developed into an outbreak (see Fig. 4). The recovery of the fluxes was relatively fast compared to the several decades necessary for the forest structure to recover (result not shown). For locations where no beetle outbreak occurred (i.e., HYY, SOR, REN, as shown in Fig. 3), the recovery was solely from the impact of the windstorm, and these locations returned to their quasi-stable state within 5 to 10 years following the windstorm. At SOR, the climate record contained two storm events within a 5-year period (one that was artificially imposed for the study and one that was naturally present in the climate series), which may have contributed to the longer recovery stage compared to HYY and THA. When considering the total net primary production over a period of 15 years, less productive sites experienced more impact from an outbreak than the more productive sites. Changes in forest functioning were evaluated through the temporal evolution of accumulated net biome productivity (NBP) over a 100-years time frame. NBP is defined as the regional net carbon accumulation after considering losses of carbon from fire, harvest, and other episodic disturbances. NBP is a key variable in the carbon cycle of forest ecosystems) as it integrates photosynthesis, autotrophic, and heterotrophic respiration. In ORCHIDEE, NBP is calculated as proposed in Chapin et al., 2006). Changes in net biome productivity are thus the result of changes in photosynthesis, which in turn is driven by changes in leaf area, autotrophic respiration, and heterotrophic respiration. The latter is influenced by the availability of litter inputs, including litter from trees that died from the bark beetle outbreak.

## 5. Results

### 5.1. Sensitivity to model parameters

The impact of spruce stand competition ( $i_{\text{hosts\_weakness}}$ ) on outbreak dynamics was examined by adjusting the parameters  $S_{\text{weakness}}$  and  $RD_{i_{\text{weakness}}}$  in equation 6a'. When  $S_{\text{weakness}}$  resulted in a linear relationship ( $S_{\text{weakness}} = -1$ ), no peak in bark beetle damage occurred for the three tested values of  $RD_{i_{\text{weakness}}}$  (permissive, reference, restrictive) at a

10% windthrow damage rate (Fig. 5, 4<sup>th</sup> row, 2<sup>nd</sup> column). However, employing a step function ( $S_{\text{weakness}} > -100$ ) led to either sporadic peaks of bark beetle damage with a permissive  $RDi_{\text{weakness}}$  or a two-year outbreak with a maximum damage rate of 60% with a restrictive  $RDi_{\text{weakness}}$  (Fig. 5, 4<sup>th</sup> row, 2<sup>nd</sup> column), neither of which aligns with the observations summarized in Table 3.

The most favorable outcome was obtained with a logistic relationship ( $-1 < S_{\text{weakness}} \ll -100$ ), where  $RDi_{\text{weakness}}$  dictated the duration of the outbreak: 11, 16, and 25 years for restrictive, reference, and permissive parameter values, respectively (Fig. 5, 4<sup>th</sup> row, 2<sup>nd</sup> column). Either the restrictive or reference parameter value could be utilized since a range of 11-16 years aligns with the observations (Table 3). To examine false positives, sensitivity tests were repeated for a 0.1% windthrow damage rate. None of the nine parameter combinations triggered an outbreak (Fig. 5, 4<sup>th</sup> row, 1<sup>st</sup> column), suggesting that false positives due to the calculation of  $i_{\text{hosts weakness}}$  are improbable.

The feedback effect of bark beetle mass attack capability ( $i_{\text{beetles mass attack}}$ ) when the bark beetle population reaches a certain threshold was evaluated by varying  $S_{\text{mass attack}}$  and  $BP_{\text{limit}}$  (Eq. 14). Linear relationships ( $S_{\text{mass attack}} = -1$ ) resulted in similar outbreak dynamics for all  $BP_{\text{limit}}$  values, with the model settling on a constant endemic damage post-outbreak, though higher than observed (Table 3). Introducing a logistic or step function minimally altered outbreak dynamics except when assuming a step function for the restrictive value, which prevented an outbreak. Repeating sensitivity tests for a 0.1% windthrow damage rate showed that assuming linear or logistic relationships could trigger an outbreak (Fig. 5, 3<sup>th</sup> row, 1<sup>st</sup> column), indicating that false positives may arise from the calculation of  $i_{\text{hosts mass attack}}$ .

The impact of bark beetle activities from the previous year ( $i_{\text{beetles activity}}$ ) on outbreak dynamics was investigated by varying  $S_{\text{activity}}$  and  $act_{\text{limit}}$  (Eq. 10). Linear or logistic relationships resulted in overly prolonged outbreaks (>30 years) compared to observations (Table 3, 1<sup>st</sup> row, 2<sup>nd</sup> column), whereas assuming a step-function relationship simulated a decline in the outbreak after 14 years. Sensitivity tests repeated for a 0.1% windthrow damage rate showed that assuming a linear relationship could trigger an outbreak (Fig. 5, 1<sup>st</sup> row, 1<sup>st</sup> column), suggesting potential false positives from the calculation of  $i_{\text{beetles activity}}$ .

To explore the effect of bark beetle activities from the previous year on outbreak dynamics ( $i_{\text{hosts generation}}$ ),  $S_{\text{generation}}$  and  $G_{\text{limit}}$  from equation 9 were varied. Bark beetle damage rate was more sensitive to  $G_{\text{limit}}$  than  $S_{\text{generation}}$ , but only a linear relationship with the reference  $G_{\text{limit}} = 1.0$  yielded an intermediate outbreak intensity consistent with the location (continental climate). Other combinations resulted in either too strong or no peak during the outbreak. Repeating sensitivity tests for a 0.1% windthrow damage rate showed that none of the nine parameter combinations triggered an outbreak (Fig. 5 2<sup>nd</sup> row, 1<sup>st</sup> column), indicating that false positives from the calculation of  $i_{\text{beetles generation}}$  are unlikely.



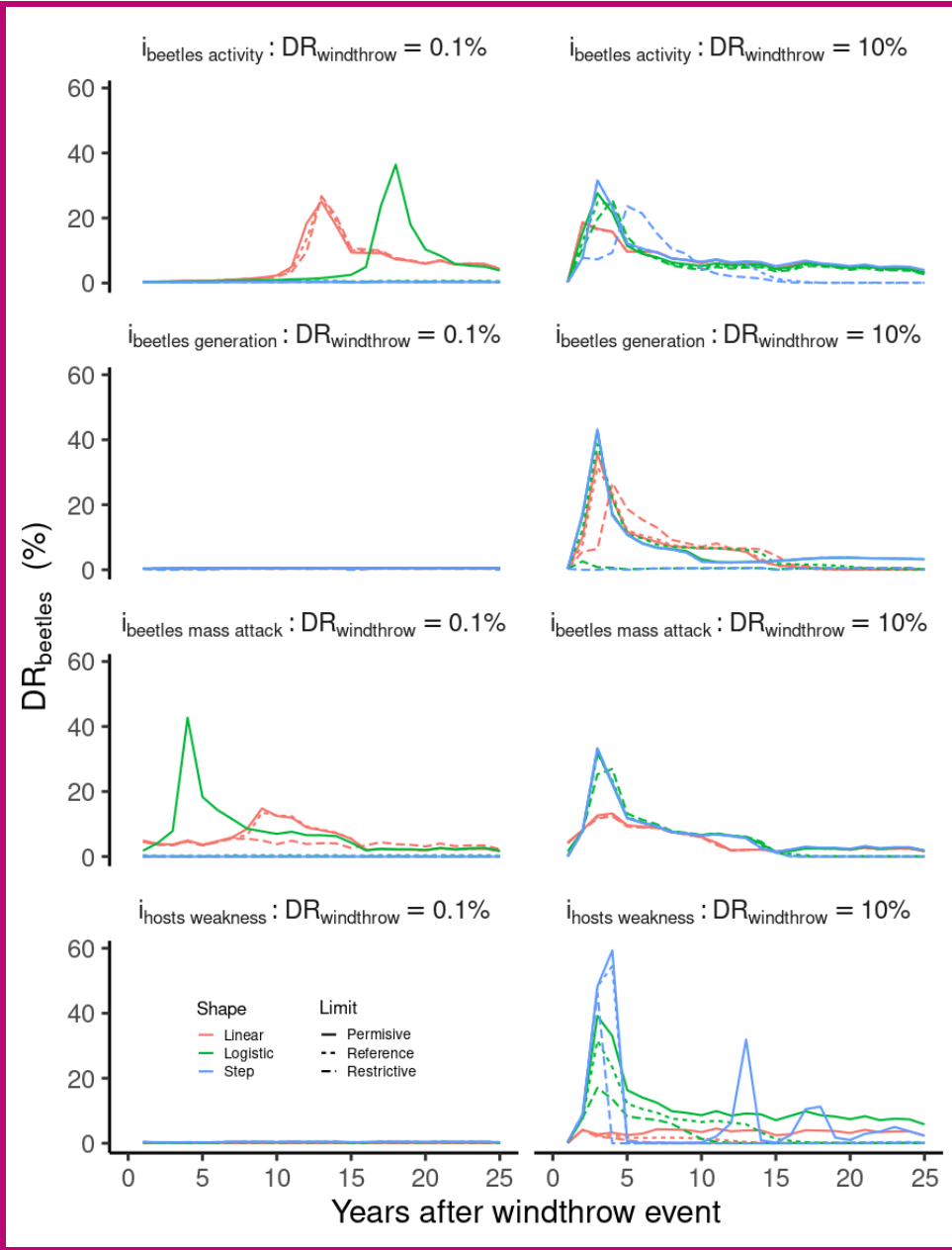


Figure 5: Simulation results from the sensitivity experiment at the THA site. Eight parameters from four equations were evaluated. Each equation represents an index from the bark beetle outbreak module ( $i_{hosts}$  weakness,  $i_{hosts}$  mass attack,  $i_{beetles}$  activity,  $i_{beetles}$  generation). Each index is represented by a logistic function defined by a shape parameter (S) and a limit parameter (L). Three values were chosen for each parameter resulting in 9 pairs of parameters for each index. Colored lines represent the shape parameter varying from linear :  $S = -1$ , logistic  $-1 < S < -100$ , to step function where  $S < -100$ . Line type represents three different values for L parameters where references are values of  $RD_{i_{weakness}}$ ,  $BP_{limit}$ ,  $act_{limit}$  and  $G_{limit}$  (given in Table 4), whereas permissive and restrictive represent a 50% decrease or increase respectively.

## 4.2. Model tuning

By comparing the outcomes of the sensitivity tests (section 4.1) to a summary of observations (Table 3), a first estimate of the values of several parameters was proposed (Table 4).

**Table 4: Parameters values from the bark beetle module tested in the sensitivity analysis. Values labeled with (\*) correspond to the parameters adjusted following the sensitivity analysis results.**

| Parameter                   | Source                                  | Value     |
|-----------------------------|---|-----------|
| $S_{\text{generation}}$     | This study: from SA (see 3.1.4)         | -1.0 (*)  |
| $G_{\text{limit}}$          | Adapted from Temperli et al. 2013       | 1.0 (*)   |
| $DD_{\text{ref}}$           | Adapted from Temperli et al. 2013       | 547.0     |
| $S_{\text{drought}}$        | Adapted from Temperli et al. 2013       | -9.5      |
| $PWS_{\text{limit}}$        | Adapted from Temperli et al. 2013       | 0.4       |
| $\max_{\text{Nwood}}$       | This study: scale dependent (see 2.4.2) | 0.2       |
| $S_{\text{activity}}$       | This study: from SA (see 3.1.3)         | -500 (*)  |
| $\text{act}_{\text{limit}}$ | This study: from SA (see 3.1.3)         | 0.06 (*)  |
| $S_{\text{weakness}}$       | This study: from SA (see 3.1.1)         | -5.0 (*)  |
| $RDi_{\text{weakness}}$     | This study: from SA (see 3.1.1)         | 0.55 (*)  |
| $RDi_{\text{limit}}$        | This study: scale dependent (see 2.4.1) | 0.4       |
| $S_{\text{mass attack}}$    | This study: From SA (see 3.1.2)         | -30.0 (*) |
| $BP_{\text{limit}}$         | This study: scale dependent (see 3.1.2) | 0.12 (*)  |
| $S_{\text{share}}$          | This study: not used (see 2.5)          | 15.5      |
| $SH_{\text{limit}}$         | This study: not used (see 2.5)          | 0.6       |

## 4.3. Impact of climate and windthrow on bark beetle damage

In ORCHIDEE, the hottest sites, HES and WET, experienced significant bark beetle outbreaks across a wide spectrum of windthrow mortality rates, whereas colder sites like REN and THA saw outbreaks only in response to the most severe windthrow events (Fig. 6). A greater average number of bark beetle generations in the years following windthrow events led to higher bark beetle damage rates at the peak of outbreaks. For instance, at a 35% windthrow mortality rate, HES reached a maximum bark beetle damage rate of 50%, whereas REN's maximum was 22% (Fig. 56).\*

### 5.1.1. ~~Back beetle outbreak dynamic across windthrow intensity gradient.~~

~~The ORCHIDEE simulation revealed a consistent correlation between the intensity of windthrow events and the dynamics of bark beetle outbreaks across all examined locations. In this study, if a windthrow resulted in less than~~

approximately 12% of timber volume loss, it did not result in an outbreak. The buildup phase, which typically lasted for three years at a 12% timber loss, reduced to two years at a 27% loss, and further shortened to one to two years at sites with a 32% loss or more (such as WET, HES, FON). The epidemic phase followed a similar trend, with its duration decreasing from six to three years at a 12% loss, to just one to two years at a 47% loss (Fig. 3). However, at a 60% timber loss, no epidemic phase was observed. Instead, an extended buildup phase lasting between five and twelve or more years was simulated. Beyond a 60% loss, the forest density became too low to trigger an outbreak, even though the vast amount of timber provided by the windthrow maintained the bark beetle population above its endemic threshold.

Analyzing the functional recovery along a gradient of windthrow intensities, it was found that a 12% loss of wood volume required 13 years to recover, while a loss of 8% required only 5 years (Fig. 4). Interestingly, when considering the total net primary production over a period of 15 years, it's apparent that the combined impact of windthrow and a bark beetle outbreak has a greater effect on ecosystem functioning than an equivalent single disturbance event, such as a windthrow that kills the same overall number of trees ( Fig. 5).

¶

## 5.2. Comparing simulated and observed bark beetle outbreak dynamics.

When confronting the simulation results with field observations reported in the literature, reasonable agreement was observed in terms of the duration of the four stages of bark beetle outbreak. A comprehensive summary of our findings for each of these four stages is presented in Table 5.

Interestingly, high windthrow mortality rates could also lead to delays and lower maximum  $DR_{\text{beetles}}$  (Fig. 6). For instance, at the HES site, 10%, 20%, and 35% windthrow damage rates triggered maximum  $DR_{\text{beetles}}$  of 50%, 43%, and 37%, respectively (Fig. 6). Conversely, low  $DR_{\text{windthrow}}$ , like 5% at WET, delayed the peak of bark beetle outbreaks by 9 years (Fig. 6). Additionally, the model simulated a post-epidemic stage during which the outbreak damage rate remained relatively low (<10%) and lasted between 3 to 10 years (Fig. 6). Overall, the simulated outbreaks lasted between 11 to 20 years, consistent with field observations (Table 3).

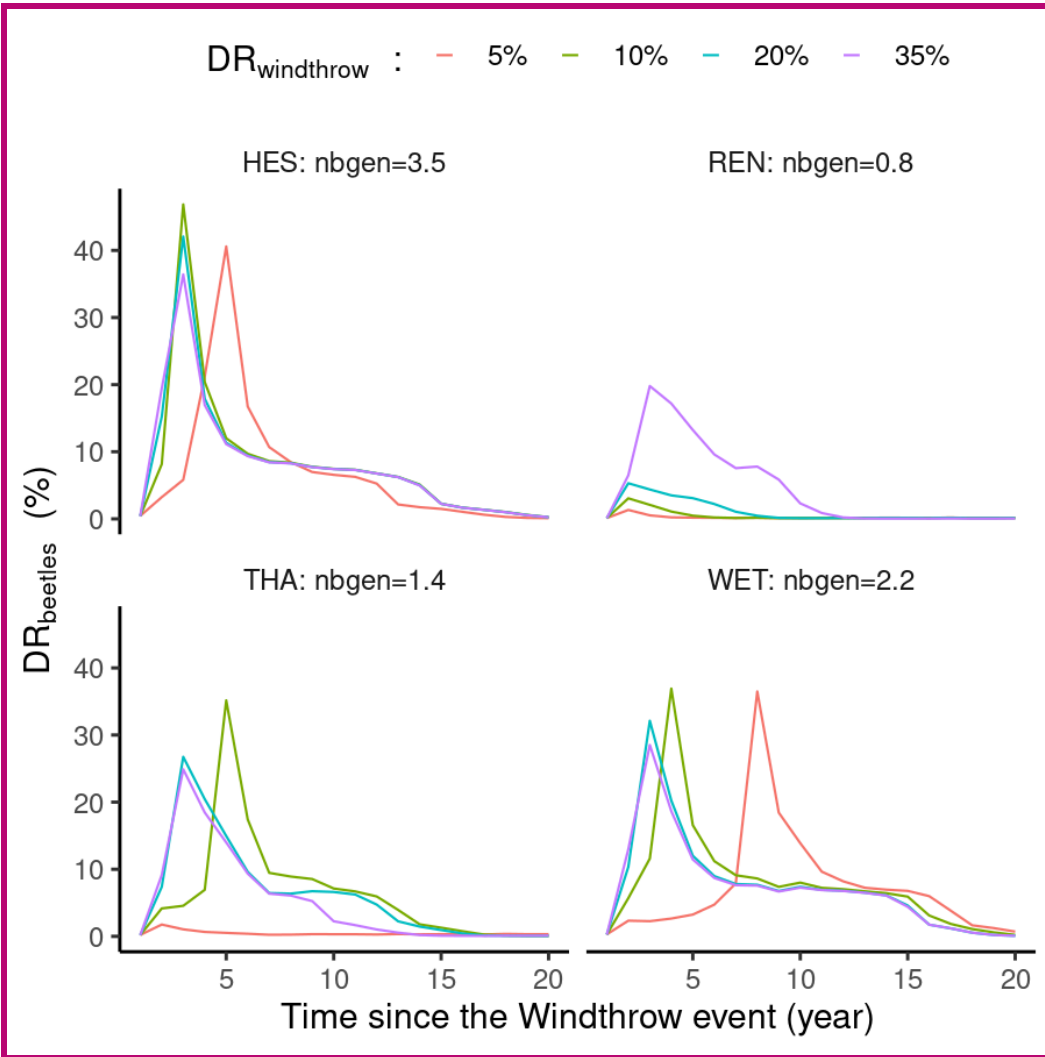


**Figure 6: Simulation results of 24 simulations (4 sites x 4 windthrow damage rate  $DR_{windthrow}$ ). Lines represent the annual bark beetle damage rate as a fraction of the total biomass ( $DR_{beetles}$ ). Nbgen is the average number of bark beetle generations during five years after the windthrow event.  $DR_{windthrow}$  represents the percentage of biomass loss by a windthrow event at the start of the simulation.**

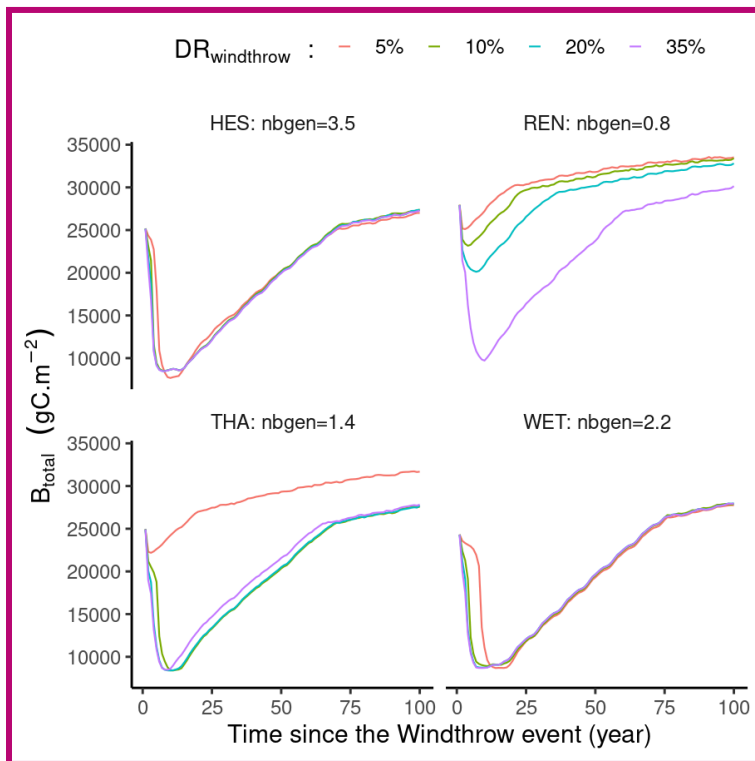
At the coldest site, HYY, ORCHIDEE predicted only a small number of bark beetle generations, preventing outbreaks from occurring. This observation validates the initial parameter tuning (Table 4), indicating that it is robust enough to prevent false positives, such as the model triggering outbreaks in sites where bark beetles cannot reproduce.

#### **4.4. Impact of climate and windthrow on stand biomass and Net Primary Production**

With the exception of REN, all sites experience a decrease in total biomass until around 9.000 gC.m<sup>-2</sup> by the end of the outbreak, which typically lasted 10 to 20 years (Fig. 7). It is noteworthy that regardless of the severity of maximum damage inflicted by bark beetles, the overall cumulative damage consistently results in the same amount

of biomass loss (Fig. 7). This characteristic is a key objective of the bark beetle module. Essentially, the model can simulate significant epidemic events even if the initial trigger, such as the windthrow event in our study, is not particularly intense. Once a tipping point is reached, at a biomass level of  $9.000 \text{ gC.m}^{-2}$  or  $\text{RD}_{\text{limit}} = 0.4$ , there's no turning back until that threshold is passed. Interestingly, at the REN site where the number of generations is approximately one, the outbreak only reaches the tipping point with a high windthrow damage rate (35%) (Fig. 7).

Throughout the outbreak period, there was a notable decrease in Net Primary Productivity (NPP), as illustrated in the second panel in Fig. 7, primarily attributed to a sharp decline in leaf area index, although not explicitly depicted. Subsequent to the epidemic phase, the forest undergoes recovery by regenerating its leaf area index. Consequently, individual leaf area indices tend to escalate to attain the overall stand leaf area index, concurrently boosting individual growth rates. Following the outbreak, the reduction in stand tree density due to bark beetle damage mitigates autotrophic respiration, albeit not displayed, and fosters recruitment, also not depicted, thereby augmenting NPP or forest growth (Fig. 7). Consequently, carbon use efficiency tends to be higher in sparsely populated stands compared to densely populated ones.



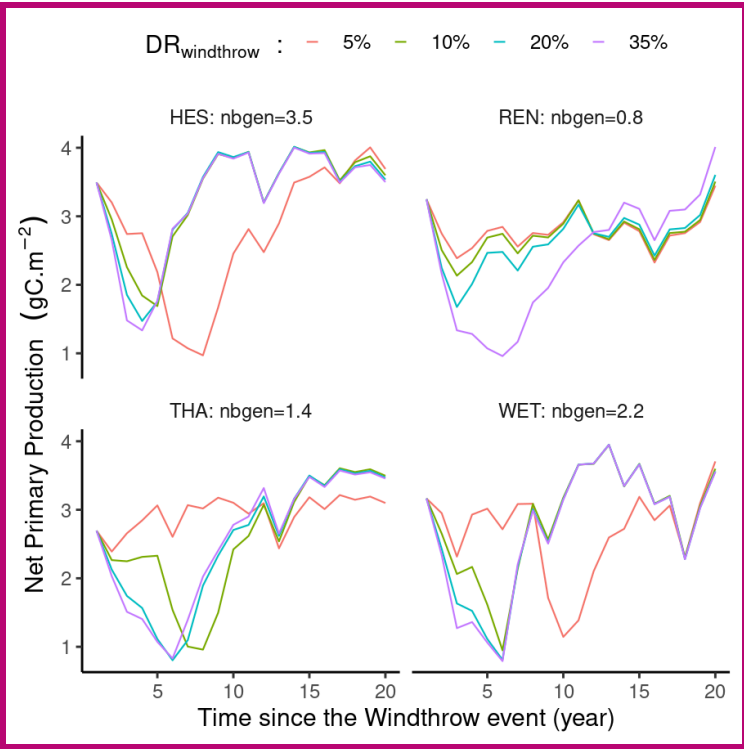


**Figure 7: Simulation results of 24 simulations (4 sites x 4 windthrow mortality rate). Lines represent the annual average net primary production (NPP) in  $\text{gC}\cdot\text{m}^{-2}$  or Total stand biomass ( $B_{\text{total}}$ ) in  $\text{gC}\cdot\text{m}^{-2}$ . Nbgen is the average number of achieved bark beetle generations during five years after the windthrow event.  $DR_{\text{windthrow}}$  represents the percentage of biomass loss by a windthrow event at the start of the simulation.**

#### 4.5. Continuous vs abrupt mortality

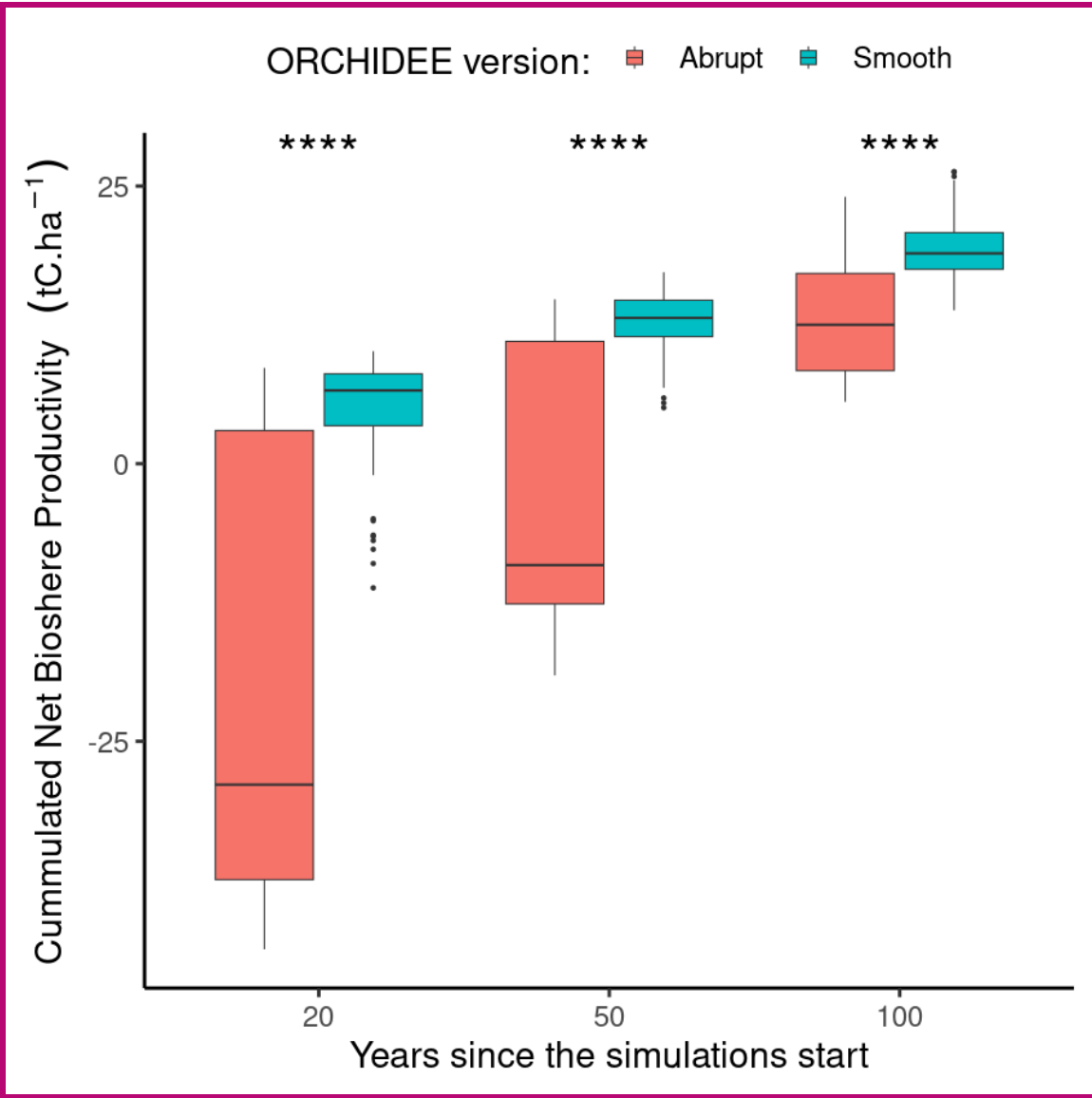


Figure 8: Difference in cumulative net biome production at three discrete time horizons (i.e. 20, 50 and 100 years) between a continuous (blue) and abrupt (red) mortality framework. Note that in the continuous mortality framework the mortality rate was adjusted to obtain a similar number of trees killed after 100 years as in the abrupt mortality framework. The variation of each boxplot arises due to different locations and prescribed storm intensities. Each boxplot displays the median value (thick horizontal line), the quartile range (box border), and the 95% confidence interval (vertical line).

The total accumulated net biome production (NBP) was evaluated for each simulation using the ORCHIDEE model across three different timeframes: 20, 50, and 100 years following a windthrow event. At the 20-year mark, the average accumulated NBP notably differed between the continuous and abrupt (Smooth) and abrupt (Abrupt) mortality frameworks:  $2.10 \pm 0.82$  and  $-19.3 \pm 2.7$  tC.ha<sup>-1</sup> for the former, and  $-9.73 \pm 10.43$  and  $34.6 \pm 0.7$  tC.ha<sup>-1</sup> for the latter.

These differences were statistically significant (t-test/Wilcoxon, p-value<0.001). While forests under the abrupt mortality framework, indicating a substantial initial reduction in NBP with the 'Abrupt' model, as ecosystems behaved as carbon sources, those whereas under the continuous mortality framework 'Smooth' model, they acted as carbon sinks (Fig. 6). Furthermore, the variability in NBP (Fig. 6)8). The variability in NBP demonstrated the broad temperature gradient in Europe and indicated that despite many locations potentially acting as sources under the abrupt mortality 'Abrupt' framework, some may transition to carbon sinks within the first 20 years following a disturbance.

When considering

Moving to the 50-year horizon, the difference between the two frameworks decreased. The, with net biome productions were  $6.00 \pm 2.09$  and  $0.77 \pm 6.15$  of  $-1.8 \pm 1.6$  and  $13.4 \pm 0.4$  tC.ha<sup>-1</sup> for the continuous and abrupt mortality frameworks, respectively. The difference in sink strength was sink strength difference remained statistically significant (t-test/Wilcoxon, p-value=<0.001), with the NBP in the abrupt 'Abrupt' framework approaching carbon neutrality. However, the variability of responses depending on climatic conditions remained pronounced under the abrupt framework in comparison persisted, with the 'Abrupt' framework showing a greater range compared to the continuous 'Smooth' one. Some locations under the abrupt mortality framework transitioned from carbon sources to carbon sinks under the continuous mortality framework 'Smooth' framework, indicating a more resilient and gradual recovery in ecosystem productivity (Fig. 6)8).

At the 100-year mark, the average accumulated NBP for the abrupt and continuous frameworks became indistinguishable (t-test 'Abrupt' and 'Smooth' frameworks became much closer (Wilcoxon, p-value=0.55<0.001), with values of  $20.98 \pm 7.90$  and  $22.90 \pm 9.77$  tC.ha<sup>-1</sup>, respectively.¶

¶

## 6. Discussion¶

### 6.1. Simulating the dynamics of bark beetle outbreaks and their interaction with windthrow¶

Given the large-scale nature of the ORCHIDEE model we opted to start with a qualitative evaluation of the bark beetle outbreak functionality rather than focusing the evaluation on matching observed damage volumes at specific case studies. Such an approach is thought to reduce the risk of overfitting the model to specific site conditions (Abramowitz et al., 2008). Qualitative evaluation enables improving the realism of the bark beetle model in ORCHIDEE without reducing its generality (Levins, 1966). The side-by-side comparison of the observed stages in a bark beetle outbreak and model behavior by ORCHIDEE (Table 6) show the ability of ORCHIDEE to simulate the dynamics of cascading disturbances. Even if some of the simulated dynamics may rarely occur in reality, the model formulation has demonstrated its capability to simulate a broad range of disturbance dynamics. The variation in the outbreak dynamics and  $14.2 \pm 0.8$  and  $20.4 \pm 0.6$  tC.ha<sup>-1</sup>, respectively (Fig. 8). The data showed a return to positive Cumulative NBP values, suggesting a long-term recovery and potential return to pre-disturbance productivity levels within the century following the windthrow events. The 'Smooth' model version displayed a consistently higher median value, suggesting a more resilient recovery over the long term.



## 7. Discussion

### 7.1. Simulating the dynamics of bark beetle outbreaks and their interaction with windthrow

Our Bark beetle outbreak model formulation has demonstrated its capability to simulate a broad range of disturbance dynamics. The variation in the outbreak dynamics and the response of the outbreak to its main drivers (Fig. 5 & 6) give confidence in the ability of ORCHIDEE to simulate various outbreak scenarios observed across the temperate and boreal zones under changing climate conditions.

Windthrow events have significant ecological meaning because such disturbances offer fresh breeding substrates, which in turn increase bark beetle populations (Lausch et al., 2011). Our modeling results align with these findings, indicating that windthrows causing damage of 5% or more may trigger beetle outbreaks (Fig. 6). Additionally, Wermelinger (2004) reported a strong increase in bark beetle populations post-windthrow, a pattern that our ORCHIDEE simulations also reflect. The model pinpoints a buildup stage—spanning 1 to 9 years, where bark beetle numbers increase prior to peaking, with the duration influenced by the severity of the windthrow and the prevailing climate (Fig. 6).

Temperature is another critical factor affecting bark beetle life cycles. Studies by Benz et al. (2005) have highlighted how intra- and interannual variation in temperature impact bark beetles, with warmer conditions fostering multiple generations per year, whereas cooler, damp climates slow breeding and survival rates. In line with these findings, ORCHIDEE's temperature-dependent simulations show variations in bark beetle impacts across different sites; cold winters at locations such as SOR and REN reduced bark beetle activity compared to warmer sites like THA and WET (Fig. 6). Lieutier et al. (2004) documented that significant bark beetle numbers can trigger mass attacks on healthy trees. Our model incorporates this dynamic, illustrated by epidemic stages where living trees become viable hosts, which then exacerbates the growth of the beetle population.

The aftermath of windthrow and subsequent bark beetle infestations also affects the forest carbon and nitrogen cycles. This impact is observed in the form of snags—standing dead trees that undergo decomposition. As Rhoades, (2019) observed, this can disrupt the link between soil and ecosystem carbon and nitrogen dynamics, a point echoed by (Custer et al., 2020). While ORCHIDEE models the ~~response decay of the outbreak to its main drivers (Fig. 3)~~ ~~give confidence in the ability of ORCHIDEE to simulate various outbreak scenarios observed around the temperate and boreal zones under changing climate conditions.~~ fallen logs, it does not account for snags. Nevertheless, the model suggests a recovery period ranging from 5 to 15 years, contingent upon the intensity of the bark beetle outbreak (Fig. 7). As snags create gaps in the canopy, conditions favorable to natural forest regeneration emerge, corroborating the affirmation of Jonášová and Prach, 2004. The ORCHIDEE model forecasts an increase in tree recruitment due to the sharp reduction in stand density, allowing more sunlight to penetrate to the forest floor, thereby stimulating growth (Fig. 7).

### 7.2. Emerging property from interacting disturbances

While this study hasn't provided a precise quantification of the impact of incorporating abrupt mortality versus a fixed continuous background mortality, it consistently demonstrated that the impact of abrupt mortality can vary across locations and over time, i.e., ecosystem functions, such as carbon storage, are affected by natural disasters like pest outbreaks, having significant impacts on short-to-mid-term carbon balance estimates.¶

The simulation experiments also highlighted that the legacy effects of disturbances can endure for decades, even in for a simplified representation of forest ecosystems such as ORCHIDEE, where the recovery might be too fast due to the absence of snags or too slow due to the absence of recruitment (Senf et al., 2019, 2017).

In the model wind speeds of less than  $20 \text{ m.s}^{-1}$  weren't powerful enough to uproot or break trees (Fig. 4).

The ability to simulate resistance as an emerging property is evident from Fig. 4 for locations SOR, REN, and HYY6 and 7 for locations REN, where no bark beetle outbreaks were observed following a windthrow medium windthrow event (5%-20%). However, in all simulated locations that couldn't resist a bark beetle outbreak, the forest was resilient and ecosystem functions were restored to the level from before the wind throw windthrow. The elasticity of, e.g., the carbon sink capacity ranged from 1 to 107 to 14 years. This elasticity is in line with current observational evidence from Millar and Stephenson (2015), 2015 who found very little evidence of ecosystem shifts due to natural disturbances in forests, Finally, after the disturbance and the recovery of vegetation structure, the ecosystems simulated by ORCHIDEE showed persistence, i.e. the ability to continue along their initial developmental path. ¶

¶

### **7.3. Are cascading disturbances important for carbon balance estimates ?**¶

The integration of abrupt mortality events instead of a fixed continuous mortality calculation has significantly complicated the ORCHIDEE model. However, does this increased realism offer any new insights into carbon balance estimates? The experiment suggests that over a century long timeframe, the net biome production, which was used to estimate carbon balance, remains consistent regardless of if a continuous or abrupt framework is used. This further corroborates the model's ability to reach the same state (Fig. 6). The time needed for both frameworks to convergence implies that after a single disturbance or a cascade of disturbances, the forest experiences a prolonged In this study we follow the definitions of Grimm and Wissel, 1997 for resistance, resilience, elasticity, and persistence.

### **7.4. Are cascading disturbances important for carbon balance estimates ?**

The enhanced complexity introduced into the ORCHIDEE model by incorporating abrupt mortality events, as opposed to a fixed-rate continuous mortality, prompts the question: does this model refinement yield significant new insights into carbon balance estimates? Our century-long timeframe analysis demonstrates that the net biome production (NBP; as defined in Chapin et al., 2006)—the metric for carbon balance—ultimately aligns between the continuous and abrupt mortality frameworks, thereby affirming the model's capacity for convergence (Fig. 8). This suggests that irrespective of the nature of the mortality events, the forest ecosystem exhibits a recovery phase, marked by a growth spurt boost that compensates for the growth deficit deficits incurred during the disturbance event.¶ The experiment, however, did not consider fluctuations in the recurrence of disturbances. Considering the significant impact.

Yet, our experiment has not taken into account the frequency of disturbances. Given the profound influence of disturbance legacy legacies on carbon dynamics, it's plausible that a recurrence interval of less shorter than the recovery period could trigger a tipping point, reducing forest's recovery time might result in a tipping point. Such a scenario could diminish the forest's carbon sequestration beyond potential in the post-100-year horizon. In extreme cases, forest ecosystems might even collapse, although this was not simulated in the current experiments nor documented in the recent period, and in extreme cases, may even lead to ecosystem collapse—outcomes not explored in the current simulations nor reflected in recent literature, such as the review by Millar and Stephenson (2015).

On the other hand, between

In the mid-term, spanning 20 to 50 years, the commonly adopted widely used continuous mortality model tends to overestimate appears to inflate the carbon sink capacity capabilities of forests compared to conditions when juxtaposed with abrupt mortality events scenarios. Since most policy recommendations target these shorter timeframes (e.g. Green Deal for Europe, 2023; Paris Agreement | CCNUCC, 2023) they should rely on policy frameworks, including the Green Deal for Europe (2023) and the Paris Agreement | CCNUCC (2023), often hinged upon these medium-term predictions, they would benefit from adopting model simulations incorporating an that integrate abrupt mortality framework events to avoid an overestimation of the sink capacity of forest. ¶

Moreover, this study emphasizes the significance of initializing the model with an accurate depiction of the forest's state. The state of the forest greatly influences the carbon assimilation rate. Integrating forests' carbon sink capacities. Furthermore, the accuracy of carbon balance estimates strongly depends upon the initial state of the forest in the model. Forest conditions markedly affect carbon uptake rates. Thus, incorporating an abrupt mortality framework into the ORCHIDEE model may help to enhance the accuracy and robustness could substantially refine and fortify the predictive power of our carbon balance estimates over assessments across short, medium, and long-term periods. ¶

¶

**Bark** scales.

## 7.5. Shortcomings of the bark beetle outbreak models shortcomings model

The bark beetle outbreak module developed in this study builds upon the strengths of the previously established LandClim model, though it also inherited some of its limitations. ¶

One notable shortcoming is the submodel module for beetle phenology, which is an empirical model making use of accumulated degrees-days. Since the model's module's conception a decade ago, Europe's climate has undergone substantial changes, primarily manifested in warmer winters and springs (European State of the Climate | Copernicus, 20232024). Because of these changes—the, chances have increased for two or even more bark beetle generations within a calendar year (Hlásny et al., 20212021a). These changes call for an update of the beetle's phenology model to align with these more recent observations (Ogris et al., 2019).

A second limitation is that our study, ORCHIDEE, has been parameterized to simulate only Ips Typographus in Europe. In order to change the Beetles/trees hosts ecosystem e.g. pine bark beetle in North America (Dendroctonus

monticolae Hopkins), the sensitivity of indexes must be revised, for example pine beetle is not breeding on the dead wood falling from withrow but very sensitive to drought event (Preisler et al., 2012).  $i_{\text{hosts defense}}$  and  $i_{\text{hosts dead}}$  as well as the phenology model will need to be revised.

Another issue is the model's consideration of drought. As outlined in the method section, drought is treated as an exacerbating factor, rather than a primary trigger as is the case for windthrow. This understanding was accurate a decade ago (Temperli et al., 2013); however, emerging evidence increasingly suggests that drought events may indeed trigger bark beetle outbreaks across Europe (Netherer et al., 2015; Nardi et al., 2022, 2023). Consequently, this extreme drought as a trigger should be incorporated in a future revision of ORCHIDEE's bark beetle outbreak module.

## 8. Outlook

This study simulated how windthrow interacts with bark beetle infestations in unmanaged forests. Future research will incorporate additional interactions, such as: the interplay between droughts, storms, and bark beetles; storms, bark beetles, and fires; as well as forest management, storms, and bark beetles.

The bark beetle outbreak module could also be enhanced by simulating: (a) standing dead trees (or snags), which would help account for differences in wood decomposition between snags and logs (Angers et al., 2012; Storaunet and Rolstad, 2004; et al., 2005), (b) the migration of bark beetles to neighboring locations, which becomes significant to account for in a model that operates at spatial resolutions below approximately 10 kilometers, ~~(c) the recruitment of trees, which would enable the simulation of ecosystem shifts (see section 4.2),~~ and (d) an up-to-date beetle phenology module which accounts for the recent change in their behavior induced by climate change.

This research provides an initial qualitative assessment of a new model feature. However, the application of the model necessitates an evaluation of the simulations against observations of cascading disturbances at the regional scale, which is the topic of an ongoing study.

## 9. Conclusion

Our approach enables improving the realism of the bark beetle model in ORCHIDEE without reducing its generality (Levins, 1966). The integration of a bark beetle outbreak module in interaction with other natural disturbance such as windthrow into the ORCHIDEE land surface model has resulted in a broader range of disturbance dynamics and has demonstrated ORCHIDEE's capacity to simulate various disturbance interaction scenarios under different climatic conditions. Incorporating abrupt mortality events instead of a fixed continuous mortality calculation provided new insights into carbon balance estimates. The study showed that the continuous mortality framework, which is commonly used in the land-surface modeling community, tends to overestimate the carbon sink capacity of forests in the 20 to 50 year range in ecosystems under high disturbance pressure, compared to scenarios with abrupt

mortality events.

Apart from these advances, the study revealed possible shortcomings in the bark beetle outbreak model including the need to update the beetle's phenology model to reflect recent climate changes, and the need to consider extreme drought as a trigger for bark beetle outbreaks in line with emerging evidence. Looking ahead, future work will further develop the capability of ORCHIDEE to simulate interacting disturbances such as the interplay between extreme droughts, storms, and bark beetles, and between storms, bark beetles, and fires.

The final step would be to realize a complete quantitative evaluation based on observation data such as produced by (Marini et al., 2017) in order to assess the capability of ORCHIDEE to simulate complex interaction between multiple sources of tree mortality affecting the carbon balance at large scale.

#### **10. Code availability**

- R script and data are available at :  
<https://doi.org/10.5281/zenodo.8004954> or DOI <https://doi.org/10.5281/zenodo.8004954>
- ORCHIDEE rev 7791 code is also available from:  
[https://forge.ipsl.jussieu.fr/orchidee/browser/branches/publications/ORCHIDEE\\_gmd-2023-05](https://forge.ipsl.jussieu.fr/orchidee/browser/branches/publications/ORCHIDEE_gmd-2023-05)

#### **11. Data availability**

- The Fluxnet climate forcing data are available at <https://fluxnet.org/>
- The simulation results use in this study are available at <https://doi.org/10.5281/zenodo.8004954>

#### **12. Author contribution**

G. Marie, S. Luysaert designed the experiments and G. Marie conducted them. Following discussions with H. Jactel, G. Petter and M. Cailleret, G. Marie developed the bark beetles model code and performed the simulations. J. Jeong integrated the wind damage and bark beetle modules with each other. G. Marie, J. Jeong, V. Bastrikov, J. Ghattas, B. Guenet, A.S. Lansø, M.J. McGrath, K. Naudts, A. Valade, C. Yue, and S. Luysaert, contributed to the development, parameterization and evaluation of the ORCHIDEE revision used in this study. G. Marie, J. Jeong, and S. Luysaert prepared the manuscript with contributions from all co-authors.

#### **13. Competing interests**

No competing interest

#### **14. Acknowledgements**

GM was funded by MSCF (CLIMPRO) and ADEME (DIPROG). SL and KN were funded by Horizon 2020, HoliSoils (SEP-210673589) and Horizon Europe INFORMA (101060309). JJ was funded by Horizon 2020, HoliSoils (SEP-210673589). BG was funded by Horizon 2020, HoliSoils (SEP-210673589). GP acknowledges funding by the Swiss National Science Foundation (SNF 163250). ASL was funded by Horizon 2020, Crescendo

(641816). C.Y. was funded by the National Science Foundation of China (U20A2090 and 41971132). MJM was supported by the European Commission, Horizon 2020 Framework Programme (VERIFY, grant no. 776810) and the European Union's Horizon 2020 research and innovation programme under Grant Agreement No. 958927 (CoCO2). AV acknowledges funding by Agropolis Fondation (2101-048). This work was performed using HPC resources from GENCI-TGCC (Grant 2022-06328). The Textual AI - Open AI GPT4 (<https://chat.openai.com/>) has been used for language editing at an early stage of manuscript preparation.

## 15. References

- Abramowitz, G., Leuning, R., Clark, M., and Pitman, A.: Evaluating the Performance of Land Surface Models, *J. Clim.*, 21, 5468–5481, <https://doi.org/10.1175/2008JCLI2378.1>, 2008.¶
- Allen, C. D., Breshears, D. D., and McDowell, N. G.: On underestimation of global vulnerability to tree mortality and forest die-off from hotter drought in the Anthropocene, *Ecosphere*, 6, art129, <https://doi.org/10.1890/ES15-00203.1>, 2015.¶
- Andrus, R. A., Hart, S. J., and Veblen, T. T.: Forest recovery following synchronous outbreaks of spruce and western balsam bark beetle is slowed by ungulate browsing, *Ecology*, 101, e02998, <https://doi.org/10.1002/ecy.2998>, 2020.¶
- ~~Angers, V. A., Bergeron, Y., Drapeau, P., and Drapeau, P.: Morphological attributes and snag classification of four North American boreal tree species: Relationships with time since death and wood density, *For. Ecol. Manag.*, 263, 138–147, <https://doi.org/10.1016/j.foreco.2011.09.004>, 2012.¶~~
- ~~¶~~
- ~~Un pacte vert pour l'Europe: [https://commission.europa.eu/strategy-and-policy/priorities-2019-2024/european-green-deal\\_fr](https://commission.europa.eu/strategy-and-policy/priorities-2019-2024/european-green-deal_fr), last access: 2 June 2023.¶~~
- ~~¶~~
- ~~European State of the Climate | Copernicus: <https://climate.copernicus.eu/ESOTC>, last access: 30 May 2023.¶~~
- ~~¶~~
- ~~L'Accord de Paris | CCNUCC: <https://unfccc.int/fr/a-propos-des-ndcs/l-accord-de-paris>, last access: 2 June 2023.¶~~
- ~~¶~~
- ~~Bentz, B. J., Régnière, J., Fettig, C. J., Hansen, E. M., Hayes, J. L., Hicke, J. A., Kelsey, R. G., Negrón, J. F., and Seybold, S. J.: Climate Change and Bark Beetles of the Western United States and Canada: Direct and Indirect Effects, *BioScience*, 60, 602–613, <https://doi.org/10.1525/bio.2010.60.8.6>, 2010.¶~~
- ~~Bergeron, Y.: Mineralization rates and factors influencing snag decay in four North American boreal tree species, *Can. J. For. Res.*, 42, 157–166, <https://doi.org/10.1139/x11-167>, 2012.~~
- ~~European State of the Climate | Copernicus: <https://climate.copernicus.eu/ESOTC>, last access: 25 March 2024.~~
- ~~Bakke, A.: The recent *Ips typographus* outbreak in Norway - experiences from a control program, *Ecography*, 12, 515–519, <https://doi.org/10.1111/j.1600-0587.1989.tb00930.x>, 1989.~~
- ~~Bentz, B. J., Régnière, J., Fettig, C. J., Hansen, E. M., Hayes, J. L., Hicke, J. A., Kelsey, R. G., Negrón, J. F., and Seybold, S. J.: Climate Change and Bark Beetles of the Western United States and Canada: Direct and Indirect Effects, *BioScience*, 60, 602–613, <https://doi.org/10.1525/bio.2010.60.8.6>, 2010.~~
- ~~Berner, L. T., Law, B. E., Meddens, A. J. H., and Hicke, J. A.: Tree mortality from fires, bark beetles, and timber harvest during a hot and dry decade in the western United States (2003–2012), *Environ. Res. Lett.*, 12, 065005, <https://doi.org/10.1088/1748-9326/aa6f94>, 2017.~~
- ~~Berryman, A. A.: Population Cycles: The Case for Trophic Interactions, Oxford University Press, 207 pp., 2002.~~
- ~~Biedermann, P. H. W., Müller, J., Grégoire, J.-C., Gruppe, A., Hagge, J., Hammerbacher, A., Hofstetter, R. W., Kandasamy, D., Kolarik, M., Kostovcik, M., Krokene, P., Sallé, A., Six, D. L., Turrini, T., Vanderpool, D., Wingfield, M. J., and Bässler, C.: Bark Beetle Population Dynamics in the Anthropocene: Challenges and Solutions, *Trends Ecol. Evol.*, 34, 914–924, <https://doi.org/10.1016/j.tree.2019.06.002>, 2019.¶~~
- ~~Boucher, O., Servonnat, J., Albright, A. L., Aumont, O., Balkanski, Y., Bastrikov, V., Bekki, S., Bonnet, R., Bony, S., Bopp, L., Braconnot, P., Brockmann, P., Cadule, P., Caubel, A., Cheruy, F., Codron, F., Cozic, A., Cugnet, D.,~~

D'Andrea, F., Davini, P., Lavergne, C. de, Denvil, S., Deshayes, J., Devilliers, M., Ducharne, A., Dufresne, J.-L., Dupont, E., Éthé, C., Fairhead, L., Falletti, L., Flavoni, S., Foujols, M.-A., Gardoll, S., Gastineau, G., Ghattas, J., Grandpeix, J.-Y., Guenet, B., Guez, L., E., Guilyardi, E., Guimberteau, M., Hauglustaine, D., Hourdin, F., Idelkadi, A., Joussaume, S., Kageyama, M., Khodri, M., Krinner, G., Lebas, N., Levvasseur, G., Lévy, C., Li, L., Lott, F., Lurton, T., Luysaert, S., Madec, G., Madeleine, J.-B., Maignan, F., Marchand, M., Marti, O., Mellul, L., Meurdesoif, Y., Mignot, J., Musat, I., Otlé, C., Peylin, P., Planton, Y., Polcher, J., Rio, C., Rochetin, N., Rousset, C., Sepulchre, P., Sima, A., Swingedouw, D., Thiéblemont, R., Traore, A. K., Vancoppenolle, M., Vial, J., Vialard, J., Viovy, N., and Vuichard, N.: Presentation and Evaluation of the IPSL-CM6A-LR Climate Model, *J. Adv. Model. Earth Syst.*, 12, e2019MS002010, <https://doi.org/10.1029/2019MS002010>, 2020.¶

~~Bugmann, H.: A Review of Forest Gap Models, *Clim. Change*, 51, 259–305, <https://doi.org/10.1023/A:1012525626267>, 2001~~  
K. M.: A Simplified Forest Model to Study Species Composition Along Climate Gradients, *Ecology*, 77, 2055–2074, <https://doi.org/10.2307/2265700>, 1996.¶

Buma, B.: Disturbance interactions: characterization, prediction, and the potential for cascading effects, *Ecosphere*, 6, art70, <https://doi.org/10.1890/ES15-00058.1>, 2015.¶

Chapin, F. S., Woodwell, G. M., Randerson, J. T., Rastetter, E. B., Lovett, G. M., Baldocchi, D. D., Clark, D. A., Harmon, M. E., Schimel, D. S., Valentini, R., Wirth, C., Aber, J. D., Cole, J. J., Goulden, M. L., Harden, J. W., Heimann, M., Howarth, R. W., Matson, P. A., McGuire, A. D., Melillo, J. M., Mooney, H. A., Neff, J. C., Houghton, R. A., Pace, M. L., Ryan, M. G., Running, S. W., Sala, O. E., Schlesinger, W. H., and Schulze, E.-D.: Reconciling Carbon-cycle Concepts, Terminology, and Methods, *Ecosystems*, 9, 1041–1050, <https://doi.org/10.1007/s10021-005-0105-7>, 2006.¶

Chen, Y., Ryder, J., Bastrikov, V., McGrath, M. J., Naudts, K., Otto, J., Otlé, C., Peylin, P., Polcher, J., Valade, A., Black, A., Elbers, J. A., Moors, E., Foken, T., van Gorsel, E., Haverd, V., Heinesch, B., Tiedemann, F., Knohl, A., Launiainen, S., Loustau, D., Ogée, J., Vessala, T., and Luysaert, S.: Evaluating the performance of land surface model ORCHIDEE-CAN v1.0 on water and energy flux estimation with a single- and multi-layer energy budget scheme, *Geosci. Model Dev.*, 9, 2951–2972, <https://doi.org/10.5194/gmd-9-2951-2016>, 2016.¶

Chen, Y.-Y., Gardiner, B., Pasztor, F., Blennow, K., Ryder, J., Valade, A., Naudts, K., Otto, J., McGrath, M. J., Planque, C., and Luysaert, S.: Simulating damage for wind storms in the land surface model ORCHIDEE-CAN (revision 4262), *Geosci. Model Dev.*, 11, 771–791, <https://doi.org/10.5194/gmd-11-771-2018>, 2018.¶

Ciais, P., Reichstein, M., Viovy, N., Granier, A., Ogée, J., Allard, V., Aubinet, M., Buchmann, N., Bernhofer, C., Carrara, A., Chevallier, F., De Noblet, N., Friend, A. D., Friedlingstein, P., Grünwald, T., Heinesch, B., Keronen, P., Knohl, A., Krinner, G., Loustau, D., Manca, G., Matteucci, G., Miglietta, F., Ourcival, J. M., Papale, D., Pilegaard, K., Rambal, S., Seufert, G., Soussana, J. F., Sanz, M. J., Schulze, E. D., Vesala, T., and Valentini, R.: Europe-wide reduction in primary productivity caused by the heat and drought in 2003, *Nature*, 437, 529–533, <https://doi.org/10.1038/nature03972>, 2005.¶

Cox, P. M., Betts, R. A., Jones, C. D., Spall, S. A., and Totterdell, I. J.: Acceleration of global warming due to carbon-cycle feedbacks in a coupled climate model, *Nature*, 408, 184–187, <https://doi.org/10.1038/35041539>, 2000.

¶

~~Deleuze, C., Pain, O., Dhôte, J.-F., and Hervé, J.-C.: A flexible radial increment model for individual trees in pure even-aged stands, *Ann. For. Sci.*, 61, 327–335, <https://doi.org/10.1051/forest:2004026>, 2004.~~

¶

~~Eswaran, H., Beinroth, F. H., and Reich, P. F.: A Global Assessment of Land Quality, Chapters, 111–132, 2003.~~

Custer, G. F., van Diepen, L. T. A., and Stump, W. L.: Structural and Functional Dynamics of Soil Microbes following Spruce Beetle Infestation, *Appl. Environ. Microbiol.*, 86, e01984-19, <https://doi.org/10.1128/AEM.01984-19>, 2020.

Das, A. J., Stephenson, N. L., and Davis, K. P.: Why do trees die? Characterizing the drivers of background tree mortality, *Ecology*, 97, 2616–2627, <https://doi.org/10.1002/ecy.1497>, 2016.


Deleuze, C., Pain, O., Dhôte, J.-F., and Hervé, J.-C.: A flexible radial increment model for individual trees in pure even-aged stands, *Ann. For. Sci.*, 61, 327–335, <https://doi.org/10.1051/forest:2004026>, 2004.



- Edburg, S. L., Hicke, J. A., Brooks, P. D., Pendall, E. G., Ewers, B. E., Norton, U., Gochis, D., Gutmann, E. D., and Meddens, A. J.: Cascading impacts of bark beetle-caused tree mortality on coupled biogeophysical and biogeochemical processes, *Front. Ecol. Environ.*, 10, 416–424, <https://doi.org/10.1890/110173>, 2012.
- Friedlingstein, P., Cox, P., Betts, R., Bopp, L., Bloh, W. von, Brovkin, V., Cadule, P., Doney, S., Eby, M., Fung, I., Bala, G., John, J., Jones, C., Joos, F., Kato, T., Kawamiya, M., Knorr, W., Lindsay, K., Matthews, H. D., Raddatz, T., Rayner, P., Reick, C., Roeckner, E., Schnitzler, K.-G., Schnur, R., Strassmann, K., Weaver, A. J., Yoshikawa, C., and Zeng, N.: Climate–Carbon Cycle Feedback Analysis: Results from the C4MIP Model Intercomparison, *J. Clim.*, 19, 3337–3353, <https://doi.org/10.1175/JCLI3800.1>, 2006.
- Grimm, V. and Wissel, C.: Babel, or the ecological stability discussions: an inventory and analysis of terminology and a guide for avoiding confusion, *Oecologia*, 109, 323–334, <https://doi.org/10.1007/s004420050090>, 1997.
- Havašová, M., Ferenčík, J., and Jakuš, R.: Interactions between windthrow, bark beetles and forest management in the Tatra national parks, *For. Ecol. Manag.*, 391, 349–361, <https://doi.org/10.1016/j.foreco.2017.01.009>, 2017.
- Haverd, V., Lovell, J. L., Cuntz, M., Jupp, D. L. B., Newnham, G. J., and Sea, W.: The Canopy Semi-analytic Pgap And Radiative Transfer (CanSPART) model: Formulation and application, *Agric. For. Meteorol.*, 160, 14–35, <https://doi.org/10.1016/j.agrformet.2012.01.018>, 2012.¶
- Hicke, J. A., Allen, C. D., Desai, A. R., Dietze, M. C., Hall, R. J., Hogg, E. H., Kashian, D. M., Moore, D., Raffa, K. F., Sturrock, R. N., and Vogelmann, J.: Effects of biotic disturbances on forest carbon cycling in the United States and Canada., <https://doi.org/10.1111/j.1365-2486.2011.02543.x>, 2012.¶
- Hlásny, T., König, L., Krokene, P., Lindner, M., Montagné-Huck, C., Müller, J., Qin, H., Raffa, K. F., Schelhaas, M.-J., Svoboda, M., Viiri, H., and Seidl, R.: Bark Beetle Outbreaks in Europe: State of Knowledge and Ways Forward for Management, *Curr. For. Rep.*, 7, 138–165, <https://doi.org/10.1007/s40725-021-00142-x>, 2021.2021a.
- Hlásny, T., Zimová, S., Merganičová, K., Štěpánek, P., Modlinger, R., and Turčáni, M.: Devastating outbreak of bark beetles in the Czech Republic: Drivers, impacts, and management implications, *For. Ecol. Manag.*, 490, 119075, <https://doi.org/10.1016/j.foreco.2021.119075>, 2021b.
- Huang, J., Kautz, M., Trowbridge, A. M., Hammerbacher, A., Raffa, K. F., Adams, H. D., Goodsmann, D. W., Xu, C., Meddens, A. J. H., Kandasamy, D., Gershenson, J., Seidl, R., and Hartmann, H.: Tree defence and bark beetles in a drying world: carbon partitioning, functioning and modelling, *New Phytol.*, 225, 26–36, <https://doi.org/10.1111/nph.16173>, 2020.
- ¶
- Jactel, H., Moreira, X., Jonášová, M. and Prach, K.: Central-European mountain spruce (*Picea abies* (L.) Karst.) forests: regeneration of tree species after a bark beetle outbreak, *Ecol. Eng.*, 23, 15–27, <https://doi.org/10.1016/j.ecoleng.2004.06.010>, 2004.
- Jönsson, A. M., Schroeder, L. M., Lagergren, F., Anderbrant, O., and CastagneyrolSmith, B.: ~~Tree Diversity and Forest Resistance to Insect Pests: Patterns, Mechanisms, and Prospects, *Annu. Rev. Entomol.*, 66, 277–296, <https://doi.org/10.1146/annurev-ento-041720-075234>, 2021.~~¶
- Guess the impact of *Ips typographus*—An ecosystem modelling approach for simulating spruce bark beetle outbreaks, *Agric. For. Meteorol.*, 166–167, 188–200, <https://doi.org/10.1016/j.agrformet.2012.07.012>, 2012.
- Kärvemo, S. and Schroeder, L. M.: A comparison of outbreak dynamics of the spruce bark beetle in Sweden and the mountain pine beetle in Canada (Curculionidae: Scolytinae), 2010.
- Kautz, M., Anthoni, P., Meddens, A. J. H., Pugh, T. A. M., and Arneith, A.: Simulating the recent impacts of multiple biotic disturbances on forest carbon cycling across the United States, *Glob. Change Biol.*, 24, 2079–2092, <https://doi.org/10.1111/gcb.13974>, 2018.¶
- Komonen, A., Schroeder, L. M., and Weslien, J.: *Ips typographus* population development after a severe storm in a nature reserve in southern Sweden, *J. Appl. Entomol.*, 135, 132–141, <https://doi.org/10.1111/j.1439-0418.2010.01520.x>, 2011.¶
- Krinner, G., Viovy, N., de Noblet-Ducoudré, N., Ogée, J., Polcher, J., Friedlingstein, P., Ciais, P., Sitch, S., and Prentice, I. C.: A dynamic global vegetation model for studies of the coupled atmosphere-biosphere system: DVGCM FOR COUPLED CLIMATE STUDIES, *Glob. Biogeochem. Cycles*, 19, <https://doi.org/10.1029/2003GB002199>, 2005.
- Kurz, W. A., Dymond, C. C., Stinson, G., Rampley, G. J., Neilson, E. T., Carroll, A. L., Ebata, T., and Safranyik, L.: Mountain pine beetle and forest carbon feedback to climate change, *Nature*, 452, 987–990, <https://doi.org/10.1038/nature06777>, 2008a.



Kurz, W. A., Dymond, C. C., Stinson, G., Rampley, G. J., Neilson, E. T., Carroll, A. L., Ebata, T., and Safranyik, L.: Mountain pine beetle and forest carbon feedback to climate change, *Nature*, 452, 987–990, <https://doi.org/10.1038/nature06777>, 2008. 

~~Lasslop, G., Thonicke, K., and Kloster, S.: SPITFIRE within the MPI Earth system model: Model development and evaluation, *J. Adv. Model. Earth Syst.*, 6, 740–755, <https://doi.org/10.1002/2013MS000284>, 2014.~~ 

Kurz, W. A., Stinson, G., Rampley, G. J., Dymond, C. C., and Neilson, E. T.: Risk of natural disturbances makes future contribution of Canada's forests to the global carbon cycle highly uncertain, *Proc. Natl. Acad. Sci.*, 105, 1551–1555, <https://doi.org/10.1073/pnas.0708133105>, 2008c.

Lasslop, G., Thonicke, K., and Kloster, S.: SPITFIRE within the MPI Earth system model: Model development and evaluation, *J. Adv. Model. Earth Syst.*, 6, 740–755, <https://doi.org/10.1002/2013MS000284>, 2014.

Lausch, A., Fahse, L., and Heurich, M.: Factors affecting the spatio-temporal dispersion of *Ips typographus* (L.) in Bavarian Forest National Park: A long-term quantitative landscape-level analysis, *For. Ecol. Manag.*, 261, 233–245, <https://doi.org/10.1016/j.foreco.2010.10.012>, 2011.

Levins, R.: The Strategy of Model Building in Population Biology, *Am. Sci.*, 54, 421–431, 1966. 

Lieutier, F.: Mechanisms of Resistance in Conifers and Bark beetle Attack Strategies, in: Mechanisms and Deployment of Resistance in Trees to Insects, edited by: 

Wagner, M. R., Clancy, K. M., Lieutier, F., and Paine, T. D., Springer Netherlands, Dordrecht, 31–77, [https://doi.org/10.1007/0-306-47596-0\\_2](https://doi.org/10.1007/0-306-47596-0_2), 2002.

Lombardero, M. J., Ayres, M. P., Ayres, B. D., and Reeve, J. D.: Cold Tolerance of Four Species of Bark Beetle (Coleoptera: Scolytidae) in North America, *Environ. Entomol.*, 29, 421–432, <https://doi.org/10.1603/0046-225X-29.3.421>, 2000.

Luyssaert, S., Marie, G., Valade, A., Chen, Y.-Y., Njakou Djomo, S., Ryder, J., Otto, J., Naudts, K., Lansø, A. S., Ghattas, J., and McGrath, M. J.: Trade-offs in using European forests to meet climate objectives, *Nature*, 562, 259–262, <https://doi.org/10.1038/s41586-018-0577-1>, 2018.

Marini, L., Økland, B., Jönsson, A. M., Bentz, B., Carroll, A., Forster, B., Grégoire, J.-C., Hurling, R., Nageleisen, L. M., Netherer, S., Ravn, H. P., Weed, A., and Schroeder, M.: Climate drivers of bark beetle outbreak dynamics in Norway spruce forests, *Ecography*, 40, 1426–1435, <https://doi.org/10.1111/ecog.02769>, 2017.

Mezei, P., Grodzki, W., Blaženec, M., and Jakuš, R.: Factors influencing the *wind–bark beetles'* disturbance system in the course of an *Ips typographus* outbreak in the Tatra Mountains, *For. Ecol. Manag.*, 312, 67–77, <https://doi.org/10.1016/j.foreco.2013.10.020>, 2014.

Mezei, P., Jakuš, R., Pennerstorfer, J., Havašová, M., Škvarenina, J., Ferenčík, J., Slivinský, J., Bičárová, S., Bilčík, D., Blaženec, M., and Netherer, S.: Storms, temperature maxima and the Eurasian spruce bark beetle *Ips typographus*—An infernal trio in Norway spruce forests of the Central European High Tatra Mountains, *Agric. For. Meteorol.*, 242, 85–95, <https://doi.org/10.1016/j.agrformet.2017.04.004>, 2017. 

Migliavacca, M., Dosio, A., Kloster, S., Ward, D. S., Camia, A., Houborg, R., Houston Durrant, T., Khabarov, N., Krasovskii, A. A., San Miguel-Ayanz, J., and Cescatti, A.: Modeling burned area in Europe with the Community Land Model, *J. Geophys. Res. Biogeosciences*, 118, 265–279, <https://doi.org/10.1002/jgrg.20026>, 2013. 

Migliavacca, M., Musavi, T., Mahecha, M. D., Nelson, J. A., Knauer, J., Baldocchi, D. D., Perez-Priego, O., Christiansen, R., Peters, J., Anderson, K., Bahn, M., Black, T. A., Blanken, P. D., Bonal, D., Buchmann, N., Caldararu, S., Carrara, A., Carvalhais, N., Cescatti, A., Chen, J., Cleverly, J., Cremonese, E., Desai, A. R., El-Madany, T. S., Farella, M. M., Fernández-Martínez, M., Filippa, G., Forkel, M., Galvagno, M., Gomasasca, U., Gough, C. M., Göckede, M., Ibrom, A., Ikawa, H., Janssens, I. A., Jung, M., Kattge, J., Keenan, T. F., Knohl, A., Kobayashi, H., Kraemer, G., Law, B. E., Liddell, M. J., Ma, X., Mammarella, I., Martini, D., Macfarlane, C., Matteucci, G., Montagnani, L., Pabon-Moreno, D. E., Panigada, C., Papale, D., Pendall, E., Penuelas, J., Phillips, R. P., Reich, P. B., Rossini, M., Rotenberg, E., Scott, R. L., Stahl, C., Weber, U., Wohlfahrt, G., Wolf, S., Wright, I. J., Yakir, D., Zaehle, S., and Reichstein, M.: The three major axes of terrestrial ecosystem function, *Nature*, 598, 468–472, <https://doi.org/10.1038/s41586-021-03939-9>, 2021. 

Millar, C. I. and Stephenson, N. L.: Temperate forest health in an era of emerging megadisturbance, *Science*, 349, 823–826, <https://doi.org/10.1126/science.aaa9933>, 2015.



~~Nageleisen, L. M. and Grégoire, J.-C.: Une vie de typographe : point des connaissances sur la biologie d'*Ips*~~

- ~~*typographus* (Linnaeus 1758), Rev. For. Fr., 73, 479–498, <https://doi.org/10.20870/revforfr.2021.5565>, 2022.~~¶
- Morehouse, K., Johns, T., Kaye, J., and Kaye, M.: Carbon and nitrogen cycling immediately following bark beetle outbreaks in southwestern ponderosa pine forests, *For. Ecol. Manag.*, 255, 2698–2708, <https://doi.org/10.1016/j.foreco.2008.01.050>, 2008.
- Nardi, D., Jactel, H., Pagot, E., Samalens, J.-C., and Marini, L.: Drought and stand susceptibility to attacks by the European spruce bark beetle: A remote sensing approach, *Agric. For. Entomol.*, ~~afe.12536~~25, 119–129, <https://doi.org/10.1111/afe.12536>, 2022.¶
- Naudts, K., Ryder, J., McGrath, M. J., Otto, J., Chen, Y., Valade, A., Bellasen, V., Berhongaray, G., Bönisch, G., Campioli, M., and others: A vertically discretised canopy description for ORCHIDEE (SVN r2290) and the modifications to the energy, water and carbon fluxes, *Geosci. Model Dev.*, 8, 2035–2065, 2015a.
- Naudts, K., Ryder, J., McGrath, M. J., Otto, J., Chen, Y., Valade, A., Bellasen, V., Berhongaray, G., Bönisch, G., Campioli, M., Ghattas, J., De Groote, T., Haverd, V., Kattge, J., MacBean, N., Maignan, F., Merilä, P., Penuelas, J., Peylin, P., Pinty, B., Pretzsch, H., Schulze, E. D., Solyga, D., Vuichard, N., Yan, Y., and Luysaert, S.: A vertically discretised canopy description for ORCHIDEE (SVN r2290) and the modifications to the energy, water and carbon fluxes, *Geosci. Model Dev.*, 8, 2035–2065, <https://doi.org/10.5194/gmd-8-2035-2015>, 2015b.
- Naudts, K., Chen, Y., McGrath, M. J., Ryder, J., Valade, A., Otto, J., and Luysaert, S.: Europe’s forest management did not mitigate climate warming, *Science*, 351, 597–600, <https://doi.org/10.1126/science.aad7270>, 2016.
- Netherer, S., Matthews, B., Katzensteiner, K., Blackwell, E., Henschke, P., Hietz, P., Pennerstorfer, J., Rosner, S., Kikuta, S., Schume, H., and Schopf, A.: Do water-limiting conditions predispose Norway spruce to bark beetle attack?, *New Phytol.*, 205, 1128–1141, <https://doi.org/10.1111/nph.13166>, 2015.¶
- Ogris, N., Ferlan, M., Hauptman, T., Pavlin, R., Kavčič, A., Jurc, M., and de Groot, M.: RITY – A phenology model of *Ips typographus* as a tool for optimization of its monitoring, *Ecol. Model.*, 410, 108775, <https://doi.org/10.1016/j.ecolmodel.2019.108775>, 2019.¶
- Pastorello, G., Trotta, C., Canfora, E., Chu, H., Christianson, D., Cheah, Y.-W., Poindexter, C., Chen, J., Elbashandy, A., Humphrey, M., Isaac, P., Polidori, D., Reichstein, M., Ribeca, A., van Ingen, C., Vuichard, N., Zhang, L., Amiro, B., Ammann, C., Arain, M. A., Ardö, J., Arkebauer, T., Arndt, S. K., Arriga, N., Aubinet, M., Aurela, M., Baldocchi, D., Barr, A., Beamesderfer, E., Marchesini, L. B., Bergeron, O., Beringer, J., Bernhofer, C., Berveiller, D., Billesbach, D., Black, T. A., Blanken, P. D., Bohrer, G., Boike, J., Bolstad, P. V., Bonal, D., Bonnefond, J.-M., Bowling, D. R., Bracho, R., Brodeur, J., Brümmer, C., Buchmann, N., Burban, B., Burns, S. P., Buisse, P., Cale, P., Cavagna, M., Cellier, P., Chen, S., Chini, I., Christensen, T. R., Cleverly, J., Collalti, A., Consalvo, C., Cook, B. D., Cook, D., Coursolle, C., Cremonese, E., Curtis, P. S., D’Andrea, E., da Rocha, H., Dai, X., Davis, K. J., Cinti, B. D., Grandcourt, A. de Ligne, A. D., De Oliveira, R. C., Delpierre, N., Desai, A. R., Di Bella, C. M., Tommasi, P. di, Dolman, H., Domingo, F., Dong, G., Dore, S., Duce, P., Dufrêne, E., Dunn, A., Dušek, J., Eamus, D., Eichelmann, U., ElKhidir, H. A. M., Eugster, W., Ewenz, C. M., Ewers, B., Famulari, D., Fares, S., Feigenwinter, I., Feitz, A., Fensholt, R., Filippa, G., Fischer, M., Frank, J., Galvagno, M., et al.: The FLUXNET2015 dataset and the ONEFlux processing pipeline for eddy covariance data, *Sci. Data*, 7, 225, <https://doi.org/10.1038/s41597-020-0534-3>, 2020.¶
- Pasztor, F., Matulla, C., Rammer, W., and Lexer, M. J.: Drivers of the bark beetle disturbance regime in Alpine forests in Austria, *For. Ecol. Manag.*, 318, 349–358, <https://doi.org/10.1016/j.foreco.2014.01.044>, 2014.¶
- ~~Pineau, X., Bourguignon, M., Jactel, H., Lieutier, F., Pfeifer, E. M., Hicke, J. A., and Sallé, A.: Pyrrhic victory for bark beetles: Successful standing tree colonization triggers strong intraspecific competition for offspring of *Ips sexdentatus*, *For. Ecol. Manag.*, 399, 188–196, <https://doi.org/10.1016/j.foreco.2017.05.044>, 2017.~~¶
- ~~Pörtner, H.-O., Roberts, D. C., Tignor, M. M. B., Poloczanska, E. S., Mintenbeck, K., Alegría, A., Craig, M., Langsdorf, S., Löschke, S., Möller, V., Okem, J. H.: Observations and modeling of aboveground tree carbon stocks and fluxes following a bark beetle outbreak in the western United States, *Glob. Change Biol.*, 17, 339–350, <https://doi.org/10.1111/j.1365-2486.2010.02226.x>, 2011.~~
- Pineau, X., David, G., Peter, Z., Sallé, A., Baude, M., Lieutier, F., and Jactel, H.: Effect of temperature on the reproductive success, developmental rate and brood characteristics of *Ips sexdentatus* (Boern.), *Agric. For. Entomol.*, 19, 23–33, <https://doi.org/10.1111/afe.12177>, 2017.
- ~~Preisler, H. K., Hicke, J. A., Ager, A. A., and Rama, B. (Eds.): Climate Change 2022: Impacts, Adaptation and Vulnerability. Contribution of Working Group II to the Sixth Assessment Report of the Intergovernmental Panel on Climate Change., 2022.~~¶

¶

~~Pugh, T. A. M., Lindeskog, M., Smith, B., Poulter, B., Hayes, J. L.: Climate and weather influences on spatial temporal patterns of mountain pine beetle populations in Washington and Oregon, *Ecology*, 93, 2421–2434, <https://doi.org/10.1890/11-1412.1>, 2012.~~

~~Pugh, T. A. M., Jones, C. D., Huntingford, C., Burton, C., Arneeth, A., Haverd, V., and Calle, L.: Role of forest regrowth in global carbon sink dynamics, *Proc. Natl. Acad. Sci.*, 116, 4382–4387, <https://doi.org/10.1073/pnas.1810512116>, 2019.~~¶

~~Ciais, P., Lomas, M., Robertson, E., and Piao, S. L.: A Large Committed Long-Term Sink of Carbon due to Vegetation Dynamics, *Earths Future*, 2017.~~

~~Quillet, A., Peng, C., and Garneau, M.: Toward dynamic global vegetation models for simulating vegetation–climate interactions and feedbacks: recent developments, ¶~~

~~limitations, and future challenges, *Environ. Rev.*, 18, 333–353, <https://doi.org/10.1139/A10-016>, 2010.~~¶

~~Raffa, K. F., Aukema, B. H., Bentz, B. J., Carroll, A. L., Hicke, J. A., Turner, M. G., and Romme, W. H.: Cross-scale Drivers of Natural Disturbances Prone to ¶~~

~~Anthropogenic Amplification: The Dynamics of Bark Beetle Eruptions, *BioScience*, 58, 501–517, <https://doi.org/10.1641/B580607>, 2008.~~

¶

~~Reeve, J. D. and Turchin, P.: Evidence for Predator–Prey Cycles in a Bark Beetle, in: *Population Cycles: The Case for Trophic Interactions*, edited by: Berryman, A., Oxford University Press, 0, <https://doi.org/10.1093/oso/9780195140989.003.0009>, 2002.~~¶

~~Rhoades, C. C.: Soil Nitrogen Leaching in Logged Beetle-Killed Forests and Implications for Riparian Fuel Reduction, *J. Environ. Qual.*, 48, 305–313, <https://doi.org/10.2134/jeq2018.04.0169>, 2019.~~

~~Ryder, J., Polcher, J., Peylin, P., Otlé, C., Chen, Y., van Gorsel, E., Haverd, V., McGrath, M. J., Naudts, K., Otto, J., Valade, A., and Luysaert, S.: A multi-layer land surface energy budget model for implicit coupling with global atmospheric simulations, *Geosci. Model Dev.*, 9, 223–245, <https://doi.org/10.5194/gmd-9-223-2016>, 2016.~~¶

~~Schumacher, S., Bugmann, H., and Mladenoff, D. J.: Improving the formulation of tree growth and succession in a spatially explicit landscape model, *Ecol. Model.*, 180, 175–194, <https://doi.org/10.1016/j.ecolmodel.2003.12.055>, 2004.~~¶

~~: The role of large-scale disturbances and climate for the dynamics of forested landscapes in the European Alps, Doctoral Thesis, ETH Zurich, <https://doi.org/10.3929/ethz-a-004818825>, 2004.~~

~~Seidl, R. and Rammer, W.: Climate change amplifies the interactions between wind and bark beetle disturbances in forest landscapes, *Landsc. Ecol.*, 1–14, <https://doi.org/10.1007/s10980-016-0396-4>, 2016.~~

~~Seidl, R., Fernandes, P. M., Fonseca, T. F., Gillet, F., Jönsson, A. M., Merganičová, K., Netherer, S., Arpacı, A., Bontemps, J.-D., Bugmann, H., González-Olabarria, J. R., Lasch, P., Meredieu, C., Moreira, F., Schelhaas, M.-J., and Mohren, F.: Modelling natural disturbances in forest ecosystems: a review, *Ecol. Model.*, 222, 903–924, <https://doi.org/10.1016/j.ecolmodel.2010.09.040>, 2011.~~¶

~~Seidl, R., Schelhaas, M.-J., Rammer, W., and Verkerk, P. J.: Increasing forest disturbances in Europe and their impact on carbon storage, *Nat. Clim. Change*, 4, 806–810, <https://doi.org/10.1038/nclimate2318>, 2014.~~¶

~~Seidl, R., Thom, D., Kautz, M., Martin-Benito, D., Peltoniemi, M., Vacchiano, G., Wild, J., Ascoli, D., Petr, M., Honkaniemi, J., Lexer, M. J., Trotsiuk, V., Mairota, P., Svoboda, M., Fabrika, M., Nagel, T. A., and Reyer, C. P. O.: Forest disturbances under climate change, *Nat. Clim. Change*, 7, 395–402, <https://doi.org/10.1038/nclimate3303>, 2017.~~¶

~~Seidl, R., Klöner, G., Rammer, W., Essl, F., Moreno, A., Neumann, M., and Dullinger, S.: Invasive alien pests threaten the carbon stored in Europe’s forests, *Nat. Commun.*, 9, 1626, <https://doi.org/10.1038/s41467-018-04096-w>, 2018.~~¶

~~Senf, C., Müller, J., Pflugmacher, D., Hostert, P., and Seidl, R.: Post-disturbance recovery of forest cover and tree height differ with management in Central Europe, *Landsc. Ecol.*, 34, 2837–2850, <https://doi.org/10.1007/s10980-019-00921-9>, 2019.~~¶

¶

~~SHINOZAKI, K., YODA, K., HOZUMI, K., and KIRA, T.: A QUANTITATIVE ANALYSIS OF PLANT~~

~~FORM THE PIPE MODEL THEORY - I. BASIC ANALYSES, 1964.~~¶

¶

~~Sitch, S., Smith, B., Prentice, I. C., Arneeth, A., Bondeau, A., Cramer, W., Kaplan, J. O., Levis, S., Lucht, W., Sykes, M. T., Thonicke, K., and Venevsky, S.: Evaluation of ecosystem dynamics, plant geography and terrestrial carbon cycling in the LPJ dynamic global vegetation model, *Glob. Change Biol.*, 9, 161–185, <https://doi.org/10.1046/j.1365-2486.2003.00569.x>, 2003.~~¶

¶

~~Staal, A., Fetzer, I., Wang-Erlandsson, L., Bosmans, J. H. C., Dekker, S. C., van Nes, E. H., Rockström, J., and Tuinenburg, O. A.: Hysteresis of tropical forests in the 21st century, *Nat. Commun.*, 11, 4978, <https://doi.org/10.1038/s41467-020-18728-7>, 2020.~~¶

¶

~~Storaunet, K. O. and Rolstad, J.: How long do Norway spruce snags stand? Evaluating four estimation methods, *Can. J. For. Res.*, 34, 376–383, <https://doi.org/10.1139/x03-248>, 2004.~~¶

Using Landsat time series for characterizing forest disturbance dynamics in the coupled human and natural systems of Central Europe, *ISPRS J. Photogramm. Remote Sens.*, 130, 453–463, <https://doi.org/10.1016/j.isprsjprs.2017.07.004>, 2017.

Storaunet, K. O., Rolstad, J., Gjerde, I., and Gundersen, V. S.: Historical logging, productivity, and structural characteristics of boreal coniferous forests in Norway, *Silva Fenn.*, 39, 2005.

Temperli, C., Bugmann, H., and Elkin, C.: Cross-scale interactions among bark beetles, climate change, and wind disturbances: a landscape modeling approach, *Ecol. Monogr.*, 83, 383–402, <https://doi.org/10.1890/12-1503.1>, 2013a.

Temperli, C., Bugmann, H., and Elkin, C.: Cross-scale interactions among bark beetles, climate change, and wind disturbances: a landscape modeling approach, *Ecol. Monogr.*, 83, 383–402, <https://doi.org/10.1890/12-1503.1>, 2013b.

~~Thurner, M., Beer, C., Santoro, M., Carvalhais, N., Wutzler, T., Schepaschenko, D., Shvidenko, A., Kompter, E., Ahrens, B., Levick, S. R., and Schmullius, C.: Carbon stock and density of northern Ciais, P., Friend, A. D., Ito, A., Kleidon, A., Lomas, M. R., Quegan, S., Rademacher, T. T., Schaphoff, S., Tum, M., Wiltshire, A., and Carvalhais, N.: Evaluation of climate-related carbon turnover processes in global vegetation models for boreal and temperate forests, *Glob. Ecol. Biogeogr. Change Biol.*, 23, 297–310, 3076–3091, <https://doi.org/10.1111/gcb.12125>, 2014.~~¶  
gcb.13660, 2017.

Van Meerbeek, K., Jucker, T., and Svenning, J.-C.: Unifying the concepts of stability and resilience in ecology, *J. Ecol.*, 109, 3114–3132, <https://doi.org/10.1111/1365-2745.13651>, 2021.¶

Vuichard, N., Messina, P., Luysaert, S., Guenet, B., Zaehle, S., Ghattas, J., Bastrikov, V., and Peylin, P.: Accounting for carbon and nitrogen interactions in the global terrestrial ecosystem model ORCHIDEE (trunk version, rev 4999): multi-scale evaluation of gross primary production, *Geosci. Model Dev.*, 12, 4751–4779, <https://doi.org/10.5194/gmd-12-4751-2019>, 2019.

Wermelinger, B.: Ecology and management of the spruce bark beetle *Ips typographus*—a review of recent research, *For. Ecol. Manag.*, 202, 67–82, <https://doi.org/10.1016/j.foreco.2004.07.018>, 2004.

Wichmann, L. and Ravn, H. P.: The spread of *Ips typographus* (L.) (Coleoptera, Scolytidae) attacks following heavy windthrow in Denmark, analysed using GIS, *For. Ecol. Manag.*, 148, 31–39, [https://doi.org/10.1016/S0378-1127\(00\)00477-1](https://doi.org/10.1016/S0378-1127(00)00477-1), 2001.

Yao, Y., Joetzjer, E., Ciais, P., Viovy, N., Cresto Aleina, F., Chave, J., Sack, L., Bartlett, M., Meir, P., Fisher, R., and Luysaert, S.: Forest fluxes and mortality response to drought: model description (ORCHIDEE-CAN-NHA r7236) and evaluation at the Caxiuana drought experiment, *Geosci. Model Dev.*, 15, 7809–7833, <https://doi.org/10.5194/gmd-15-7809-2022>, 2022.

Yi-Ying, C., Gardiner, B., Pasztor, F., Blennow, K., Ryder, J., Valade, A., Naudts, K., Otto, J., McGrath, M. J., and Planque, C.: Simulating damage for wind storms in the land surface model ORCHIDEE-CAN (revision 4262), *Geosci. Model Dev.*, 11, 771, 2018.

Yue, C., Ciais, P., Cadule, P., Thonicke, K., Archibald, S., Poulter, B., Hao, W. M., Hantson, S., Mouillot, F., Friedlingstein, P., Maignan, F., and Viovy, N.: Modelling the role of fires in the terrestrial carbon balance by incorporating SPITFIRE into the global vegetation model ORCHIDEE – Part 1: simulating historical global burned area and fire regimes, *Geosci. Model Dev.*, 7, 2747–2767, <https://doi.org/10.5194/gmd-7-2747-2014>, 2014.¶

Zaehle, S. and Dalmonech, D.: Carbon–nitrogen interactions on land at global scales: current understanding in modelling climate biosphere feedbacks, *Curr. Opin. Environ. Sustain.*, 3, 311–320,

<https://doi.org/10.1016/j.cosust.2011.08.008>, 2011.¶

Zaehle, S. and Friend, A. D.: Carbon and nitrogen cycle dynamics in the O-CN land surface model: 1. Model description, site-scale evaluation, and sensitivity to parameter estimates, *Glob. Biogeochem. Cycles*, 24, <https://doi.org/10.1029/2009GB003521>, 2010.¶




Zhang, Q.-H. and Schlyter, F.: Olfactory recognition and behavioural avoidance of angiosperm nonhost volatiles by conifer-inhabiting bark beetles, *Agric. For. Entomol.*, 6, 1–20, <https://doi.org/10.1111/j.1461-9555.2004.00202.x>, 2004.¶

Zscheischler, J., Westra, S., van den Hurk, B. J. J. M., Seneviratne, S. I., Ward, P. J., Pitman, A., AghaKouchak, A., Bresch, D. N., Leonard, M., Wahl, T., and Zhang, X.: Future climate risk from compound events, *Nat. Clim. Change*, 8, 469–477, <https://doi.org/10.1038/s41558-018-0156-3>, 2018.

¶

**Figures :** ¶

¶

-  Developed for ORCHIDEE
-  Developed for ORCHIDEE but inactivated
-  Not developed for ORCHIDEE

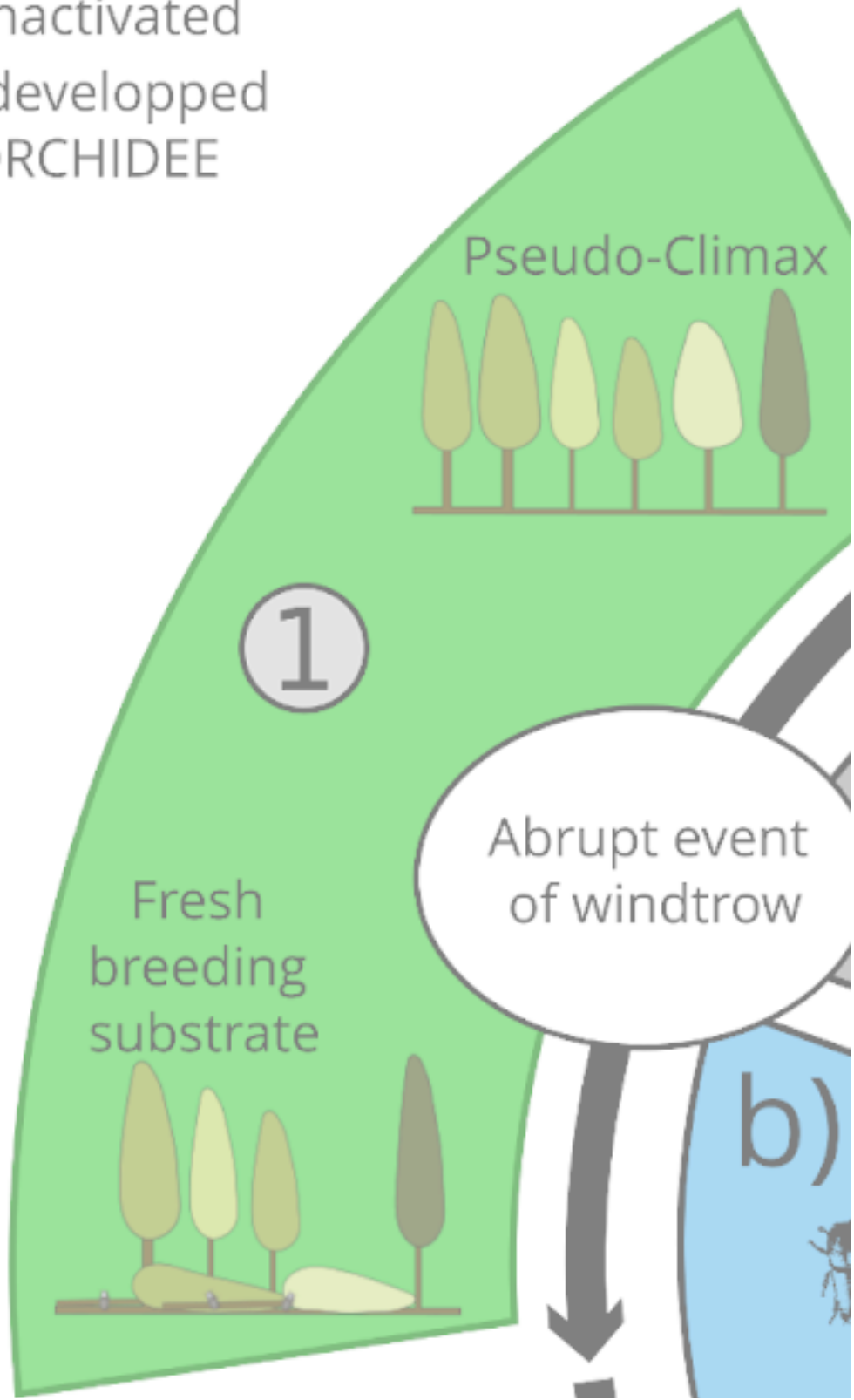
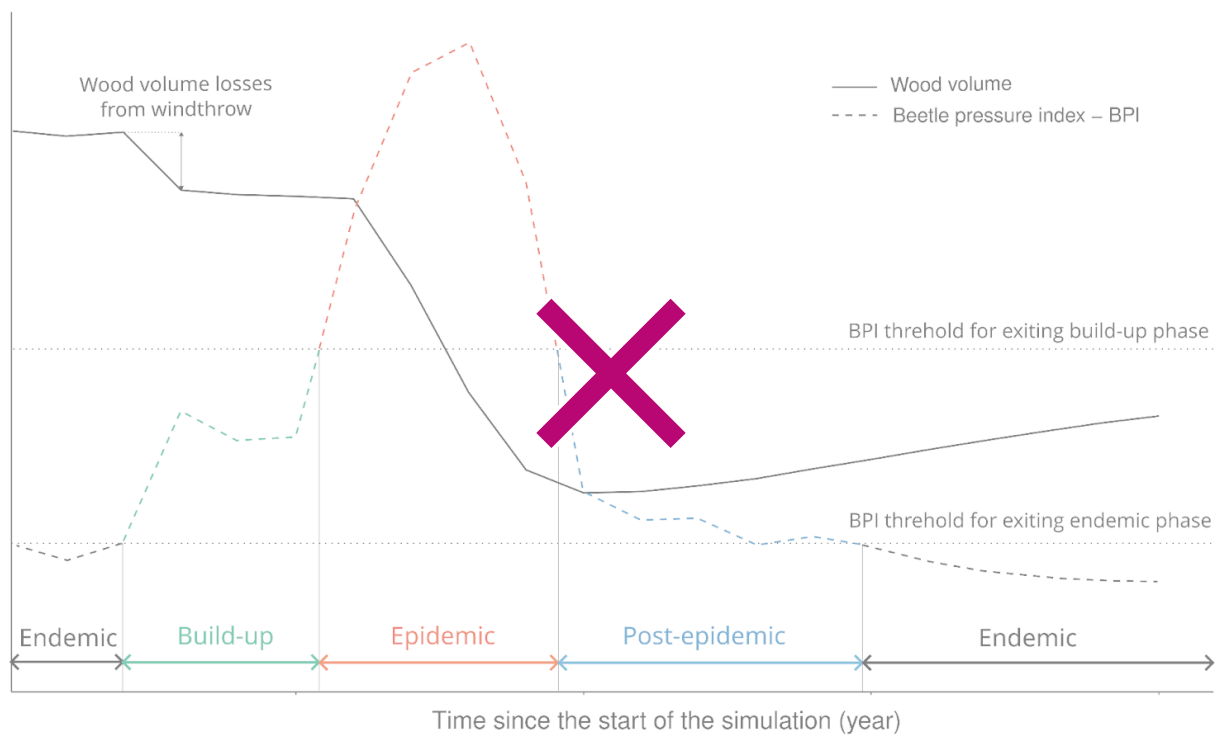


Figure 1: Life cycle of a bark beetle outbreak and subsequent dynamics of a forest stand. The life cycle of an outbreak includes the following stages: a) the “endemic stage” at which the forest stand experiences low bark beetle pressure enabling the forest to maintain a pseudo-climax or climax depending on whether the stand is managed or not (shown as stage 1). b) The “build-up” stage is characterized by a rapid increase in the bark beetle population due to an event that weakened part of the trees but without visible impact on healthy trees (stage 1 & 2). c) During the “epidemic stage” bark beetles are so numerous that they can successfully attack healthy trees causing a change in leaf colour (stage 2 & 3). d) In the “post-epidemic stage” a significant reduction in the bark beetle population occurs due to a lack of substrate for feeding and breeding (stage 3 & 4). Stage 4: In the “gray stage” infected trees that retain their leaves and remain standing, gradually die turning into so-called snags. Stage 5: in the “ecological transition” stage degradation from wind throws and bark beetles result in openings in the canopy reducing between-tree competitions. In Stage 6 bark beetles return to their initial population level resulting in a new endemic stage during which recruitment may help the forest to reach a (pseudo-)climax stage.

¶  
¶  
¶

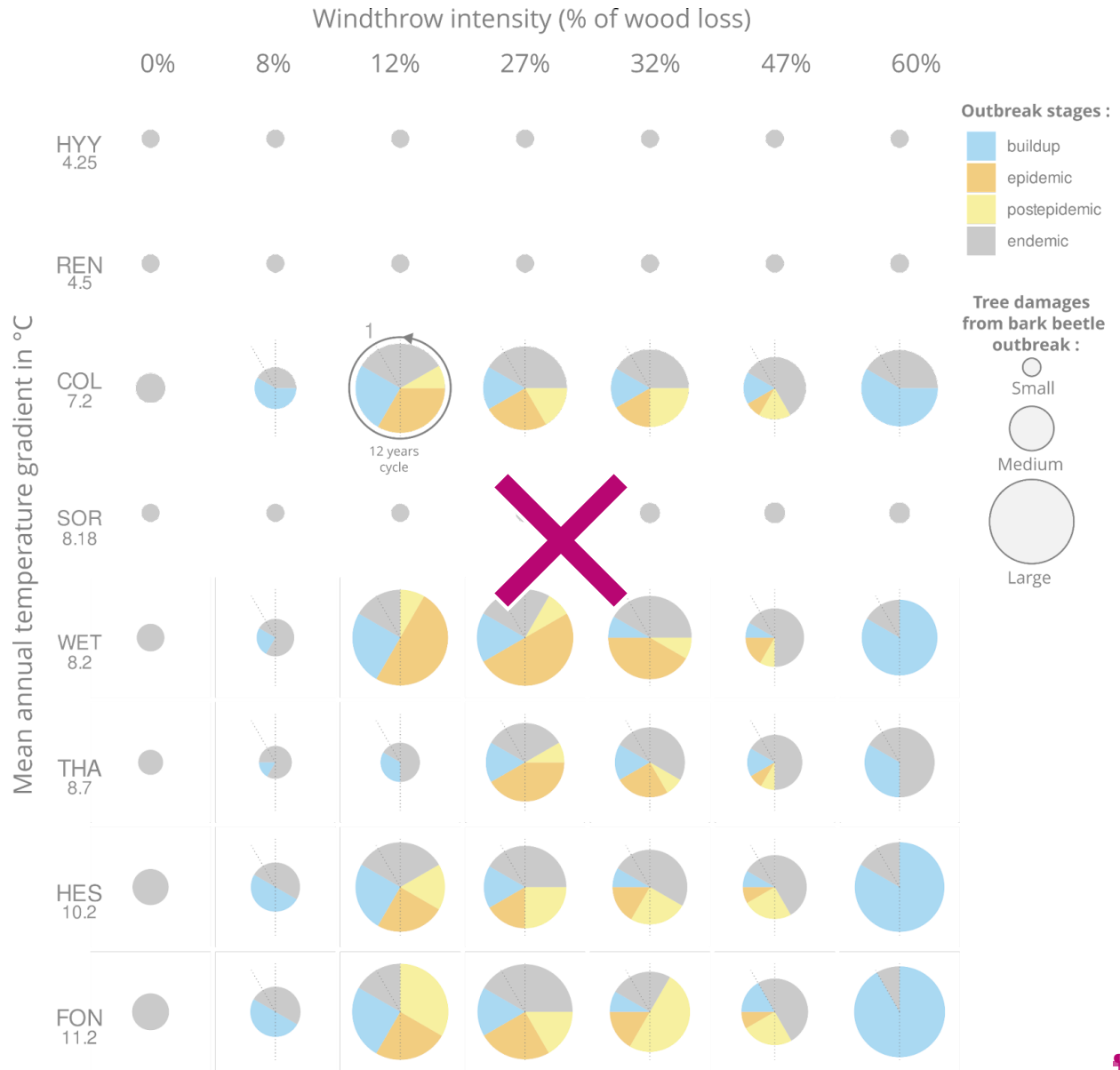


¶

Figure 2: The endemic, build-up (green), epidemic (red), and post-epidemic (blue) stages in the development of a bark beetle outbreak based on synthetic data. The beetle outbreak stages are defined on the basis of the beetle pressure index (unitless) which is a proxy of beetle population size and shown as the dotted line. The full line represents the evolution of wood volume ( $m^3/ha$ ).

¶  
¶



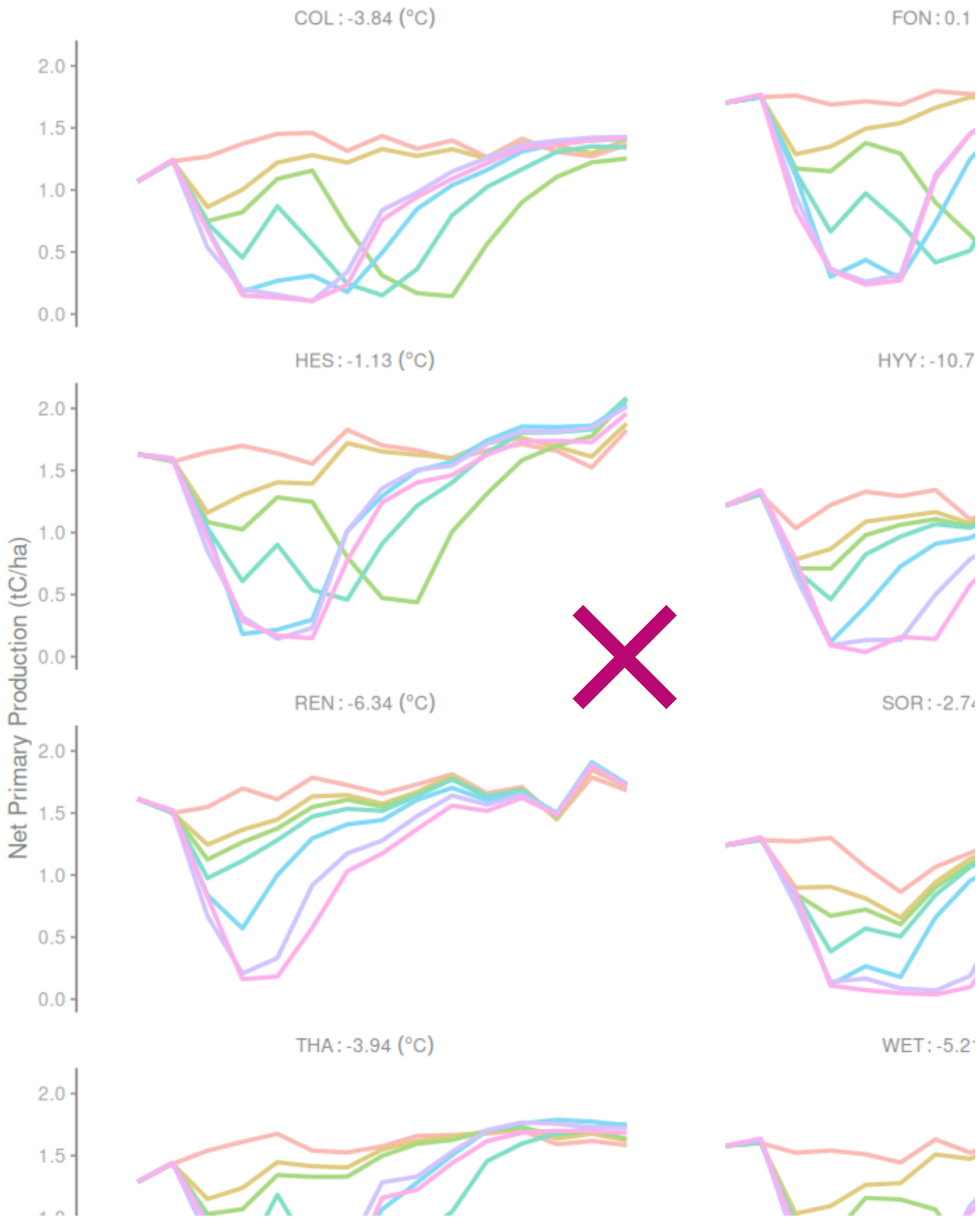


~~Figure 3: Simulated dynamic of bark beetle outbreaks in spruce forests in the first 20 years after a windthrow event. The criteria used to attribute the simulated beetle population to the different outbreak stages is detailed in table 5. In the left panel an identical and fixed relative wood volume loss from windthrow (i.e., 12%) was applied for each site. The eight sites (Table 4) were used as reference sites for which seven additional simulations were run in order to evaluate the impact of windthrow intensity (outbreak trigger intensity) on the length of the outbreak stages. The simulated relationship between wind speeds and relative wood losses from windthrow are given in Table 3.~~



Wind speed max(m/s)    19    23    29    35

21    25    35



~~Figure 4: Net primary production for a simulation period of 15 years. At the beginning of year two a windthrow event is forced based on its maximum wind speed (colored line). Each wind speed corresponds to a certain amount of wood loss (see Table 3 for the corresponded value). Each panel represents one of the eight FLUXNET sites studied.~~

~~¶  
¶  
¶~~

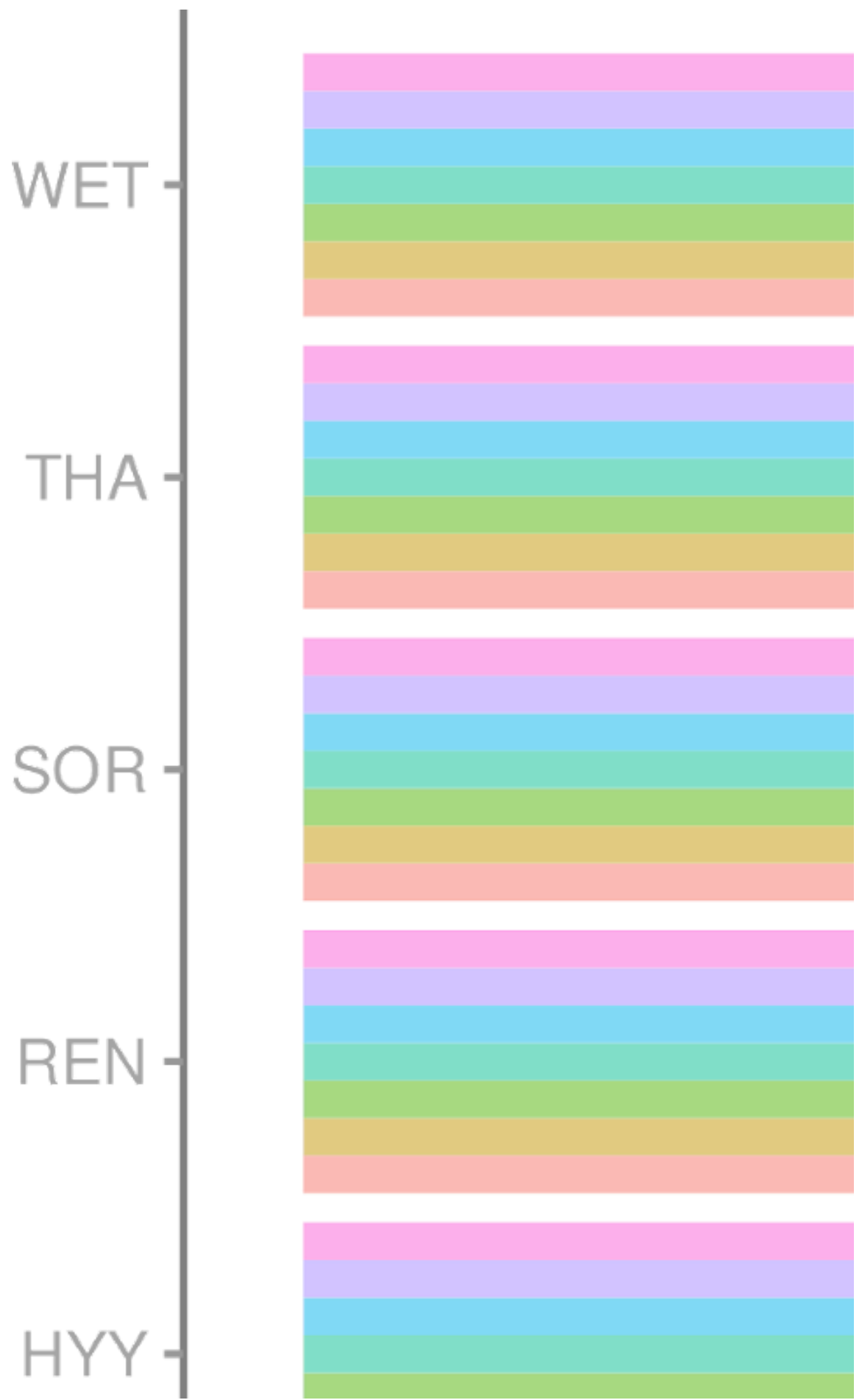


**Figure 5:** Accumulated net primary production over 15 years. Each group of colored bars represents a Fluxnet site for which seven wind storm intensities have been tested. Higher values mean undisturbed forests and lower values mean highly disturbed forests. See table 3 for the corresponding wood loss % at each max wind speed.

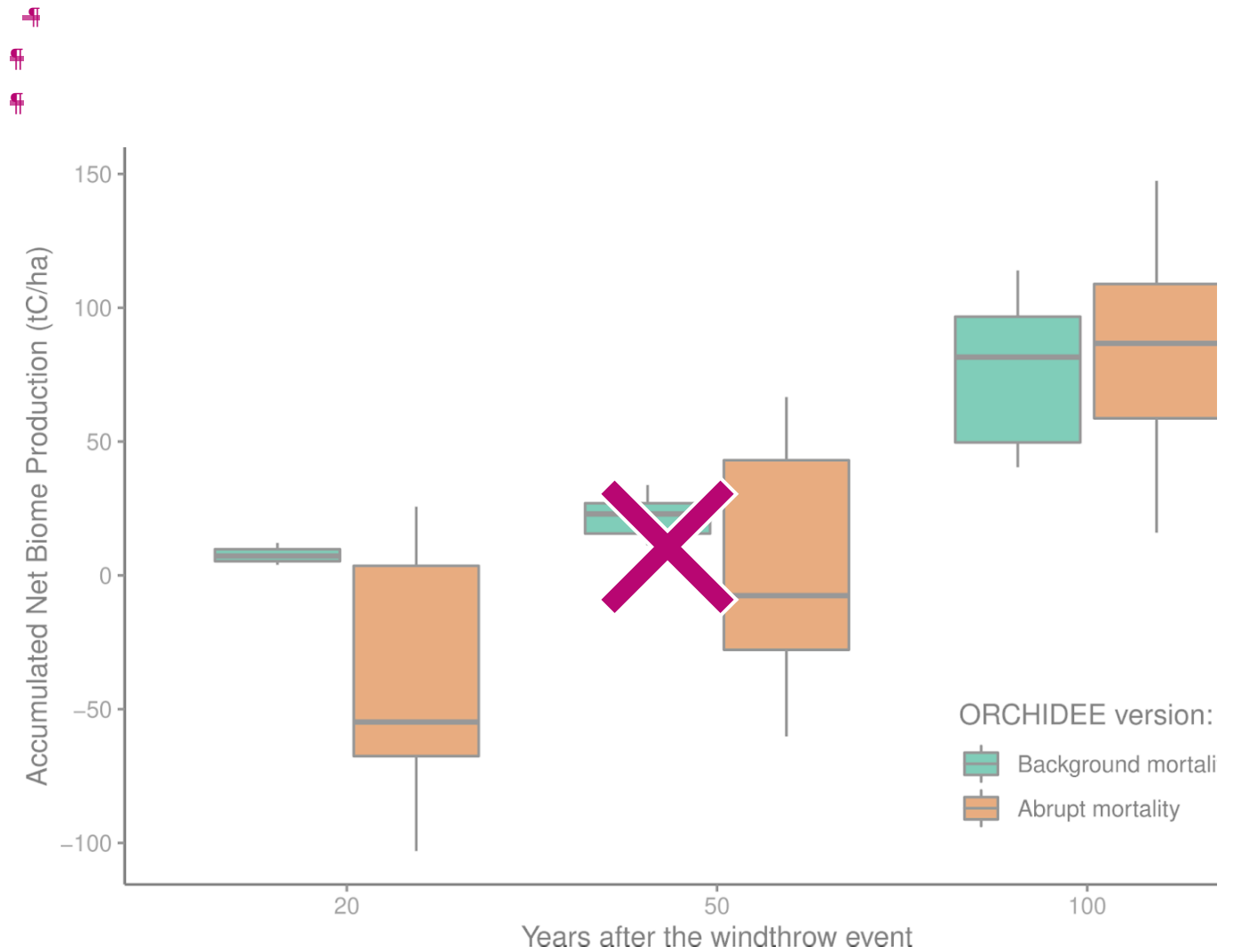


**Figure 6:** Difference in cumulative net biome production at three discrete time horizons (i.e. 20, 50 and 100 years) between a continuous (green) and abrupt (orange) mortality framework. Note that in the continuous mortality framework the mortality rate was adjusted to obtain a similar number of trees killed after 100 years as in the abrupt mortality framework. The variation of each boxplot arises due to different locations and prescribed storm intensities. Each boxplot displays the median value (thick horizontal line), the quartile range (box border), and the 95% confidence interval (vertical line).

## Tables :

**Table 1:** List of abbreviations

| Symbol | Description | Units |
|--------|-------------|-------|
|--------|-------------|-------|

|                              |  |                          |
|------------------------------|--|--------------------------|
| <del>Act<sub>y-1</sub></del> | <del>Bark beetle activity index in the previous year</del>                     | <del>unitless</del>      |
| <del>Age</del>               | <del>Age of the dominant spruce trees in a spatial entity</del>                | <del>year</del>          |
| <del>BA</del>                | <del>Basal area of trees in a spatial entity</del>                             | <del>m<sup>2</sup></del> |
| <del>Bdb</del>               | <del>Dead biomass from bark beetle attack</del>                                | <del>t/ha</del>          |
| <del>Bdw</del>               | <del>Dead biomass from windthrow</del>   | <del>t/ha</del>          |
| <del>Binf</del>              | <del>Living biomass infested by bark beetles</del>                             | <del>t/ha</del>          |
| <del>Bmax</del>              | <del>Maximum potential biomass of a European Forest</del>                      | <del>t/ha</del>          |
| <del>Bt</del>                | <del>Actual total biomass of spruce forest</del>                               | <del>t/ha</del>          |
| <del>Bw</del>                | <del>Actual woody biomass of spruce forest</del>                               | <del>t/ha</del>          |
| <del>BPI</del>               | <del>Bark beetle pressure index</del>  | <del>unitless</del>      |
| <del>D</del>                 | <del>Distance between two patches</del>  | <del>m</del>             |
| <del>Dw</del>                | <del>Maximum distance for which windthrow can affect surrounding patches</del> | <del>m</del>             |
| <del>Cbp</del>               | <del>Spatial scaling coefficient</del>   | <del>unitless</del>      |
| <del>Est</del>               | <del>Temporal scaling coefficient</del>  | <del>unitless</del>      |
| <del>Frac</del>              | <del>Area fraction within a pixel</del>  | <del>unitless</del>      |
| <del>G</del>                 | <del>Bark beetle generation index</del>  | <del>unitless</del>      |
| <del>K</del>                 | <del>Thermal sum of degrees days for one bark beetle generation</del>          | <del>°C/day</del>        |
| <del>Litw</del>              | <del>Woody biomass left on the forest floor</del>                              | <del>t/ha</del>          |
| <del>Litt</del>              | <del>Litter to stand biomass ratio at which Siw is maximum</del>               | <del>unitless</del>      |
| <del>m</del>                 | <del>Midpoint of the function for degree days</del>                            | <del>unitless</del>      |
| <del>r</del>                 | <del>Logistic growth rate</del>  | <del>unitless</del>      |
| <del>Si</del>                | <del>Susceptibility index [0,1]</del>  | <del>unitless</del>      |
| <del>Sir</del>               | <del>Susceptibility index for stand density [0,1]</del>                        | <del>unitless</del>      |
| <del>Sid</del>               | <del>Susceptibility index for tree health [0,1]</del>                          | <del>unitless</del>      |
| <del>Sis</del>               | <del>Susceptibility index for spruce abundance [0,1]</del>                     | <del>unitless</del>      |
| <del>Siw</del>               | <del>Susceptibility index for tree mortality from windthrow [0,1]</del>        | <del>unitless</del>      |
| <del>SumTeff</del>           | <del>Sum of effective temperature for bark beetle reproduction</del>           | <del>°C/day</del>        |
| <del>Wr</del>                | <del>Weight for stand density index</del>                                      | <del>unitless</del>      |

|       |                             |          |
|-------|-----------------------------|----------|
| $W_d$ | Weight for drought index    | unitless |
| $W_s$ | Weight for spruce abundance | unitless |
| $W_w$ | Weight for windthrow damage | unitless |

**Table 2: Definition of the stages used in the study.**

|                            |   |
|----------------------------|---|
| <b>Outbreak stages</b>     | Stages representing the evolution of the bark beetle population from an endemic to an epidemic situation. There are four stages represented by latin lower case a, b, c, and d representing endemic, build-up, epidemic, post-epidemic, respectively. |
| <b>Stand forest stages</b> | Stages representing the health status of a forest before, during and after a bark beetle outbreak. The six stages represented by arabic numbers from 1 to 6 representing pseudo-climax, green, red, gray, growth and recruitment, respectively.       |

**Table 3: Simulated wood volume loss for the different wind speeds prescribed in this study. Wind storms were used as the disruptive event to trigger change in the ecosystem structure. Seven different wind speeds were used in the experimental setup.**

|                                    |    |    |    |     |     |     |      |
|------------------------------------|----|----|----|-----|-----|-----|------|
| Max wind speed ( $m.s^{-1}$ )      | 19 | 21 | 22 | 23  | 29  | 35  | 40   |
| Relative wood volume loss (%)      | 0  | 8  | 10 | 12  | 27  | 47  | >60  |
| Wood volume loss ( $m^3.ha^{-1}$ ) | 0  | 50 | 70 | 100 | 200 | 300 | >300 |

**Table 4: Climate characteristics of the eight sites used in the gradient underlying our experimental setup. The site acronyms refer to the sites used in the FLUXNET database (Pastorello et al. 2020).**

| Site (FLUXNET abv.)                     | HYY      | SOR     | THA      | WET               | HES    | FON               | REN   | COL   |
|---|----------|---------|----------|-------------------|--------|-------------------|-------|-------|
| Full name                               | Hyytiälä | Sorø    | Tharandt | Trebon            | Hesse  | Fontaine<br>bleau | Renon | Colle |
| Country                                 | Finland  | Danmark | Germany  | Czech<br>republic | France | France            | Italy | Italy |
| Latitude ( $^{\circ}N$ )                | 61.8     | 55.5    | 50.9     | 49.0              | 48.4   | 48.7              | 46.5  | 41.8  |
| Longitude ( $^{\circ}E$ )               | 24.3     | 11.6    | 13.6     | 14.8              | 7.1    | 2.8               | 11.4  | 13.6  |
| Mean annual temperature ( $^{\circ}C$ ) | 3.8      | 8.2     | 8.2      | 7.7               | 9.5    | 10.2              | 4.7   | 6.3   |
| Min annual temperature ( $^{\circ}C$ )  | -10.8    | 2.7     | -3.9     | -5.2              | 0.1    | -1.1              | -6.3  | -3.8  |

|   |      |      |      |      |      |      |      |      |
|---|------|------|------|------|------|------|------|------|
| Mean annual precipitation (mm.y <sup>-1</sup> ) | 522  | 811  | 734  | 587  | 653  | 989  | 752  | 1050 |
| Mean annual net radiation (w.m <sup>-2</sup> )  | 42.1 | 49.4 | 52.5 | 68.0 | 53.7 | 50.3 | 67.7 | 68.3 |

**Table 5. Key components of a bark beetle outbreak.** We conducted a comprehensive literature review, specifically focusing on peer-reviewed articles that outlined the duration of one or multiple stages of the outbreak. In total, 11 papers were identified and utilized in this evaluation.

|   |  |
|---|--|
| erved elements of a bark beetle outbreak (Fig. 1)   | ORCHIDEE behavior  |
| max with endemic stage (Fig. 1; outbreak stage a)   | <p>In colder regions, an increase in temperature following a windthrow event could accelerate the growth of the beetle population and potentially instigate an epidemic situation, as demonstrated in the case of COL (Fig. 3).</p> <p>Conversely, in warmer locations, colder temperatures after a windthrow event could halt the increase in the beetle population, thereby preventing epidemic situations, as seen in the case of THA (Fig. 3).</p> <p>Strong windthrow events resulting in more than 27% damage may lead to a shorter outbreak, as there are fewer living trees available and not all the fresh fallen wood can be utilized by the bark beetles for breeding during the buildup stage (Fig. 3).</p> <p>For weaker windthrow events causing approximately 12% of damage, the likelihood of an epidemic situation will greatly depend on the specific temporal climatic conditions (Fig. 3).</p> |
| en or buildup stage (Fig. 1; outbreak stage b)  | <p>Based on our simulations, the duration of the buildup stage varied from 1 to 3 years, contingent on the intensity of the windthrow events and the prevailing climate conditions (Fig. 3).</p>   |
| l or epidemic stage (Fig. 1; outbreak stage c)  | <p>The ORCHIDEE model simulates epidemic stages where all trees with a diameter greater than 20 cm become potential hosts. During these stages, the bark beetle population escalates, reaching levels 6 to 8 times higher than those in the endemic stage (Fig. 2).</p>  |
| ge-scale tree mortality leads to resource scarcity for the bark beetles, subsequently causing a reduction in their population due to intraspecific competition. The duration of the bark beetle epidemic stage ranges from 1 to 5 years, contingent on the severity of the outbreak and the density of the forest (Burg et al. 2012, Hlásny et al. 2021). | <p>The ORCHIDEE model simulates an epidemic stage lasting between 1 to 6 years, depending on the prevailing climate conditions (Fig 3). A significant decline in the beetle population is observed when the relative stem density drops too low (around 0.4).</p>  |

|   |  |
|---|--|
| <p>factors that instigate a bark beetle outbreak, such as climate conditions and the availability of fresh dead woody biomass, are different from those that lead to the conclusion of an outbreak, namely resource limitations (Edburg et al. 2012).</p>   | <p>The ORCHIDEE model emulates the observed hysteresis, or delay in response, in the dynamics of the beetle population, as outlined in the model description.</p>  |
| <p>pre- or post-epidemic stage (Fig. 1; outbreak stage d)</p> <p>grey stage represents an extended period, spanning years to decades, during which trees die and decompose while still standing, also known as snags (Edburg et al. 2012). During this stage, a disconnection between the soil and ecosystem carbon and nitrogen cycles may be observed (Hlásny et al. 2021).</p> | <p>The ORCHIDEE model simulates logs but not snags. In the model, tree death is instantaneous, with 90% of logs from wind throw and bark beetle damage decomposing within a span of 1 to 3 years (data not shown). This is applicable when logs are lying on the ground. To accurately represent the process in the ORCHIDEE model, snags must be explicitly represented, or the rate of log decomposition must be artificially decreased.</p> |
| <p>ecological transition in endemic stage (Fig. 1; outbreak stages 4 to 6)</p>  |  |
| <p>the aftermath of a bark beetle outbreak, which resulted in a 52% reduction in tree numbers, a combination of observational and modeling approaches estimated a recovery period of 25 years (Pfeifer et al. 2011).</p>  | <p>Without snag decomposition, the model simulates an extended period of functional recovery, ranging from 5 to 15 years depending on the intensity of the bark beetle outbreak (Fig. 4).</p>  |
| <p>the gradual disappearance of snags tends to favor natural regeneration (Jonášová et al. 2004, Carlson et al. 2020).</p>  | <p>The ORCHIDEE model does not simulate natural regeneration in this study. This limitation, along with the model's inability to accurately represent snags, could be responsible for its overestimation of the recovery stage.</p>  |

¶

### Supplementary material S1: The original bark beetle outbreak model of LandClim and the two step integration into ORCHIDEE

Table S1: Main equations of the three versions of the bark beetle outbreak model presented in this study. Subscript “org” refers to the original model (BBO<sub>org</sub>) as presented in Temperli et al. 2013. The subscript “imp” refers to the spatially implicit formulation of the model (BBO<sub>imp</sub>), subscript “orc” refers to the bark beetle outbreak model in ORCHIDEE (BBO<sub>orc</sub>). Subscript “p” represents a patch, “l” represents a landscape, and “ac” represents a diameter class. Subscript “dc” refers to diameter classes in C

| Process                   | Change in formulation   | secondary                           |
|---------------------------|---|-------------------------------------|
| Susceptibility to drought | $(1a) SId_{org} = \sum_{p_t}^{p=1} (1 + e^{d1 \times (Dlmax_p - d2)})^{-1} \times \frac{1}{p_t}$ $(1b) SId_{imp} = (1 + e^{d1 \times (Dlmax_{lc} - d2)})^{-1}$ $(1c) SId_{orc} = \sum_{nac}^{ac=1} (1 + e^{d1 \times ((1 - MOmax_{ac}) - d2)})^{-1} \times \frac{Frac_{ac}}{ndc}$ | $Dlmax_p$ $Dlmax_{lc}$ $MOmax_{ac}$ |



|  |  |   |
|--|--|---|
| <p><del>Susceptibility to windthrow</del></p>  | <p>(2a) <math>SIw_{org} = \max\left(\frac{Bdw_p}{Bmax}, \frac{Bdw_k}{Bmax} \in D(p, k) \leftarrow Dw\right)</math></p> <p>(2b) <math>SIw_{imp} = \frac{Bdw_{lc}}{Bmax}</math></p> <p>(2c) <math>SIw_{orc} = \frac{Litw_{sp}}{Bw_{sp}} / Lit_{thres}</math></p>   | <p><del><math>Bdw_{lc}</math></del></p> <p><del><math>Lit_{thres}</math></del></p> <p><del>windthrow</del></p>  |
| <p><del>Susceptibility to stem density</del></p>                                     | <p>(3a) <math>SIra = \sum_{p_t}^{p=1} (a1 + (1 - a1)/(1 + e^{a2 \times (Age_p - a3)})) \times \frac{1}{p_t}</math></p> <p>(3b) <math>SIa_{imp} = (a1 + (1 - a1)/(1 + e^{a2 \times (Age_{lc} - a3)}))</math></p> <p>(3c) <math>SIr_{orc} = (a1 + (1 - a1)/(1 + e^{a2 \times (RDI_{sp} - a3)}))</math></p>   | <p><del><math>RDI_{lc}</math></del></p>   |
| <p><del>Susceptibility to patch purity</del></p>                                     | <p>(4a)</p> <p><del><math>SI_s_{org} = \sum_{p_t}^{p=1} (s1 + (1 - s1)/(1 + s2 \times e^{s3 \times (Sh_p - s4)})) s5^{-1} \times</math></del></p> <p>(4b) <math>SI_s_{imp} = (s1 + (1 - s1)/(1 + s2 \times e^{s3 \times (Sh_{lc} - s4)})) s5^{-1}</math></p> <p>(4c) <math>SI_s_{orc} = (1 + e^{s1 \times (sh_{sp} - s2)})^{-1}</math></p>                                   | <p><del><math>Sh_p = \frac{BA}{BA}</math></del></p> <p><del><math>Sh_{lc} = \sum_{p_t}^{p=}</math></del></p> <p><del><math>Sh_{sp} = \frac{Fr}{Fr}</math></del></p> |
| <p><del>Susceptibility of trees to bark beetle infestation</del></p>                 | <p>(5a) <math>SI_{org} = \frac{SIw_{org}}{2} + \frac{SI_{d_{org}} + SI_{a_{org}} + SI_{s_{org}}}{6}</math></p> <p>(5b) <math>SI_{imp} = \frac{SIw_{imp}}{2} + \frac{SI_{d_{imp}} + SI_{a_{imp}} + SI_{s_{imp}}}{6}</math></p> <p>(5c)</p> <p><del><math>SI_{orc} = SIw_{orc} \times Ww + SIr_{orc} \times Wr + SI_{d_{orc}} \times Wd + SI_{s_{orc}} \times</math></del></p> | <p><del>Risk_{orc}</del></p> <p><del><math>Ws = 0.1</math></del></p> <p><del><math>Wr = (1 +</math></del></p> <p><del><math>Ww = 1 -</math></del></p>               |
| <p><del>Susceptibility of trees to mortality after bark beetle infestation</del></p> | <p>(6a) <math>SI_{p,co} = \max(SIw_{p,co}, (SIa_{p,co} + SI_{d_{p,co}})/2)</math></p> <p>(6b) <math>SI_{p,co} = \max(SIw_{p,co}, (SIa_{p,co} + SI_{d_{p,co}})/2)</math></p> <p>(6c) <math>SI_{ac} = SIr_{ac} \times Wr + SI_{d_{ac}} \times (1 - Wr)</math></p>  | <p><del></del></p>  |
| <p><del>Beetle pressure index</del></p>  | <p>(7a) <math>BPI_{org} = Cbp \times SI_{org} \times (GI + \frac{Bdb_{p,n-1}}{Bmax})/2</math></p> <p>(7b) <math>BPI_{imp} = Cbp \times SI_{imp} \times (GI + \frac{Bdb_{imp,n-1}}{Bmax})/2</math></p> <p>(7c) <math>BPI_{orc} = Cbp \times SI_{orc} \times (GI + \frac{Bdb_{pix,n-1}}{Bt \times Cst})/2</math></p>   | <p><del></del></p>  |

|  |   |  |
|--|---|--|
| <p>Risk index <math>\mathbb{H}</math></p>                      | <p>(8a) <math>RI_{org} = SI_{org} \times BPI_{org} \mathbb{H}</math></p> <p>(8b) <math>RI_{imp} = SI_{imp} \times BPI_{imp} \mathbb{H}</math></p> <p>(8c) <math>RI_{orc} = SI_{orc} \times BPI_{orc} \mathbb{H}</math></p>  | <p><math>\mathbb{H}</math></p>   |
| <p>Infested biomass by bark beetle <math>\mathbb{H}</math></p> | <p>(9a) <math>Binf_{org} = 150 \times SI_{org} \times BPI_{org} + r_{beta} \mathbb{H}</math></p> <p>(9b) <math>Binf_{imp} = 150 \times SI_{imp} \times BPI_{imp} \mathbb{H}</math></p> <p>(9c) <math>Binf_{orc} = Bt \times Cst \times SI_{orc} \times BPI_{orc} \mathbb{H}</math></p>  | <p><math>r_{beta} \mathbb{H}</math></p> <p><math>\mathbb{H}</math></p>                             |
| <p>Killed biomass by bark beetle <math>\mathbb{H}</math></p>   | <p>(10a) <math>Bdb_{org} = \sum_{p_t}^{p=1} \sum_{nco}^{co=1} \frac{SI_{p,co} + BPI_{org}}{2} \times Binf_p \times \frac{BA_{sp,co}}{BA_{sp}} \mathbb{H}</math></p> <p>(10b) <math>Bdb_{imp} = \sum_{nco}^{co=1} \frac{SI_{lc,co} + BPI_{imp}}{2} \times Binf_{imp} \times \frac{BA_{lc,co}}{BA_{sp}} \mathbb{H}</math></p> <p>(10c) <math>Bdb_{orc} = \sum_{nac}^{ac=1} \frac{SI_{ac} + BPI_{orc}}{2} \times Binf_{orc} \times \frac{BA_{ac}}{BA_{sp}} \mathbb{H}</math></p> | <p><math>\mathbb{H}</math></p> <p><math>\mathbb{H}</math></p> <p>Retrieving</p> <p>Temperli et</p> |